ČESKÉ VYSOKÉ UČENÍ TECHNICKÉ V PRAZE

Fakulta stavební

Katedra technologie staveb

Critical assessment of 3D printing technology regarding its general applicability under technological and material constraints

DISERTAČNÍ PRÁCE

Ing. Michal Kovářík

Doktorský studijní program: (P3604) Stavební inženýrství

Studijní obor: (3608V001) Pozemní stavby

Školitel: doc. Ing. Pavel Svoboda, CSc.
Školitel - specialista   prof. Ing. Petr Štemberk, Ph.D., D.Eng.
Školitel - specialista   prof. Dr. Henri Hubertus Achten

..

Praha, 2023

PROHLÁŠENÍ

Jméno doktoranda: Ing. Michal Kovářík

Název disertační práce: Critical assessment of 3D printing technology regarding its general applicability under technological and material constraints

Prohlašuji, že jsem uvedenou disertační práci vypracoval/a samostatně pod vedením školitele doc. Ing. Pavel Svoboda, CSc.

Školitel - specialista   prof. Ing. Petr Štemberk, Ph.D., D.Eng.

Školitel - specialista   prof. Dr. Henri Hubertus Achten.

Použitou literaturu a další materiály uvádím v seznamu použité literatury.

V Praze dne ⎯⎯⎯⎯⎯⎯⎯⎯⎯   ⎯⎯⎯⎯⎯⎯⎯⎯⎯⎯⎯⎯⎯⎯⎯⎯⎯⎯

                                                                        podpis

Acknowledgments

This thesis presents my work performed as a PhD student at Czech Technical University in Prague, Faculty of Civil Engineering, Department of Construction Technology over the course of the past seven years. Many people, directly or indirectly, have contributed to this final result.

Firstly, I would like to thank my supervisor, associate professor Pavel Svoboda, for giving me the opportunity to pursue the novel topic of 3D printing within the Department of Construction Technology and supporting me in my choice of the thesis topic despite the initial scepticism of my colleagues and minimal research facilities.

Secondly, I would like to thank my supervisor specialist prof. Petr Štemberk, for his guidance and feedback during the research and towards the completion of this thesis. I am forever grateful for his trust, humour and encouraging me during moments of doubts and hardship. My sincere appreciations go out to all his team members for their support and helpful assistance during elaborating this thesis.

Many thanks go also to my second supervisor specialist prof. Henri Achten, for organizing my inspiring consultation at BRG, ETH and his international insight.

I am very thankful to my colleagues at the Department of Construction Technology, especially Dr. Rostislav Šulc for his insight in materials and technology.

The author also acknowledges the support from Master Builders, and SIKA for donating the materials and sharing their know-how.

Last but not least, I would like to thank my family members and friends. I would like to thank my mother Marie for her support of the 3D printing workshop in her house and for her inspiring insight as the first tester of our products. I would like to thank my brother Petr for his inspiring insight in mechatronic and all his effort during developing Fabrilium project. Thanks also go to my friends Vít Kolovrat, Petr Kašpárek and Vojta Kašák for their contribution to this project.

I would like to thank my wife Magdalena, who was always there for me. I thank her for her patience and understanding when I spent days and nights in our workshop or at the office. Without her support, this thesis would never have been possible.

Anotace

Technologie 3D tisku z betonu je od svého prvního masivnějšího proniknutí do mediálního prostoru po roce 2007 mnohými pasována do role gamechangera, který změní budoucí tvář stavební výroby a podobu budov jako takových. Do vývoje této robotické technologie bylo v posledních deseti letech v globálním měřítku investováno velké množství úsilí i prostředků, přesto nejsme ani po letech svědky jejího masivního pronikání na staveniště.

Tato práce se snaží popsat specifika technologie 3D tisku z betonu i tiskového materiálu a odpovědět na otázku, jaké oblasti jsou klíčové pro využitelnost 3D tisku vytlačováním jednokomponentních směsí při výrobě prefabrikátů s vysokými požadavky na kvalitu. Práce je podpořena více než šestiletou zkušeností autora s tématem práce a praktickými dovednostmi, nutnými pro jeho zvládnutí, tj. návrhem a stavbou tiskáren, výrobou výtlačných trysek a tiskových hlav, přípravou a zkoušení tiskových materiálů i programováním ovládacích skriptů.

Autor v úvodu práce shrnuje dosavadní stav poznání v oblasti 3D tisku vytlačováním malty. V hypotéze pojmenovává kritické oblasti, jejichž zvládnutí bude klíčové pro praktické využití technologie. V návazné části navrhuje metody pro dosažení cílů práce. Popisuje postup návrhu tiskových materiálů a možné způsoby návrhu ovládacích skriptů. Zabývá se použitelností vybraných zkušebních metod pro ověření parametrů tiskového materiálu. Na konkrétních případových studiích poté v praktické části demonstruje úskalí, provázející proces tisku z důvodu specifik strojního zařízení, kolísání kvality vstupních surovin i vlivu okolního prostředí na proces 3D tisku i na kvalitu finálního výtisku.

Autorem získané výsledky jsou dále podrobeny analýze s cílem posoudit jednotlivé aspekty procesu přípravy materiálu i samotného tisku. V závěru poté shrnuje provedené poznatky a naznačuje podmínky využitelnosti dané technologie 3D tisku v praxi.

Klíčová slova

Betonové konstrukce, aditivní výroba, 3D tisk z betonu, robotická technologie, řízení kvality

Abstract

Since its first massive media breakthrough after 2007, the concrete 3D printing technology has been hailed by many as a game-changer that would change the future face of construction manufacturing and the face of buildings in general. A great deal of effort and resources have been invested in the development of this robotic technology on the global scale over the past decade, yet even after all these years, we have not witnessed its massive deployment on the construction site.

This thesis seeks to describe the specifics of the concrete 3D printing technology from both technology and material perspective and to answer the question of what are the key areas regarding applicability of the 3D printing by extruding one component mixtures in the production of concrete components with high quality requirements. The work is supported by the author's more than six years of experience with the topic of the thesis and the practical skills required to master it, i.e. designing and building printers, manufacturing extrusion nozzles and print heads, preparing and testing printing materials and programming the controlling scripts.

In the introduction of the thesis, the author summarizes the current state of knowledge in the field of 3D printing by mortar extrusion. In the hypothesis, he names critical areas, the mastery of which will be crucial for the practical application of the technology. In the following sections, methods for achieving the objectives of the thesis are proposed. The process of designing printing materials and possible ways of designing the controlling scripts are described and the applicability of selected test methods for verifying print material parameters is discussed. Then, using specific case studies, the practical part demonstrates the pitfalls accompanying the printing process due to the specifics of the machinery, variations in the quality of input raw materials and the influence of the surrounding environment on the 3D printing process and the quality of the final print.

The results obtained by the author are further analysed in order to assess individual aspects of the material preparation process and the printing process itself. In the conclusions, the author summarizes the findings and suggests the conditions for the applicability of the 3D printing technology in practice.

Keywords

Concrete structures, additive manufacturing, 3D concrete printing, robotic technology, quality control

List of Abbreviations

AM: Additive Manufacturing

FFF: Fused Filament Fabrication

CAD: Computer Aided Design

CAM: Computer Aided Manufacturing

CNC: Computer Numeric Control

DOF: Degrees of Freedom

3DCP: 3D Concrete Printing

FEM: Finite Element Method

Table of Contents

„For a successful technology, reality must take precedence over public relations, for Nature cannot be fooled.“

Richard P. Feynman

1. MOTIVATION

Since 2009, thanks to the first experimental construction 3D printing projects, the first examples of real constructions have started to reach the public [1-3]. [Fig.1]. This construction technology, using automated fabrication machinery, special materials and optimization algorithms, has gradually become one of the synonyms for the future of construction, thanks to a great deal of media interest and significant investments by renowned companies [4]. Bold plans by governments to massively incorporate this technology into construction are being presented to the public [5-7], space agencies are promising to use the technology to facilitate the construction of human bases on the Moon and Mars [8, 9], and 3D printing is credited with solving the global housing crisis [1, 10] or reducing the carbon footprint of construction [11].

The potential to revolutionise construction on a global scale by 3D printing shall be quite promising. Cutting waste, pollution, time, labour, and cost, this technology shall soon have the capacity to break down the traditional design boundaries that have stood in the way of architectural innovation [10]. The technology's ability to produce material-saving, digitally optimised shapes also appears to be an advantage for the future, as is the waste-free nature of production, promising to reduce concrete consumption at a time of social pressure to increase sustainability in construction.

Fig. 1: a) Radiolaria pavilion developed by Andrea Morgante of Shiro Studio and 3D printed by D-Shape technology b) Simple building, made of 3D printed walls by WinSun technology c) Model of a castle, made of 3D printed parts by Andrey Rudenko, TotalCustom

The fundamental question that the author has set as the goal of his research and of this thesis is based on a simple consideration. According to a number of scholarly articles and the growth in the number of projects, it seems that the future of the construction industry belongs to concrete 3D printing technology (3DCP). Significant financial resources have been invested in research in this field over the last 10 years or so, yet we still do not see significant application of this technology on construction sites, all projects are limited to experimental or verification purposes, the cost of

commercial projects exceeds the price of comparable buildings realized by conventional technologies and their number is thus negligible in the construction production.

The author therefore asks the logical questions: "What is the reason for the difference between the proclamations and the actual low use of the technology? Is the low use of 3D printing in practice due to the technical immaturity of the technology, high material and operating costs or other reasons? Are there ways to successfully address these issues and fulfil media predictions about 3D printing as the future of construction?"

The work presented in this thesis is the result of six years of intense experimentation and thousands of hours spent searching for the right paths, lined with many dead ends. It can be considered a pioneering work in the Czech context and at the given time.

2. STATE OF ART

The 3D printing technology generally represents the creation of physical 3D objects through an additive manufacturing process, thus it is also referred to as additive manufacturing. Extrusion based 3DCP technology, similar to fused filament fabrication (FFF) 3D printing technology, is based on extruding material in a form of a filament from a nozzle and depositing it in stacked layers according to spatial and technological parameters defined within a digital printing script. The structural stability of objects produced in this manner is not ensured by formwork, but by the rapid solidification of the filament material after being extruded from the nozzle. In 3DCP, solidification is usually ensured on microstructural scale by accelerating or amplifying the interactions between cement particles or by accelerating the cement hydration itself [12].

Geometric and model constraints

Worldwide so far, the 3DCP technology has been used to fabricate elements and structures with dimensions in the order of 10^{-1} to 10^{1} m. The size of the printed elements is then limited/defined by the dimensions of the printing space of the fabrication facility, i.e. a printer. The 3D printing technology relies on the materialisation of physical objects in layers of a defined thickness and width in the range of 10^{-3} to 10^{-2} m. The resulting elements do not have solid infill as in monolithic concreting, but they are rather 2D, 2.5D or 3D surfaces and their combinations [13]. Another feature of the 3DCP technology, which distinguishes it from monolithic concreting in terms of quality and mechanical properties of the resulting products, is the printing resolution, i.e. the size of the smallest fabricatable detail of the element. The resolution is related to the nozzle cross-section size, material type and deposition rate and defines the application of the resulting products. A different resolution is desirable for printing building support structures, another for printing design components with aesthetic requirements. The key to the design of the technology is then the production method of the final work, i.e. in-situ or prefabrication. In the case of in-situ printing, high demands are placed on the technology in terms of the dimensions and rigidity of the printer, or its mobility, as well as demands arising from

2

the specifics of in-situ production, i.e. mainly resistance to climatic influences. In the case of printing prefabricated elements in the factory, similarly to prefabricated elements produced by mould casting, the design of the element joints, the consideration of the influence of assembly load cases and the constraints imposed by the technology for transport and assembly in-situ, such as the weight and dimensions of the element, play a crucial role. The key to the design of the technology is the method of fabrication of the resulting structure, i.e. in-situ or off-site prefabrication. In the case of in-situ printing, heavy demands are placed on the technology in terms of the size and rigidity of the printer or its mobility. The limitations resulting from the specifics of in-situ production, i.e. mainly the effects of climatic influences are also crucial.

Machinery

The 3D printing process itself is performed via robotic fabrication device called a 3D printer. It consists of a robotic manipulator that delivers the position and orientation of the production tool, i.e. the extrusion nozzle or complex print head fitted with a nozzle. Extrusion nozzles can be of a circular, oval, or rectangular section. Six DOF industrial robots or custom-built Cartesian kinematics are typically utilized as printers, yet other types of kinematic structures can be also employed [14]. The 3D printer is controlled by a computer control unit in which the firmware is installed. The control unit, using firmware, converts data from an externally generated control script into commands to individual motors that control the printer's kinematic axes and usually the extrusion screw inside the nozzle.

The material supply to the nozzle is provided via a pressure hose from a pump, usually working under the progressive cavity or peristaltic [15] principle. The pump can be fitted with an RPM controller to ensure smooth control of the material delivery during printing.

The material is provided using a mixer. Two basic material preparation approaches can be used. First, the fresh mixture is mixed in multiple batches using a horizontal mixer or a gear stirrer with single or double rods and the fresh mixture is then delivered manually or automatically to the hopper of the pump. It is mainly preferred in a small-scale application, e.g., printable material development and other experimental activities. Second option, a continuous system, relies on an in-line mixing machine. A dry bulk material mixture is transferred by gravity from the hopper to the mixing chamber, where it is mixed with water in a controlled manner. Fresh mortar is then continuously pushed to the outlet of the mixer where it travels into the pump hopper. It is mainly used for large-scale construction. If the mixer and pump are controlled digitally, they can be connected to the 3D printer in order to control the material feed to the nozzle using a printing script.

Printing strategies

The extrusion based 3DCP technology employs the principle of extruding material in form of a filament from a nozzle and depositing it in stacked layers. The envelope of each layer is created by translating a cross-section of the layer [Fig.2] along the control curve representing the printing path, i.e. path of a nozzle. The print path can be of different types depending on the shape of the printed element and the

slicing method, i.e. the division of the element geometry into layers [16]. To convert a 3D model into a control script used by a 3D printer, it is necessary to process the model in a CAM tool, which in 3D printing is called the slicer. To generate the printing path strategies for the 3DCP, we can borrow from clay printing [17]. There are several types of printing paths possible, i.e. slicing into horizontal or inclined paths with travels, horizontal or inclined paths with ramps, or spiral paths. When printing in horizontal or inclined layers [Fig.2a] with travels, the path of each layer is an open or closed planar curve oriented parallel to the print base surface. At the connection point at the start and the end points of closed contour curves visible seams are formed. Paths generated in such a manner consist of a set of parallel contours connected with travels without extrusion. The challenge related to this method of printing is to guarantee a constant nozzle pressure caused by the extrusion interruption during travels to prevent the nozzle pressure from fluctuating between the seams of subsequent layers and degrading the printout with excessive material. To deal with the problem of fluctuating pressure and visible seams, the parallel layers can be connected into one continuous extrusion path using inclined ramps instead of interrupting it with non-extrusion travels. The second option for the continuous printing path is spiral printing, when the complete printing path corresponds to a single 3D curve with a constant stroke in the positive direction of the Z-axis. Besides the standard slicing methods, recently a technology of printing with variable layer heights was developed [18] [Fig.3b].
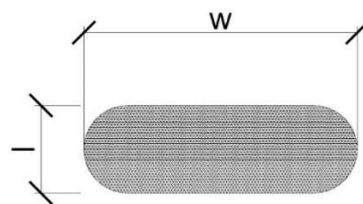

Fig. 2. Oval layer cross-section details

The cross section of a layer can be characterized by the height (l) and the width (w) and is determined by the nozzle profile, extrusion flow and nozzle movement velocity as well as the consistency of the material. Dimensions of both the layer width and height vary in the range of $5 - 50$ mm for most processes. The shape of the cross-section of the layer can be rectangular or oval [19], depending on the shape of the nozzle cross-section and whether the sides of the layer are trowelled after extrusion. The cross-section, and with it the envelope of each layer, is deformed during the printing of subsequent layers due to loading from their own gravity and increases with the number of layers [12]. This can be corrected by gradually lowering the layer height depending on the increment of the layer Z coordinate, or by accelerating the solidification of the material.

In order to maintain uniform appearance of layers from below up to the top, it is crucial to maintain a constant deposition rate, i.e. the layer profile. Besides the printing strategy, the layer appearance and therefore the quality is also crucially influenced by the material properties.
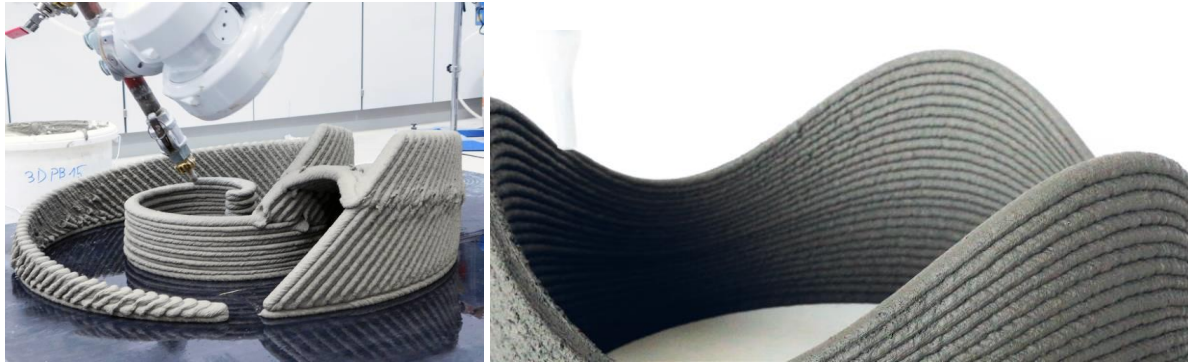
Fig.3. a) Inclined layer printing with the BauMinator [20]
b) Non-laminar printing with variable layer height [18]

Material requirements

In the 3DCP, the material parameters are derived from contradictory requirements defined by the unique character of fabrication technology employing robotic controlled deposition of a flowing material to create solid objects without formwork. The material behaviours are therefore primarily constrained by the printing strategy, i.e. the printing system and process. A key criterion to consider when designing printing materials applicable in the 3DCP technology is their properties and behaviour in the fresh state.

Material components

The vast majority of projects use fine-grained Ordinary Portland cement (OPC) based mortars as the printing material, but concrete and geopolymers were also investigated [21]. Mixtures can be custom prepared from individual components on demand or, commercial industrial premix mixtures can be used. High-strength cements with a rapid initial setting are used as binders in cementitious mixes and concretes to meet the requirement for rapid setting. Supplementary cementitious materials, such as fly ash, blast furnace slag, calcined clay and limestone can be used to improve properties of mixtures or to increase sustainability [21]. Fine sands with $d_{max} < 2$ to 3 mm are mainly used as an aggregate due to easy permeability through the pumping system and nozzle, in the case of concretes up to $d_{max} < 8$ mm fraction. In order to ensure the required rheology, additives such as plasticizers, viscosity modifiers or solidification retarders and accelerators are key components of the mixtures. Fibres are also often added, most often monofilament plastic fibres of 6 to 12 mm in length. Mixtures can be designed as single (1K) or two-component (2K), depending on whether a second component is added to the mix in the form of a liquid suspension of a setting accelerator in the mixing nozzle.

Fresh properties and rheometry

Printable Materials behave roughly as visco-plastic Bingham materials. They display a viscous behaviour, i.e. they flow, when submitted a to stresses higher than a critical threshold value τ_c called yield stress. During the flowing phase, they exhibit shear rate, that is proportional to the stress in excess of the yield stress through a constant μ_p called plastic viscosity [22]. This behaviour is required only for the short time of pumping and extrusion. After being deposited, materials stay in rest and

instead its plastic viscosity they start demonstrating elasto-plastic behaviour [23]. Below the yield stress, these materials exhibit a roughly elastic behaviour. Their shear elastic modulus can be expressed as $G = \tau_c / \gamma_c$ with γ_c the critical shear strain at flow onset. A key feature in most printing applications is the thixotropy of these materials and more generally their ability to build up an internal structure at rest. When the material is deposited, it exhibits an initial yield stress τ_{c0}, an initial critical shear strain γ_{c0} and an initial elastic shear modulus G_0. In the consecutive phase these rheological parameters evolve in time making material stronger (higher yield stress) and also more rigid (higher elastic modulus) [12].

At a microscopic scale, fresh properties are based on same principles as typical cementitious materials. The ability to display a yield stress and build up a structure at rest originates from its ability to flocculate along with its ability to the nucleate early hydrates at the pseudo-contact points between cement grains in the flocculated structure formed by the cement grains [12]. From a practical point of view, hydration may have reversible macroscopic consequences as long as the available mixing power is sufficient to break the hydrates bridges between cement particles. Hydration is however at the origin of workability loss as soon as the available mixing power becomes insufficient to break all these inter-particle connections [12]. Following these principles, the most efficient ways to create very thixotropic concrete is to introduce hydration accelerating products in the mixture or fine silica or limestone particles that will act as intercalated grains with strong nucleating properties. As soon as the mixing power available during industrial processes is sufficient to break the additional CSH bonds created by these products, they enhance thixotropy without any workability loss [23]. To assess fresh state of materials in 3DC, several rheological requirements were defined [19, 24, 25]

Pumpability

As a part of the printing process successive to mixing, the material has to be delivered from the mixing machine via hose to the extrusion nozzle or printhead where it must be extruded as a continuous filament [25]. Pumpability is defined as an ability of material to flow smoothly through the pump and hose. Necessary fluidity is indeed expected to be above a threshold value, which depends on the pumping system used (technology, pumping distance, diameter etc.). To maintain pumpability, the material should manifest visco-plastic behaviour, i.e. low-to-moderate yield stress and low plastic viscosity during the pumping and extrusion phase [26]. A main factor that governs rheology and fluidity of concrete paste in the fresh state is the particle grading. Generally, a wider particle size distribution would contribute to a higher packing density and yield a better flowability [27, 28]. In most cases, superplasticizers are preferred to improve the flowability of cement paste while maintaining comparable or higher mechanical strength to increasing so it has positive impact on both pumpability and extrudability.

To measure fluidity of slurry and its stability against the segregation during the flow, there are several testing methods to be used over decades. Slump test is used to describe the concrete of relatively low flowability by the drop in height of concrete. V-funnel test is used to evaluate the viscosity of fresh concrete and the deformability to

pass through restricted areas by the V-funnel flow time. The L-Box test is employed to evaluate the flowable performance and in particular the passing ability of concrete mixtures. Results obtained from this test can be used to assess the passing ability of concrete flow through narrow pipes in the printing system and small openings formed by the deposition head. Viscosity behaviour of concrete mixture can be measured by digital viscometers [30].

Extrudability

In 3DCP, extrudability describes the ability of material to be continuously delivered through the hose and deposited from extrusion nozzle (usually linked to the hose via printing head) [30]. Similarly to pumpability, the increase in the fineness of solid constituents reduces the extrudability if the water content remained unchanged [31]. But not only grain size distribution should be considered, also the size of grains. Compared to angular aggregates, employing round shape aggregates would enable a better control of extrudability and decrease blocking potential for a given water to powder ratio. Generally, basic principle of grading design for printing material is to use a considerable volume of cementitious paste to fill the voids formed between smooth graded aggregate particles [30]. Malaeb et al. [32] recommended that the mass ratio of fine aggregate to cement is 1.28 and fine aggregate to sand is 2.0. And the maximum size of aggregates is set as 1/10 of the diameter of the printing nozzle. Le et al. [25] selected sand with a maximum size of 2 mm to manufacture concrete paste used for a small nozzle with a diameter of 9 mm, which ensures a high printing resolution. For the quantitative evaluation of extrudability, simple flow tests are inapplicable. Rheological measurements by means of viscometer, however, can serve as indicators for variation in extrudability. In literature novel testing methods were suggested, but they have their own difficulties [26, 31. Chen et al [21] suggested that for characterizing the fresh properties of printable Cementitious materials during the pumping, and extrusion processes, offline methods, like flowability, ram extrusion, and rheometry (CSR/hysteresis loop) tests can be employed.

Workability

Le et al linked workability with consistence [25] Khoshnevis described workability of printing mixtures in terms of print quality, shape stability, and printability window [33]. In order to evaluate workability, the slump, compacting factor and flow tests as conventional methods are available regarding various national standards [21, 25]. However, these do not measure fundamental physical properties [30].

Open time / Printable window

Le et al [25] determined the open time as the time period in which the workability of fresh concrete was at a level that maintained extrudability. As a different concept, Khoshnevis [33] introduced the term "printable Window" to timespan during which the printing mixture could be extruded by the nozzle with an acceptable quality, considering the workability loss that happens over time. Two time limits were introduced to define the printability window of a mixture:

(1) Printability limit: The time when the quality of printed layer is affected as a result of workability loss, recognized by triple "print quality" requirement

(2) Blockage limit: The time when the concrete cannot be guided out of printing nozzle at all, and further delay would result in mixture solidification and damage to the nozzle.

The results indicated that nozzle blockage could happen long before the initial setting time of each mixture and setting time could not be used as an alternative indicator. Nozzle blockage can result in significant time loss, nozzle damage and extra cost during construction. As such, measuring the blockage limit for each mixture is recommended during mixture design and laboratory testing [33].

The open time of a cementitious material has a relationship with its setting time, usually measured with a Vicat apparatus. However, this equipment is designed to determine the initial and final setting time which are not particularly helpful in characterising the change of workability with time of fresh concrete [25]. An effective way for continually monitoring the setting performance of concrete was demonstrated via ultrasonic method. The method has been shown to be sensitive and reliable to monitor the hydration process of cement paste as affected by different w/c ratios, different curing temperatures, and different cement types and fineness [34]. Recently, ultrasonic wave reflection method has been proved to be effective to monitor the early age setting and hardening process of concretes non-destructively and continuously [35].

Buildability

Le et al characterized it as a material ability to be laid down correctly, remain in position, be stiff enough to support further layers without collapsing and yet still be suitable to provide a good bond between layers [25]. Alternatively, Lim et al. [36] defined buildability as "the resistance of deposited wet material to deformation under load". Kazemian et al [33] defined shape stability as "the ability to resist deformations during layer-wise concrete construction" and specified "three main sources of deformation: self weight, weight of following layers, and extrusion pressure". Nerella et al [31] defined it as the ability of an extruded cementitious material to retain its geometry (shape and size) under sustained and increasing loads in fresh or transient state. Buildability is a complex and process-specific property which depends not only on material composition, but also on process parameters such as layer geometry. Nerella et al [31] further recognized three primary parameters defining any buildability tests when applied in laboratory investigations for material characterization: 1) the height of the wall to be printed, 2) the section geometry of each layer, thus, the total number of layers to be printed, and 3) the time interval (TI) between subsequent layers. The shape of the layers and that of the element (e.g. inclination) also influence buildability. Perrot et al. [37] considered the following primary criterion: "the flow resistance of a substrate-layer should always be higher than the vertical loads acting on top of it". Chen et al. [21] noted that the printing parameters, i.e., the geometry and length of printing/ nozzle path (shape of the designed object for printing), nozzle variables (shape, dimension, and flow direction), the time intervals between two subsequent layers (also known as cycle time), nozzle standoff distances and printing speeds, may significantly influence the buildability assessment. Detail explanation of fresh-state properties of cementitious materials and their influence on buildability were formulated by Roussel [12]. After material

8

deposition, the quantification of buildability and structural build-up becomes critical. Development of yield stress/stiffness with time can be quantitatively determined using the green strength test, penetration test, and rheometry (static yield stress measurement with time, SAOS, and LAOS tests). The inline buildability test incorporating experiment monitoring systems can be implemented to evaluate the developed mixtures directly [21].

Printability

This key characteristic is still not unified across the literature. Lim et al [19] defined printability as the ease and reliability of depositing material through a deposition device. Ketel et al [38] defined printability index (Ip) which quantitatively describes the ability of given slurry to be used as a printing medium for a particular geometry. It is quantified by assessing the extent of external dimensional mismatch between a digital CAD input design and its corresponding printed counterpart. The index offers a robust basis for comparing the geometric fidelity of a specimen printed using any nature of slurry, thereby facilitating identification of how changes in the rheological properties (e.g., yield stress, viscosity and shear modulus) may affect printability.
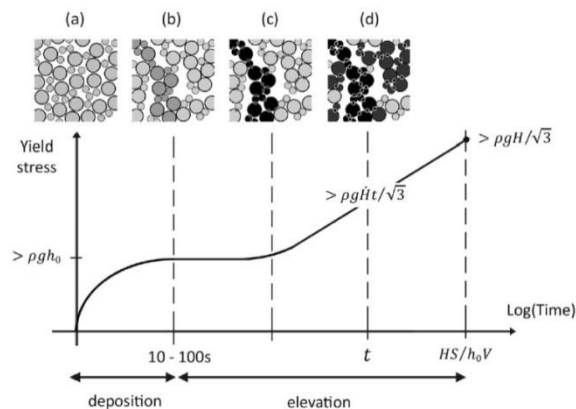

Fig.4. Yield stress requirement as a function of time. On short time scales, flocculation allows for the printing of a filament with well-controlled geometrical features while, on longer time-scales, hydrates nucleation allows for the printing of vertical slender objects. Adapted from [12]

Tripathi et al [39] noted that appropriate binding materials, water content, and the use of chemical admixtures to ensure high particle packing help in optimization of the material, whereas appropriate mixing processes, rest time, and printer characteristics forms part of the process optimization to ensure desired printability, on which the properties of the 3D printed concrete structure rely significantly on. Roussel [12] suggested that "printability" or "buildability" seem to include a combination of various aspects of the rheological behaviour of the material and, as such, shall reach a practical limit when it comes to mix-design [Fig.4]. It moreover suggests that the rheological window, in which the material is "printable" May be extremely narrow, raising some major questions of robustness and quality control. Wrangler et al [40] distinguished two types of approaches depending on material consistency. Extrusion of very high/sufficiently stiff materials is still the most common printing strategy in the field of 3DCP. However, the pumping distance for extrusion of

stiff materials is limited due to the high pumping pressure induced by the high yield stress and plastic viscosity. Compared to the very high/sufficiently, stiff material, the material for set-on-demand printing exhibits exceptionally high fluidity during mixing, pumping, and extrusion processes, which may be more suitable for large-scale construction projects. However, the study of set-on-demand printing is still limited and requires further investigations. To facilitate laboratory testing of printing mixtures, Khoshnevis suggests 5-stepped framework [Fig.5].
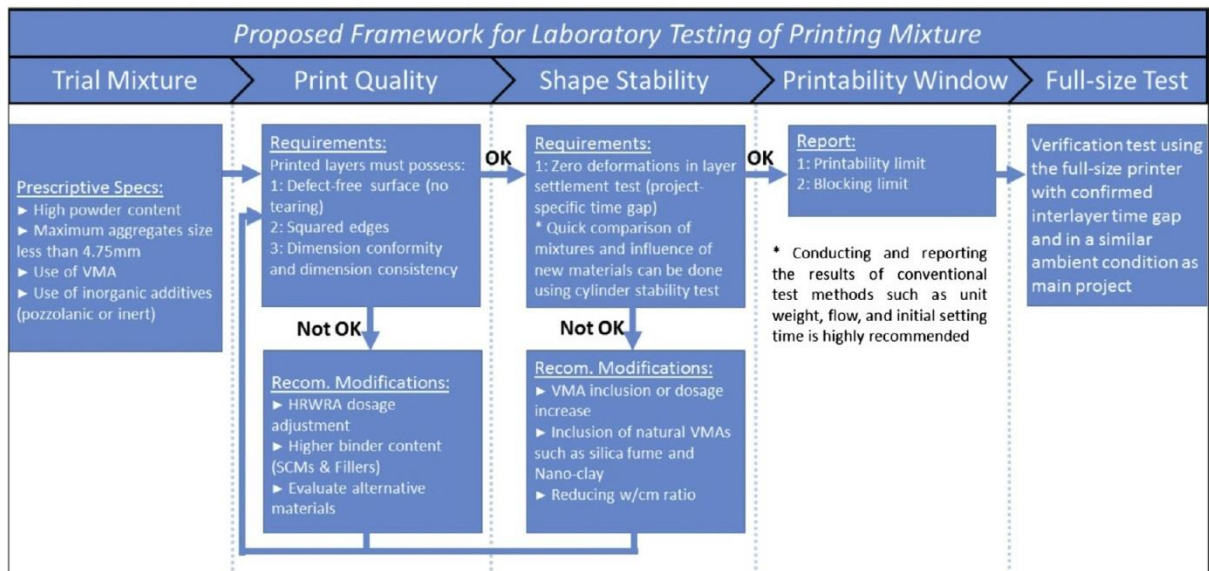

Fig.5. Proposed framework for laboratory testing of printing mixture in fresh state [33]

To analyse material behaviour during printing process, Mohr-Coulomb material model was suggested by Wolfs et al [41]. The essential time-dependent material properties were determined by triaxial compression testing of 3D-printed concrete.as material density ρ, the Young modulus E function of time (t), Poisson's ratio ν, cohesion c function of time (t), the angle of internal friction φ and the dilatancy angle ψ. To analyse and optimize the printing of straight wall structures, a mechanistic model was proposed by Suiker [42]. His model distinguishes between two failure mechanisms: elastic buckling of the global structure and plastic collapse at the bottom layer. This model was further developed [43] and incorporated into digital modelling tools employing FEM [44, 45]. Roussel [12] suggested that for complex shapes, some structural and morphological effects could reinforce the printed object against buckling.

Green strength

To avoid collapse during printing, it is crucial to determine the yield stress evolution of the bottom layers. One of the ways to determine the applicable building rate and to assess shape stability for specific printable Materials can be applying direct load on the fresh cementitious materials [46]. Perrot et al [37] simulated the loading induced by the layer-by-layer construction process on the first deposited layer by using a plate-stacking test. Monitoring of the very early-age strength development of studied mixtures can be facilitated by measuring the uniaxial unconfined compressive strength test. In such a test, cylindrical samples with an

aspect ratio of 2 are commonly used [41, 47]. Experiments suggest that the young age sample fails with a barrelling effect, in contrast, for the samples with older ages (after 1 or 2 h), a strain-softening behaviour is observed after the stress reached the peak value. Mix design of materials with higher tensile strength in the fresh state could imply flexible organic fibres or high molar-mass binding polymers allowing for an improvement of the ductility of the fresh material [12].

Cracking in fresh state

Bos et al. [48] reported that small radii of curvature in the nozzle path may result in tearing and/or cracking of the outer edge of the material due to the tensile. A minimum radius of curvature should be maintained, the value of which, however, is highly dependent on the printing process and the layers geometry. According to Roussel [12], the mix design of materials with higher tensile strength in the fresh state could imply flexible organic fibres or high molar-mass binding polymers allowing for an improvement of the ductility of the fresh material.

Print quality

Khoshnevis et al [33] referred to the properties of a printed layer such as surface quality and dimensional conformity/consistency, when using a specific printing mixture. A printing mixture could be considered acceptable When the three following requirements are satisfied:

1. The printed layer must be free of surface defects, including any discontinuity due to excessive stiffness and inadequate cohesion.

2. The layer edges must be visible and squared (versus round edges).

3. Dimension conformity and dimension consistency must be satisfied by printed layer.

Hardened state properties and performance

Wangler et al [40] noted that the specifically adjusted material compositions as well as the characteristics of the various digital fabrication processes have such an influence on the hardened state properties that the performance of the printed objects in-use is not a trivial issue. Regarding the materials, noteworthy deviations from conventional concrete include the use of high ratios of cement and alternative binders, chemical admixtures such as retarders, accelerators, and viscosity modifiers, as well as a lack of normal and large size aggregates (aggregates larger than approximately 2mm are rarely used). On the process side, the filament deposition, the pressure versus print nozzle speed, the formation of distinct layers, the lack of compaction as well as the incompatibility with traditional reinforcement strategies, are some of the remarkable differences to the well-known casting process. Duballet et al [13] suggested that as printable Materials are often accelerated in order to improve their ability to quickly build up a structure, some increase in temperature resulting from this increase in chemical activity can be expected. This may lead to increase of a drying rate and make these printable Materials extremely sensitive to the external environment (temperature and humidity) or to the so-called printing environment.

Anisotropy and interlayer bonding

The anisotropy of printed concrete has already been pointed out in an early stage by Le et al [25]. Who found that both the compressive and flexural-tensile strength were directionally dependent. Other studies resulted in similar findings: perpendicular to an interface the tensile strength is lower than in the other directions [49]. Wolfs et al [41] suggested that the cohesion was found to be a linear function of time, and the angle of internal friction independent of age, within the time frame of a typical printing process. Khoshnevis et al [50] assumed that high structuration rates could lead to so called "cold joints" and weak interfaces between layers. Roussel [12] suggested that the waiting time between layers and/or thixotropy increase layer cohesion in direct proportion. Chen et al [21] suggested that the presence of air voids appears to be an important reason for weak interlayer bond strength and anisotropy of printed cementitious materials. The air voids in 3D printed samples can be quantitatively characterized using optical image scanning and X-ray computed tomography. Chen et al [21] noted that next to the effect of material compositions, printing parameters, i.e., time intervals, nozzle standoff distances, printing environmental conditions, and nozzle types, can also affect the interlayer bond strength of printed cementitious materials. The current strategies for enhancing interlayer bonding can be summarized as increasing the contact area (for instance by interlocking), and the adhesion between layers.

Reinforcement

Comparing to standard monolithic reinforced concrete structures, those fabricated of printable cementitious mortars are inherently brittle. Their failure behaviour is characterized by a low ratio of tensile to compressive strength, and low ultimate tensile strain compared to their fracture strain. To facilitate safe structural behaviour, technological and design approaches from conventional concrete construction are being adapted and new innovative strategies are being developed [51].

Scripting

Majority of projects use modeling and slicing framework based on Rhinoceros and Grasshopper. In the Rhinoceros CAD software environment [52] with the built-in plugin for parametric design Grasshopper, various plugins were developed thanks to a large community of developers, integrating CAM technologies into the design. To generate GCodes for 3D printers, tools incorporated in Grasshopper core using custom text generation can be used as for clay printing [17]. 3D printing plugins such as Silkworm [53] or HAL [15], enabling generation of robot control scripts directly from 3D models are also an option.

During the elaboration of the thesis, two plugins for Grasshopper were published by the Concre3Dlab team at Ghent University, allowing FEM simulation of the model behaviour during the 3DCP to be included in the design process. VoxelPrint can transform any three-dimensional shape into a set of identical finite elements and produce ready-to-use Input files for simulation in ABAQUS. The term 'voxelization' is to describe the process of transforming a random 3D shape into a set of 3D unit cubes (voxels). The main contribution of this plug-in is providing an extensive, yet easy-to-

use plugin to be used by both non-experts (e.g. architects and designers that are familiar with the parametric toolbox that is provided by Grasshopper) and more advanced users (that can experiment with the broad range of input parameters in an attempt to optimize their print design). The core component generates .INP files for ABAQUS; and is based on state-of-the art numerical methods for simulation of concrete printing [54]. In CobraPrint plug-in, a structured mesh is generated by sweeping a cross-section of the printed concrete layer along the print path. This mesh discretization is realized by a custom Grasshopper code; by first dividing the print path into several segments, and projecting vertices tangential to the path and in the z-direction. By careful parametrization, the approximate size of the mesh elements along the path can be used as an input. The final FE model contains a number of meshed layers, divided into segments, which toolpath are, similar to the previous method, activated sequentially to simulate the printing process. Using the Abaqus Model Change command, the new sets of elements are activated step by step. In this method, the transformation from the 3D-printed structure to the FE mesh is much more accurate and even allows for bevels on the layer's edges. However, attention must be paid to the minimum curvature of the print path in order to avoid intersecting neighbouring elements. Also, layer contact is much more difficult to model, as all intersecting elements must be determined beforehand [44].

Origins

The first concept of using the cement-based additive technology for rapid fabrication of large-scale building elements was firstly published by Pegna in 1997 [55]. He used layered fabrication of steamed Portland cement over a layer of silica matrix material to create 76/140/76 mm H-O shaped specimen. The resulting material was denser than regular cast concrete and had a similar compressive strength. First large-scale 3D printing technology, based on extrusion deposition was developed by the team of B. Khoshnevis at the University of Southern California (USC) under the name Contour Crafting (CC) [56]. CC is an additive fabrication technology that uses computer control to exploit the superior surface-forming capability to create smooth and accurate planar and free-form surfaces. Several CC machines were developed at USC to research fabrication with various materials including thermoplastics, thermosets and various types of ceramics [Fig.6]. These machines include a XYZ gantry system, a nozzle assembly with three motion control components (extrusion, rotation and trowel deflection) and a six-axis coordinated motion control system [57].

Further development resulted in advanced printing head with 3 extrusion nozzles and incorporated surface smoothing trowels to create walls with internal zig-zag structure. First prototype of concrete wall made by Contour Crafting technology was presented in 2005 [58]. 3D printing technology named Mega-scale rapid manufacturing for construction became the subject of research at Loughborough University in 2005 [59]. Its concept under name the Concrete Printing technology and was firstly described in 2009 [60] [Fig.7]. In 2014, Chinese company WinSun used their own 3D printing technology similar to Contour Crafting, to make buildings of 3D printed concrete prefabricates [2] [Fig.8].
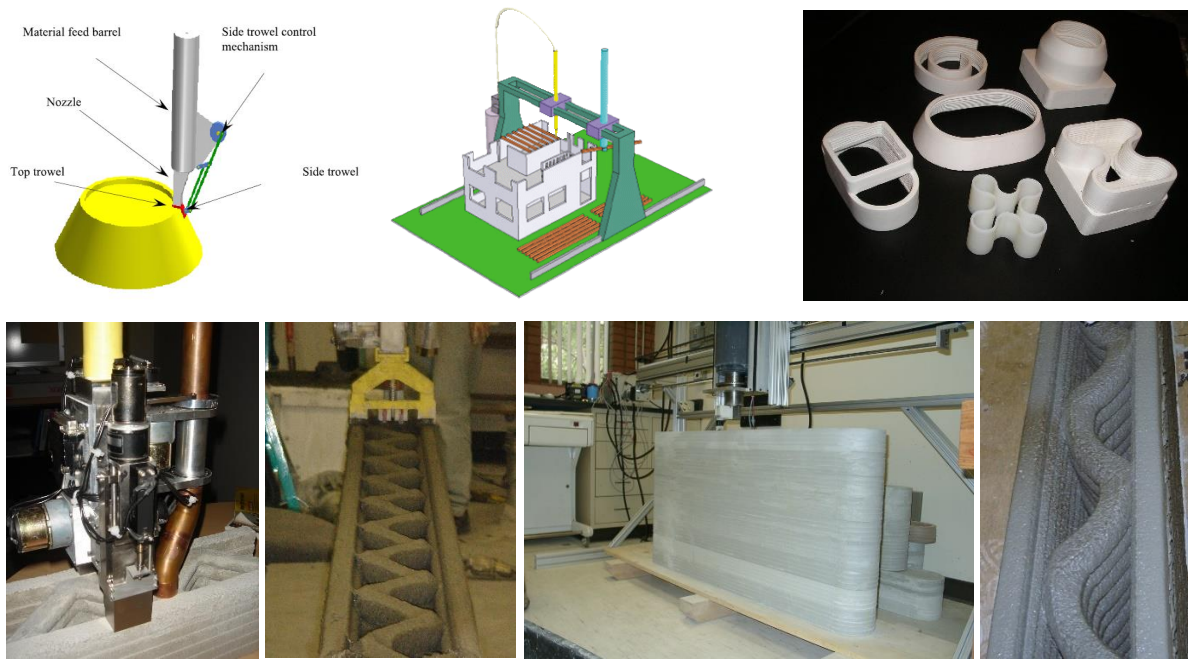
Fig.6. 3D printing by Contour Crafting, USA
a) The extrusion assembly with top and side trowels. B) Residential building construction
c) Various prints d) CC Printhead e), f), g) Examples of concrete walls made by CC

Fig.7: 3D printing at Loughborough University, UK
a) Gantry 3D printer b) Printhead c) 3D wall section with the team

Fig.8 : 3D printing at WinSun, China a) 3D printed wall prefabricates b) Final assembly of walls
c) 5 story residential building made of 3D printed wall prefabricates

In Holland, the CyBe Additive Industries company started working on the development of concrete 3D printing technology in 2013 [Fig.9]. Their original 3D printer ProTo R 3DP with a range of 3.150mm was first printer in history to be based on 6-axial robotic arm. They also developed original cement-based mortar [61]. CyBe

technology allowed printing at speed of 175mm/sec while using a printhead with extrusion nozzle 30mm x 30mm to make a 30mm layers. In 2014, the founder of Total Kustom company [62] Andrey Rudenko presented 3D printed mini castle and in 2016 pictures of printed ground floor of a hotel in Phillipines in progress [63] [Fig.10]. In 2015, a unique concrete printing facility with a build space of 11 by 5 by 4 meters was commissioned at Eindhoven University of Technology (TUe) [48] [Fig.11]. This gantry 3D printer, built by Dutch company ROHACO, featured a build space of 11 by 5 by 4 meters. It costed about 650,000 euros and was financed by ten companies and the university [64]. Since 2012, the number of projects of 3D printing in architecture including 3DCP has started exponential-like growth as demonstrated on infographics made by Langenberg in 2015 [65].
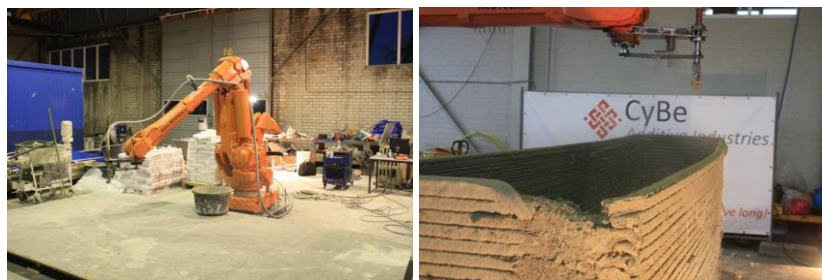

Fig.9. 3D printing at CyBe, Netherlands a) Printing setup b) 3D printed wall

Fig.10. 3D printing at Total Kustom, USA
a)Printing process b) Printed parst of a castle c) 3D printed hotel in Phillipines in progress

Fig.11: 3D printing at Tue, Netherlands
a) Gantry 3D printer b) Printhead c) 3D printed wall detail

3. BASIC ASSUMPTIONS

Chapter 2 summarised the current knowledge of 3DCP technology, i.e. printing strategies, materials, testing, machinery, scripting methods, as well as case study

examples. This technology is very different from conventional methods for the realization of concrete structures due to the use of robotic production equipment, the need to ensure the stability of the structures during the maturation of the material other than by formwork, and the different static properties of the resulting elements. The specificity on the material side is mainly due to the contradictory requirements for its properties at different stages of the printing process, resulting in a specific mix composition. In order to achieve thixotropic behaviour, a high proportion of fine particles and chemical additives are included in the formulations, which affects the resulting shrinkage and the price of the mixtures. The production technology itself is also very demanding with regard to the continuous production, pumping and deposition of homogeneous material, the properties of which change over time. Also crucial to the efficiency of the process is the ability to assess the printability of individual objects before the actual printing begins and the ability to flexibly modify the models.

On the basis of these aspects, it can be concluded that 3DCP technology requires mastering a spectrum of very complex engineering tasks, to adopt and put into practice, it is necessary to further develop the existing research potential. It is questionable to what extent the presented solutions and methods are illustrative in a situation where a number of hitherto neglected external and internal variables and boundary conditions on the side of material, technology and human operator factors enter the model. The current 3DCP technologies are, according to available information, still very sensitive to changes in these conditions, so the robustness of the whole technology, necessary for application in real conditions, remains a big question. The compatibility of materials and production technologies needs to be verified, especially in the area of mixers and pumps. Also critical to the successful mastery of the technology is the incorporation of environmental influences into the printing process, which is a challenge especially for on-site printing. The question is to what extent it will be possible to control the material properties and printing technology in such a complex process to avoid quality defects in the prints. In the field of printing design elements, it will thus be necessary to find a suitable quality control process to take into account the variations in external and internal variables and boundary conditions. During his study of 3D printing technology, the author asked himself whether this technology could be used for custom architectural elements of complex shapes of high quality.

Therefore, the following questions were posed by the author in the context of this thesis:

- Is there a sufficiently robust concrete 3D printing technology to be applied in real production conditions? If so, what are the requirements for its applicability?
- What are technology constraints to achieve consistent high print quality?
- What printing material, in combination with the production equipment, will enable stable production quality without failures and quality fluctuations?
- Can the printing material be an alternative to conventional concrete, which has a significant carbon footprint but is a relatively cheap and technologically robust material?

- What is the feasibility and realism of using material alternatives using raw materials with lower carbon and energy footprints or waste materials such as fly ash to increase sustainability in construction?
- According to the research, most 3D printing technologies are based on modelling and slicing in Grasshopper. Is this application flexible enough to be used in real production where the technological and economic parameters of production also need to be modelled?
- Is it realistic to print elements of thickness of 20 to 30 mm to allow manual assembly and handling of components in interiors?
- What will be the durability of such thin prints in terms of structural performance, allowing safe use in interior and exterior design and artwork?
- What will be the durability of printed elements in exteriors exposed to the weather?

The fundamental question of this thesis was: "To what extent the previous questions can be answered in terms of commercially applicable 3D printing?"

4. OBJECTIVES

In 2015, when the author was looking for answers to the above questions, there were no projects or experts in this field in the Czech Republic, from which the author could draw information to refine the topic of the thesis. The only sources were foreign literature and media. In order to understand the nature of a multidisciplinary technology such as 3DCP, it was necessary to acquire knowledge from many disciplines that had been lacking so far. It was also necessary to build the missing facilities to enable serious research on 3DCP technology and materials.

The objectives of the thesis were therefore as follows:

- To develop a printing material enabling stable print quality.
- Finding suitable test methods to verify the properties of printing materials.
- Specification and eventual in-house development of material preparation and pumping equipment to enable stable print quality.
- Development and construction of 3D printer and print head including control system.
- Design of suitable 3D models of architectural prefabricates.
- Development of control scripts to ensure the transfer of 3D models to production equipment.
- Development of 3D printing technology for the production of architectural prefabricates.
- Conducting case studies.

5. METHODS

5.1. Definition of technology and material parameters

Due to the novelty of the 3DCP technology, no printing machinery, scripts, material or test apparatus and procedures were available on the Czech market at the time of the work. Part of the machinery could be provided on the market and adapted for 3D printing purposes, while the key components of the system, i.e. nozzle, 3D printer, material and scripts had to be developed as part of the project.

Due to spatial and transport limitations inside the faculty building and also limitations on manual handling of printed objects, the maximum size of prints was defined at 1000 x 1000 x 1000 mm. The weight of the printed elements was further defined to be in the range of 5 to 180 kg. This size makes it possible to verify the basic parameters of the technology on the printing of design prefabricates, which can then be manually assembled on the construction site into dimensionally unlimited objects. After defining the size of the printed objects, it was necessary to define the parameters of the layers. Printing the design prefabricates in an exposed concrete quality requires the ability to capture the fine details of the designs, which results in the requirement for the finest possible print resolution and therefore the smallest possible print layer size. In addition, thin layers also generate lower weight prints and therefore make them easier to handle. At the same time, however, the width of the layers must be adjustable within a certain range to allow the formation of stable structures of different sizes and shapes, i.e. buildability. For the sake of structural stability of the layers during printing, it was chosen that the width of the layers would be 15 to 32 mm and the height of the layers would be from 5 to 10 mm, so that the ratio $w/l = 3/1$. The range of layer widths w was designed at 15, 18, 22, 25, 32 mm, the range of layer heights l at 5, 8, 10 mm. The author has introduced layer marking in the format w/l, i.e. e.g. 25/8. The nozzle diameter in the range of 10 to 25 mm was chosen to fit this parameter. The nozzle diameter then defined the requirements for the material properties in terms of extrudability.

The properties governing extrudability for a given nozzle geometry can be determined by the material properties, primarily the material grain curve, maximum grain size and consistency. For the purpose of the 3DCP by extruding material from the nozzle, it was necessary to design a material that could be extruded without the risk of nozzle clogging by material grain buckling. A nozzle value of /5 was chosen as the limiting value, i.e. a maximum grain size of 2 mm, which also introduced a coarser particle content into the mixture and thus the assumption of lower shrinkage. This parameter narrowed the field of materials to special cement mortars and composites, and concrete printing was not considered further due to the standard requirement for grain size content of 4 mm [66].

The workability and open-time values of the mixes also had to be determined as part of the work. These are defined by the author with regard to design requirements as the time interval when the material will be capable of pumping, extruding and forming layers achieving stability and high quality without obvious defects such as cracks or profiling.

Furthermore, it was necessary to define a way to ensure buildability to maintain the shape and stability of the printed layers during the printing process, when the bottom layers are stressed. Conventional cementitious binder setting time is not fast-enough for the needs of 3D printing of elements with layer lengths in order of meters. An option to reduce the hydration time is to use a hardening accelerator. Hardening accelerators based on alkaline reactive inorganic salts are commonly used, which, at a sufficient dosage, can provide a set-up time of just a few seconds. The use of an accelerator directly in the mixture significantly reduces the workability and open time of the mixture. It is therefore advisable to combine it with continuous mixing and pumping technology, which ensures a constant supply of material with the same degree of consistency while minimising the risk of the mixture solidifying in the mixer or hose. This solution seemed ideal for the actual 3D printing technology. Therefore, a key factor in defining the rise time of the material solidification was the definition of the parameters of the mixing technology and material transport to the nozzle. To facilitate this task, it was planned to use a continuous mixer in combination with a pump. To determine the volumetric output of both the mixer and the pump, it was necessary to determine the volumetric output of the printer. A calculation was made based on the maximum and minimum layer dimensions and the nozzle speed, given by the maximum nozzle holder speed in the proposed printer.

Tab.1. Calculation of the volumetric capacity range of the pump

	Layer width w	Layer height l	Nozzle velocity v	Nozzle profile A	Q
units	mm	mm	m/min	mm^2	l / min
max	32	10	6 000	320	**1,92**
min	15	5	6 000	75	**0,42**

The maximum horizontal speed of the nozzle movement was chosen to be 100 mm/s, i.e. 6000 mm/min. The vertical speed, which determines the speed of passage between layers, was limited to 600 mm/minute, which is 10 mm/s, i.e. with a layer height of 5 to 10 mm, the passage between layers takes a maximum of 1 second, which is sufficient for printing purposes. From these data, the pump output was determined to be Q_{max} = 1.92 l/min and Q_{min} = 0.42 l/min [Tab 1]. These parameters were subsequently used as the basis for the printer design in the subsequent part of the thesis.

From this calculation it is clear that the pump supplying the printing mortar to the nozzle must be capable of a very small output in the range of 0.42 to 1.92 l/min, which corresponds to a mass output of 1 to 5 kg/min at a bulk density of 2.5 kg/l.

In order to find a suitable machine, a research of continuous mixers was first carried out. All available types are designed for the preparation of plaster, mortar or concrete for flooring, plastering or masonry purposes. The output of these mixers is also set for this purpose, reaching tens of litres per minute [Tab. 2] The smallest STROBL Stromixer D 1000 has a volumetric output of 15 l/min, i.e. 35 times the required minute output. This mixer would produce 37.5 kg of wet mix per minute, which would have to be consumed before the open time expires, greatly reduced using a solidification accelerator. This seemed unworkable for the printing needs of 5

to 150 kg elements. In addition, inline mixers were also investigated in which mortar preparation is combined with mix pumping, where the volumetric output is an order of magnitude lower compared to continuous mixers, reaching 1.5 l /min in the case of the PFT Ritmo M machine, and even reducing to zero in the case of the PFT Bolero machine according to the manufacturer's data [Tab. 3]. This output is already usable for the purpose of 3D printing layers of the above parameters. However, in the course of this work it became clear that these machines have one major character that made it impossible to use them for the purposes of this work. The technology of the machine mixers and also the continuous mixers is adapted for mixing industrially produced dry mixtures with water, fed from the water line via a valve. It therefore does not allow the gradual addition of individual liquid or solid components, which later proved to be a limiting factor for the purposes of experimental testing of tailor-made materials under development. These technological limitations, together with the aim of extending the workability time of the mixture and eliminating the risk of material solidification in the conveyor path if the printing process had to be interrupted, it was decided not to add the accelerator directly to the mixture.

The most advantageous solution to this situation seemed to be to ensure that the mixture solidifies by hydrating the cement at the end of this path directly in the nozzle, similar to shotcrete technology. This solution makes it possible to maintain the workability of the mix in the high tens of minutes, similar to conventional mortars or concretes. Unlike shotcrete, 3D printing does not involve transporting the material and mixing it with compressed air, but simply by extrusion. In the field of machine extrusion of mortars, no such solution was available on the Czech market at the time of the work. The costs and time required for the development of the mixing nozzle in the form of an advanced press head were unknown to the author and it could not be excluded that its development would be beyond the technical and financial capabilities of the author and his workplace and thus could significantly slow down this research project and jeopardize the completion of the work.

It was therefore necessary to find another solution. A review of published materials for 3D printing showed that such a solution was possible by using one component (1K) mixtures, providing solidification by thixotropy. It was therefore decided to focus on printing from a single component mixture where buildability is ensured by thixotropy of the material in the nozzle without the need of adding an accelerator. For 1K mixtures, similarly to mixtures with accelerator, the workability and open time of the material is defined due to the time required to work with the material.

The processing time for this material was chosen by the sum of the time required for material preparation 10 minutes, the time for tuning the pumping and printing technology 5 minutes and the open time i.e. the printing time itself 15 minutes, i.e. 30 minutes in total. During printing, the layers should be fully bonded, i.e. cold joints between layers should be eliminated. To fully bond the layers, it is necessary that the new layer is laid before the previous layer has set, i.e. before the open time is reached. Open time thus defines the maximum printing time of one layer and thus its maximum length. With a printing time of one layer equal to the open time, i.e. 15 min and a nozzle speed of 6 000 mm/min, the maximum length of one layer is 90 m, which roughly corresponds to a layer width of 11 mm when the printing

area of the printer is fully filled with 1000 x 1000 mm. The minimum layer width was previously chosen to be 15 mm for technological reasons, which allows the print area of 1000 x 1000 mm to be filled with a layer length of 66.6 m, so we are on the safe side in terms of maximum layer length.

In this part of the work, it was not clear to what extent the buildability principle based on a thixotropic 1K compound would be limiting, especially when printing objects with overlapping and low wall angles. The author wondered if with a 1K compound in combination with a given material preparation and pumping technology it would be possible to solve the buildability problem and achieve high quality layers. This is further verified experimentally in the following part of the thesis.

5.2.   Material

5.2.1. Material components

CEM I 42.5 R (hereinafter referred to as CEM ČM) (producer Českomoravský cement, a.s. branch Radotín) [29]

It is high quality Portland cement with a rapid increase in strength and a rapid and high development of hydration heat. It was supplied from the HORNBACH hobby market in 25kg paper bags.

Tab.2. Compressive and flexural tensile strength of CEM ČM

Compressive strength [MPa] EN 196-1	1 day	2 days	7 days	28 days	56 days	90 days
	16	30,2	50	59,5	64	66
Flexural tensile strength [MPa] EN 196-1	1 day	2 days	7 days	28 days	56 days	90 days
	4.0	5,9	8	9,4	9,4	9,4

Tab.3. Physical and mechanical characteristics of CEM ČM

Parameter	Units	Values	Reference method
Normal consistency	%	28,4	EN 196-3
Onset of setting	min	199	EN 196-3
End of setting	min	280	EN 196-3
Volume stability	mm	1.4	EN 196-3, Le Chatelier
Specific surface area	$m^2.kg^{-1}$	364	EN 196-6, Blaine
Specific gravity	$kg.m^{-3}$	3150	EN 196-6
Bulk density in silo	$kg.m^{-3}$	1200-1600	EN 196-6

CEM I 42,5 R (hereinafter referred to as CEM EX) (producer CEMEX, a.s., Prachovice) [67]

It is high quality Portland cement with a rapid increase in strength and a rapid and high development of hydration heat. It was supplied from DEK construction stores in 25kg paper bags.

Tab.4. Physical and mechanical characteristics of CEM EX

Parameter	Units	Requirements of EN 197-1	Average values achieved
SO$_3$ content	%	max. 4,0	2,6 – 3,2
Cl content	%	max. 0,1	0,03 – 0,09
Volumetric stability	mm	max. 5%	3,5
Hardening onset	minutes	max. 5%	0,5
Loss on ignition	%	max. 10	0 – 1,5
Insoluble residue	%	min. 60	190 – 240
Compressive strength 2 days	MPa	min. 20	28 – 36
Compressive strength 28 days	MPa	42,5 – 62,5	53 – 59
Specific surface area (Blaine)	cm2.g-1	not applicable	3200 – 3800

Sorfix (producer and supplier: ČEZ Energetické produkty, s.r.o.) [68, 69]

Sorfix is a composite dry material based on a salt-free hydraulic binder. As an admixture, it improves the strength of concrete and resistance to water seepage. It was developed in cooperation between the Czech University of Chemical Technology, the Czech Technical University and ČEZ Energetické produkty s.r.o. Waste materials from coal combustion are used for its production, while it is linked to the production of clean resources, so the ash for the production of the binder must not be contaminated with anything after the combustion process. Despite the diversity of ashes from multiple sources, Sorfix binder achieves long term stable. Physical and mechanical properties, this is achieved by the optimal composition and homogenization of at least three components, the ash from the first source, the ash from the second source and the activator. It has been proven that for every 1% replacement of CEM I 42.5 R with Sorfix, an increase in the amount of water by 0.17 %. Sorfix was supplied in a 1 m^3 big bag.

Tab.5. Chemical composition of the binder Sorfix

Component	SiO$_2$+ Al$_2$O$_3$	total CaO	free CaO	SO$_3$	MgO	Na$_2$O	K$_2$O	Cl-
Content (%)	50 – 70	15-30	8 – 20	5 – 10	< 1,5	< 0,5	< 1	<0,05

Tab. 6 Chemical elements in aqueous leachate of the binder Sorfix

	pH	Chloride	Fluoride	Sulphates
Value	11-13	< 4 mg/l	< 0,3 mg/l	< 15 mg/l

Tab.7. Compressive and flexural tensile strength of the binder Sorfix

Compressive strength [MPa] EN 196-1	2 days	7 days	14 days	28 days	60 days	120 days
	12.3	39.0	37.7	42.5	52.4	53.1
Flexural tensile strength [MPa] EN 196-1	2 days	7 days	14 days	28 days	60 days	120 days
	1.6	3.3	5.5	6.1	6.2	6.3

Tab.8. Physical and mechanical characteristics of the binder Sorfix

Parameter	Units	Values	Reference method
Normal consistency	%	45	EN 196-3
Onset of setting	min	123	EN 196-3
End of setting	min	190	EN 196-3
Volume stability	mm	< 0.15	EN 196-3
Specific surface area	cm^2/g	8500 − 9500	EN 196-6, Blaine
Specific gravity	$kg.m^{-3}$	2800 ± 100	EN 1097-6, 7
Bulk density	$kg.m^{-3}$	< 690	ČSN 72 2071
Shaken bulk density	$kg.m^{-3}$	< 850	ČSN 72 2071
Loss on annealing	%	< 4	ČSN 72 0103

Tab.9. Granulometry of Sorfix [69]

Granulometry	d20	d50	d75	d97
Grain (µm)	< 5	< 25	< 65	< 250

Ground limestone (hereinafter ref. to as GLS), (producer KRVAP Kunčice, a.s.), [70]

Very finely ground limestone, class V − VI, 5600, grade No. 10 (grade B) acc. to ČSN 72 1217 and ČSN 72 1220. It was supplied from ZZN store in 20kg paper bags.

Tab.10. Granulometry of GLS

Residue on the nets	Net 0,50 mm	Nets 0,071 mm
Grain (µm)	approx. 1 %	18 − 30 %

Tab.11. Chemical composition of GLS

Component	$CaCO_3$	$MgCO_3$	SiO_2	Al_2O_3	Fe_4O_3
Content (%)	88 − 94 %	2 − 6 %	1.5 − 6 %	0.7 %	0.2 %

Microsilica MasterLife MS 120 D (supplier Master Builders Solutions CZ s.r.o.) [71]

Admixture for screeds, mortars and concrete made of fine, amorphous silica powder SiO_2. The main field of application is therefore concrete demanding strength, chemical resistance and durability. Due to the considerable specific surface area of the microsilica of about $20m^2/g$ and its glassy nature, the reaction with $Ca(OH)_2$ resulting from the hydration of the cement is very intense.

Tab.12. Physical characteristics of MS 120 D

Appearance	Grey powder, compact
Bulk density	500—700 $kg.m^{-3}$
Chlorides content max.	≤ 0,3 % of weight
Alkali content	≤ 1,0 %

The recommended dosage is between 2-15% by weight of cement. It was supplied in 25kg bags.

Quartz flour ST 6 (hereinafter referred to as ST 6), (producer Sklopísek Střeleč, a.s.) [72]

Micromilled sand (quartz flour) is produced by dry grinding in a non-ferrous environment and sorting using wind classifiers. It was supplied in 25kg paper bags.

Tab.13. Physical characteristics of ST 6

Parameter	Units	Values
Grain size range	mm	0.045−0.00 1
Medium grain size (d50)	mm	0.016
Specific surface area	cm^2/g	3 760
Bulk density	kg.m^{-3}	2 650
Moisture content	%	0.2 max
pH	-	7.2
Mohs hardness	-	7

Tab.14. Chemical composition of ST 6

Component	SiO$_2$	Al$_2$O$_3$	NaO+KO	CaO+MgO	Fe$_2$O$_3$
Content (%)	99,6%	0,2%	0,1%	0,1%	0,05%

Fine sand ST 53 (hereinafter referred to as ST 53), (prod. Sklopísek Střeleč, a.s.) [73, 74]

Quartz sand from Střeleč, it is a treated natural raw material. It was supplied in 50kg paper bags.

Tab.15. Physical and chemical characteristics of ST53

Parameter	Units	Values
Grain size range	mm	0,10 − 0,63
Medium grain size (d50)	mm	0,27
Bulk density	kg.m^{-3}	2 650
Moisture content	%	5 − 8
SiO$_2$ content	%	99,2

Technical sand ST 06/12 (hereinafter ref. to as ST 06/12), (producer Sklopísek Střeleč, a.s.), [75, 76]

Tab.16. Physical and chemical characteristics of ST06/12

Parameter	Units	Values
Grain size range	mm	2.00 − 0.63
Medium grain size (d50)	mm	0.93
Specific surface area	cm^2/g	-
Bulk density	kg.m^{-3}	2 650
Moisture content	%	0.2 max
pH	-	7.2
Mohs hardness	-	7
SiO$_2$ content	%	99,2
Fe$_2$O$_3$ content	%	0.03

ST 06/12 is treated natural quartz sand from Střeleč. It was supplied in 25kg PP bags.

MasterFiber 006 (hereinafter referred to as MF006), (producer and supplier Master Builders Solutions CZ s.r.o.) [77]

It is a polypropylene single hair microfiber for concrete EN 14889-2. It is mainly used in industrial floor construction and for fire protection. It can significantly reduce the risk of early shrinkage cracks. Adhesion of water on the fibre surface slows down the process of drying and concrete strength can develop faster than stresses from shrinkage. Length of fibre is 6 mm ± 10%. The bulk density is 0.91kg/dm^3. It has a straight shape in longitudinal direction, round in cross section, with diameter 34 μm. The recommended dosage is 0.6-3.0 kg/m^3 of fresh concrete. According to the manufacturer, these technical data are the result of statistical surveys and do not represent guaranteed minimum values. MasterFiber 006 can be mixed both in the concrete batching plant, where a mixing time of 90-120 seconds is recommended after the fibres have been added, and in the on-site mixer, provided sufficient time is allowed for the fibres to disperse perfectly throughout the mixing batch (mixing time in the mixer is about 5 minutes). It was supplied in 1kg paper bags.

MasterGlenium ACE 430 (hereinafter referred to as PCA), (producer and supplier Master Builders Solutions CZ s.r.o.) [78]

It is a super plasticizing additive based on polycarboxylate ether. The molecular structure causes a significant increase in the free surface area of the cement particle for hydration reactions. This is followed by very rapid absorption of the molecule onto the surface of the cement particle and an effective dispersion effect (electrostatic stabilization). The consequence of these reactions is an early hydration reaction. The resulting hydration heat is efficiently utilized and leads to a high increase in initial strengths. It allows the production of concrete with very low v/c values, especially for obtaining durable concrete with high initial and final strengths. The use of MasterGlenium ACE 430 is not limited by the required consistency class of the concrete. The admixture allows the production of concretes with consistency grades F1 – F6 and is suitable for production of self-compacting concretes. The bulk density at +20 °C is 1.06 ± 0.02 g/cm3. The pH value at +20 °C is 5.5 ± 1.0. Chloride content is max. 0.1 % by weight. The recommended dosage is 0.3 % - 1,0 % by weight of cement. For the purpose of the project, it was supplied in 20 kg plastic canisters or 1 kg bottles.

Master Matrix SDC 100 (hereinafter referred to as VMA), (producer and supplier Master Builders Solutions CZ s.r.o.) [79]

It is a highly effective viscosity modifying admixture for liquid concrete. It is an aqueous solution of a high molecular weight synthetic copolymer. Thanks to its targeted mechanism of action, MasterMatrix SDC 100 affects the viscosity of the mix, ensuring the right balance between the fluidity of the mix and its resistance to segregation – apparently opposing properties. It ensures economically and ecologically advantageous saving of fine particles (< 0.125 mm). The bulk density at +20 °C is 1.0-1.02 g/cm3. The pH value at +20 °C is 9 ± 1.5 after production. Chloride content is max 0.1 % by weight. The recommended dosage is 0.1-1.5 % by weight of fines. MasterMatrix SDC 100 is compatible with all types of cements. The rheological properties of MasterMatrix SDC 100 are optimally influenced by the simultaneous use

of the superplasticizer MasterGlenium. MasterMatrix SDC 100 prevents segregation and bleeding, can be used with all types of cement, does not affect the onset of setting and makes the mix less sensitive to changes in the amount of water added. It was supplied in 20 kg plastic canisters or 1 kg plastic bottles.

MasterRoc HCA20 (hereinafter referred to as HCA), (producer and supplier Master Builders Solutions CZ s.r.o.) [80]

It is a liquid ingredient that, when added to wet or dry concrete, completely stops the hydration process by forming a protective barrier around the cement particles. The bulk density at +20 °C is 1.09 g/cm^3 ± 0.02. The recommended dosage is 2 − 33 ml/kg of cement, i.e. 0.2 − 2% of the weight of cement, the dosage of which should lie in the range of approximately 400 − 460 kg. The approximate dosage according to the effects is 0.6 % for 3 hours of stabilisation or 2,0 % for 72 hours of stabilisation. The exact dose should be determined by test. It is possible to control the hydration effect of MasterRoc HCA 20 for all types of cementitious minerals (C3S, C3A, C2S, C4AF, gypsum). When wet spraying concrete, the aggregate is mixed with cement and half of the amount of mixing water. HCA 20 and a superplasticizer (e.g. MasterGlenium) are then added with stirring and the mixture is mixed with the other half of the mixing water. Normal concrete mixing time is quite sufficient. It was supplied in 20 kg plastic canisters or 1 kg plastic bottles.

MasterKure 220WB (hereinafter referred to as Kure 220WB), (producer and supplier Master Builders Solutions CZ s.r.o.) [81]

It is a protective spray in the form of a milky white liquid for retarding evaporation from the surface of concrete structures. It forms a non-degrading protective film on the surface, preventing water evaporation during the most important hydration phase. Bulk density (+20 °C) is 1.00 g/cm^3, application temperature > + 5 °C. Recommended dosage is 150 to 200 g/m^2 for unpolished surfaces. It was supplied in 1 kg plastic bottles.

MasterFlow 3D 100 (hereinafter referred to as Flow 3D 100), (producer and supplier Master Builders Solutions CZ s.r.o.) [82]

MasterFlow 3D 100 is a hydraulic prefabricated one-component mortar for 3D printing. It has very low shrinkage and is volume stable. When mixed with water, it forms a well-pumpable mortar that achieves high compressive and flexural tensile strengths (depending on w/c) in a short time interval. The maximum permissible temperature of the application mortar is +32 °C.

For small volume quantities MasterFlow 3D 100 can be mixed using a paddle mixer, but test applications should always be carried out to assess the effectiveness of the mixing process and equipment. The mixing process may vary depending on the mixing equipment used; however, it is advisable to start by pouring 80% water into an empty mixing vessel and then adding MasterFlow 3D 100 while stirring continuously for 1 minute. Add the remaining water, keep stirring and continue stirring for another 3 minutes. For larger quantities use high speed colloid mixer (1400 rpm), agitator and pump. Pour all necessary water into the mixer and add the mixture in a controlled manner so that no lumps form. Continue mixing for about 3 minutes from the time

you add the mixture. If you stir for a longer period of time, the temperature could rise significantly, and the product would begin to solidify prematurely. When mixing is complete, pass the application mortar into the agitator through a sieve with 2mm holes, the mortar should not remain in the agitator for more than 30 minutes. In most applications, MasterFlow 3D 100 should be pumped by a membrane or piston pump or other special pump for mixtures cement-based mixtures. The pump chosen should provide an uninterrupted supply of application material. The pump should be equipped with a pressure limiter to prevent pressure exceeding 2 MPa. Shelf life is 6 months when stored in a cool, dry environment.

*Tab.17. Physical and mechanical characteristics of Flow 3D 100 (** Values achieved under laboratory conditions: Temperature +23 °C and 50% RH)*

Parameter	Units	Values
Intake of mixing water	ml/kg	156
Max grain size	mm	0.5
Volume change in 24 hours	%	+0.8
Bulk density of hardened mortar	$kg.m^{-3}$	2000-2200
Compressive strength after 8 h**	MPa	min. 1 MPa
Compressive strength after 1 day**	MPa	min. 25
Compressive strength after 28 days	MPa	min. 50
Flexural tensile strength after 1 day	MPa	5
Flexural tensile strength after 28 days	MPa	6.5

Sikacrete 751 3D (producer and supplier SIKA CZ, s.r.o.), [83]

Sikacrete 751 3D is a 1-part micro-concrete for use with 3D robot or gantry printers. It contains Portland cement, selected aggregates and additives. Maximum grain size is ~2 mm.

For small volume quantities it can be mixed with an electric single or double paddle mixer (<500 rpm) or using a forced action mixer capable of mixing 2 to 3 bags at a time. Add the recommended amount of clean water in a suitable mixing container. Stir slowly, add the powder to the water and mix thoroughly for a minimum of 3 minutes. Add more water during the mixing time if necessary to the maximum specified amount to achieve a smooth consistent of mix. If necessary and before pumping, let the material stand to allow the air bubbles from entrained air to finish. Stir gently if required. Shelf life is 9 months minimum from date of production. Pumping and printing is usually a continuous process. The application specifics of the extrusion and printing speed must be optimised between the mixer, pump, pump line length and printer head. Keep pump lines wetted and cool. Condition the material between 15°C and 25°C for a minimum 24 hours before use. Use warm water at low temperatures and cold water at high temperatures to maintain application performance. Condensation due to certain curing methods and curing agents may cause some discoloration to the surface appearance.

Tab.18. Technical and application information on Sikacrete 751 3D [83]

TECHNICAL INFORMATION

Compressive Strength	+25 °C W/P = 0.14 (3.5 L water per 25 kg bag)	1 day ~20 N/mm²	7 days ~40 N/mm²	28 days ~50 N/mm²	(EN 196-1)
Tensile Strength in Flexure	~7 N/mm² (28 d / 25 °C)				(EN 196-1)
Water Penetration under Pressure	~20 mm				(EN 12390-8)
Service Temperature	+100 °C max.				

APPLICATION INFORMATION

Mixing Ratio	14 – 16% water (by weight of powder)
Fresh Mortar Density	~2,20 kg/l
Yield	~12 litres per 25 kg This figure is theoretical and does not allow for any additional material due to surface porosity, surface profile, variations in level or wastage etc.
Layer Thickness	~10 – 50 mm (subject to trials)
Ambient Air Temperature	+5 °C min. / +45 °C max.

5.2.2. Design of cement-based printing mixture

At the time of the start of this project, no commercially available material designed for 3D printing by mortar extrusion was available on the Czech market. Therefore, it was decided to outsource the development of the material to an external supplier. As the input for the company Redrock s.r.o., the technical parameters of the 1K mixture (workability 30 minutes, d_{max} = 2 mm) were defined. Based on this, 3 types of cement-based 3D printing mortar F1, R1 and P1, differing in rheological properties and water content, were delivered in Dec. 2015. Information on mixtures was limited to a listing of the types of ingredients (mixture of Portland and special cements, silica sand, pozzolanic additives, accelerators, plasticizers and stabilising additives). As neither a pump nor a 3D printer was yet available at the time of delivery of the mortar samples, testing was carried out only on a small scale by hand extrusion and standard test methods, as described in Chapter 6.3.1. As discussed further, due to the high cost (30 CZK/kg), which is 25 times of cost of a standard concrete and the inability to flexibly modify the recipe, it was decided to abandon the cooperation with Redrock and develop the printing material within the project.

The first mixture was designed on the basis of a research of 1K mixtures, which resulted in the indicative recipes of functional mixtures for 3D printing. These were the mixtures of University of Southern California [33] (hereafter USC) [Tab.19], Loughborough University [25] (hereafter LU) [Tab.20], TU Delft [84] [Tab.21], (hereafter TUD) and Hebei University [85] (hereafter HBU) [Tab.22]. The w/c ratio 0.13 of HBU mixture was considered too low to be feasible, so this mixture wasn't taken in account.

Tab.19. Composition of USC mixture

Component	Type	ϱ (kg/m³)	
Water			45
Cement	Not specified	Not specified	125,0
Sand	Not specified	Not specified	80,0
Fine aggregates	Not specified	Not specified	160,0
Superplasticizer	-	-	-
Accelerating agent			
Retarder			
w/c	0,36		
c/a	0,52		

Tab.20. Composition of LU mixture

Component	Type	ϱ (kg/m³)	m (g)
Water			Not specified
Cement	CEM Type 1 52,5		700,0
Fly ash	Not specified		200,0
Microsilica	Not specified		100,0
Superplasticizer	Not specified		10,0
Retarder	Not specified		5,0
Micropropylene fibres	Not specified		1,2kg/m3
Accelerating agent			
w/c			
b/a	2,33		

Tab.21. Composition of TUD mixture

Component	Type	ϱ (kg/m³)	m (g)
Water			228,0
Cement	Not specified	3000	659,0
Fine sand	Baskarp 15	2650	915,0
Coarse sand	Baskarp 95	2650	228,0
Fly ash	Not specified	2280	87,0
Microsilica		2600	83,0
Superplasticizer	Sikament EVO26	1080	8,3
Retarder	Not specified	1160	3,3
Sika Crack Stop		900	1,2
Micropropylene fibres			
Accelerating agent			
w/c	0,35		
c/a	0,50		

Subsequently, the ingredient ratios for the actual mixture were determined by empirical approximation and further refined to the desired properties in the

experimental part. A wider range of scientific methods and the experience gained from the design and testing of the first mixture were used in further formulations and testing of later mixtures. The reference recipes shared a number of common characteristics. They contained aggregates of fine fractions with d_{max} = 1 to 2 mm and achieved pumpability by containing a PCA based superplasticizer. In most cases, these formulations used CEM I 42.5 R Portland cement as a binder to quickly build up strength to the highest possible value.

Tab.22. Composition of HBU mixture

Component	Type	ϱ (kg/m³)	m (g)	V (ml)
Water		1000	27.0	27.0
Cement	Not specified	3000	210.0	70.0
Sand	Not specified	2650	318.0	120.0
Fly ash	Not specified	2300	46.0	20.0
Microsilica	Not specified	2600	26.0	10.0
Superplasticizer				0.3
Retarder				
Micropropylene fibres			1.2kg/m3	
Accelerating agent				
w/c	0.13			
c/a	0.54			

They also contained admixtures such as microsilica, fly ash or ground limestone to increase thixotropy. To ensure buildability, they used either a setting accelerator or VMA to ensure thixotropic behaviour. Based on presented reference recipes, an original cementitious mortar CM276 was designed using available components [Tab.23]. The author decided to use Portland cement CEM I 42,5 R from Českomoravský cement, a.s. branch Radotín as a binder. This cement was supplied in 25 kg bags for the purpose of testing the mixture in the Hobby Market Hornbach, which later proved to be critical for maintaining a uniform quality of the printing mixture.

The aggregate used was technical sands from Sklopísek Střeleč. These sands are quartz sand ST06/12 with d_{max} = 2 mm with d_{50} = 0.93 mm, quartz flour ST53 with d_{50} = 0.27 mm and silica flour ST06 with d_{50} = 0.016 mm. Furthermore, ELKEM microsilica was used as an admixture to improve the rheology of the mixture. For each of these mixtures, the water and additive content also had to be designed. The water content positively affects the consistency of the mixture and negatively affects its final strength, so an attempt is made to reduce it to a minimum by using plasticising additives. The designed water coefficient was higher than in reference mixes, it was based on values common for fine-grained mixtures, it was further refined in the experimental part. MasterGlenium ACE 430 (hereafter PCA) was proposed as a plasticising additive to reduce the water coefficient, with a recommended dosage of 0.3% to 1.0% by weight of cement. The PCA content was designed to be 3 ml/kg dry mix, this value was further refined in the experimental part. To ensure thixotropic behaviour of the mixture, it was proposed to add the viscosity modifying additive MasterMatrix SDC 100 (hereafter VMA) with a

recommended dosage of 0.1-1.5% by weight of the fines. The MM content was selected at the upper limit of the recommended dosage of 3 ml/kg dry mix, this value was further refined in the experimental part. In order to reduce cracking and improve buildability, MasterFiber 006 monofilament (MF6) was added to the mix with a recommended dosage of max 1 g/litre wet mix. The MF6 content was chosen to be 0.6 g/kg dry mix, this value was further refined in the experimental part [Tab.23]. Testing and adjustments of this mixture are presented in Chapter 6.3.2.

Tab.23. Composition of CM276 mixture

Component	ϱ (kg/m³)	m (g)
Water	1000	135.0
CEM I 42,5 R – CEM ČM	3150	276.0
MS	700	31.0
ST06/12	2650	255.0
ST53	2650	255.0
ST6	2650	183.0
PCA	1060	3.0
VMA	1000	5.0
MF6	910	0.5
w/c		0.49
c/a		0.38

During the elaboration of the thesis, a requirement arose to develop a cementitious mixture that would modify the commercially produced Master Flow 3D 100 (F3D100) mixture in order to extend its workability and improve its applicability to the printing technology. According to the supplier, the MF3D mix contained approximately 450g of CEM I 42.5 R type CEMEX Prachovice, ground limestone and a setting accelerator. The use of microsilica was eventually abandoned in further research due to its high price, which was 45 CZK/kg at the time of the mix design, and the small proportion in the mix, which complicated the dosing and mixing of the dry mix in larger quantities, as revealed in the experimental part.

The mix design [Tab.24]. was made using the freely available EMMA version 352 application [86]. This software generates the efficient granulometry design of the mortar and concrete mixtures according to given parameters. For the purpose of mix design, the first step was creating libraries of the components (cement, aggregates, limestone) according to the granulometry parameters given in their technical data sheets. Once the virtual materials were defined, the mixture was designed. In the mix design, the cement content was first selected and then the weight fractions of the other components were calculated by successive iterations to determine the ratio that best represented the ideal gradation curve [Fig. 12]. As an internal rheology parameter, Modified Andreassen was chosen as the computational model with a q value setting the packing coefficient at 0.25. The q-value for self-compacting concretes was chosen because of their easy pumpability, thixotropy ensuring buildability was further solved by VMA.
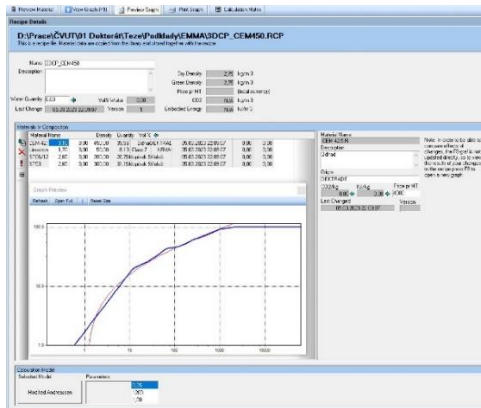
Fig.12. Packing design of CX450 using EMMA 352

Tab. 24. Composition of CX450 mixture

Components	ϱ (kg/m^3)	m (g)
Water	1000	150.0
CEM I 42,5 R – CEMEX	3150	450.0
ST06/12	2650	200.0
ST53	2650	300.0
GLS	1500	50.0
PCA	1060	3.0
VMA	1000	1.0
MF6	910	0.5

5.2.3. Design of Sorfix based printing mixture

In March 2022, following the research of Dr. Šulc's team, it was decided to design the 3D printing mortar using the original Sorfix non-cementitious binder produced by modifying of fly ash. This binder had been successfully tested as a cement substitute [87] and could therefore be expected to be useful for creating 3D printing mortar. The advantage of such a binder over cement is the significantly lower carbon footprint and the fact that natural raw materials are not used for the production of Sorfix, but energy products, i.e. waste material. It is manufactured using materials that have a zero-carbon footprint and its use therefore results in a very significant reduction in CO_2 production. One tonne of Sorfix saves 0.72t of CO_2 compared to using conventional cement [87]. Compared to other cement-free binders such as the geopolymers used in 3D printing, Sorfix is not strongly alkaline, so 3D printing technology may not be alkali-resistant, and it also brings economic benefits as the price of Sorfix is lower than cement.

The aggregate used was similar to the design of CM450 using technical sands from the supplier Sklopísek Střeleč quartz sand ST06/12 with d_{max} = 2 mm with d_{50} = 0.93 mm, quartz flour ST53 with d_{50} = 0.27 mm and silica flour ST06 with d_{50} = 0.016 mm. In order to improve the rheology of the mixture, an admixture in the form of ground limestone grade 7 from KRVAP, supplied in bags of 20 kg, was also used. Similarly to CM450 design, the EMMA application was used to design the dry mix [Fig.13-14a]. Modified Andreassen was chosen as the calculation model, with a q value setting the packing coefficient at 0.25, corresponding to self-compacting concrete. In the design of each mix, the Sorfix content was first selected and then the mass fractions of the other components were calculated by successive iterations to best represent the ideal gradation curve. In order to achieve a faster set-up and thus buildability, higher binder content was set for the mixtures with Sorfix. This increased binder content of Sorfix, unlike cement, does not have a negative effect on the carbon footprint of the mix and is also advantageous due to the lower cost of Sorfix compared to aggregates. In this way, a total of 3 mixes containing Sorfix were designed. The mixture with 350 g of Sorfix was named SF350, the mixture with 450g of SF450 and the mixture with 550g of SF550 [Tab.25].
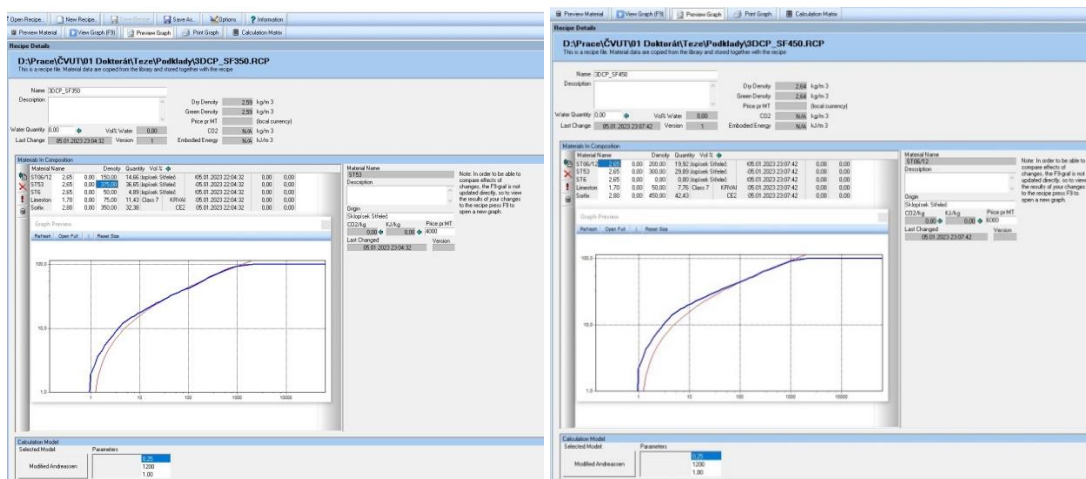
Fig.13. Packing design of mixtures using EMMA 352 a) SF350 b) SF450

Fig.14. a) Packing design of mixture SF550 using EMMA 352
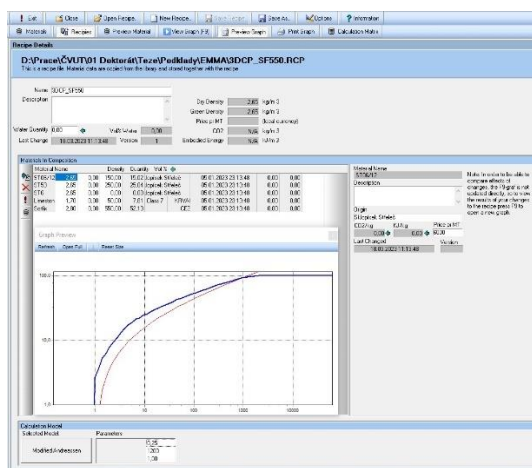
Tab. 25.
Composition of SF350, SF450 and SF550

	SF350	SF450	SF550
Sorfix (g)	350	450	550
ST06/12 (g)	150	200	150
ST53 (g)	375	300	250
ST06 (g)	50	0	0
Limestone (g)	75	50	50

For each of these mixtures, the water and additive content also had to be designed. The water coefficient was chosen in the range of 0.4-0.5. Thus, water coefficients of 0.4, 0.45 and 0.5 were subsequently assigned to each of the mixtures SF350, SF450, SF550. This value was further refined in the experimental part. MasterGlenium ACE 430 (henceforth PCA) from Master Builders was proposed as a plasticizing additive to reduce the water coefficient with a recommended dosage of 0.3%-1.0% by weight of cement. The initial PCA content was chosen to be 4 ml/kg dry mix, this value was further refined in the experimental part. To ensure thixotropic behaviour of the mixture, it was proposed to add MasterMatrix SDC 100 viscosity modifying additive (hereafter VMA) with a recommended dosage of 0.1-1.5% by weight of fines. The VMA content was selected at the upper limit of the recommended dosage of 4 ml/kg dry mix, this value was further refined in the experimental part. In order to reduce cracking and improve buildability, MasterFiber 006 monofilament fibre (MF) was added to the mix with a recommended dosage of max 1 g/litre of the wet mixture. The MF content was chosen to be 0.6 g/kg dry mix, this value was further refined in the experimental part.

This process produced 3 mixtures, which were tested in the experimental part in order to select the mixture with the best properties for 3D printing with the given printing technology [Tab 25].

5.3. Design of machinery equipment

For the purpose of large-scale testing, it was necessary to design a suitable apparatus for preparing and transporting the mixture to the ejection nozzle, as well as a programmable positioning device for manipulating the ejection nozzle, i.e. the printer itself, equipped with a control system and a print head.

5.3.1. Design of material preparation equipment

A DWT BM-720 M mixer with a mortar mixing whisk was dedicated for mixing fresh mixes up to 6 kg [Fig.15a]. A RUBI Rubimix 50 N mixing station was specified as mixing equipment for batches up to 50 kg of dry mix [Fig.15b]. This 0.88 kW mixer is equipped with a 65 L mixing vessel and achieves a mixing speed of 60 rpm is designed to pump up to 50 L of mortar and adhesives, according to the manufacturer. Gear stirrer FESTOOL MX 1600/2 EQ DUO with two rods was also available as a backup [Fig.15c].

Fig.15. a*) DWT BM-720 M gear stirrer with a mixing whisk b) RUBI Rubimix 50 N mixing station c) Gear stirrer FESTOOL MX 1600/2 EQ DUO*

In order to maintain flexibility during material preparation, enabling mixing of 5 kg test samples, it was decided to mix the material in batches and to adapt the mixing technology accordingly. See Chapter 5.1.

5.3.2. Design of material supply system

In addition to mixing, the transport of fresh mortar to the extrusion nozzle had to be solved. To this end, a detailed mortar pump survey was carried out, based on the previously determined minimum pumping capacity of 0.42 l/min and material properties such as a maximum grain size of 2 mm and the assumed rigid consistency due to thixotropy of the pumped material. It was planned to print layers of different parameters and also assumed different consistency of the tested materials, which required the possibility to vary the pumping power. Therefore, the pump had to allow continuous speed control to a minimum output close to zero, connection to a standard 240 V single-phase power socket, and its weight and dimensions were

limited to 750 x 750 x 1000 mm and 80 kg for ease of handling in the spatially confined laboratory.

Tab.26. Research of continuous mixers, inline mixing stations and pumps available in CZ

Machine type	Q [l/min]	Max. grain [mm]	Pump type	Type of mixture	Pressure (bars)	m [kg]	Dimensions (w/d/h) [mm]	Power (kW)	Voltage (V)	Pipe diameter [mm]	Hopper volume [l]	Materials	Cost (CZK)	Rent	Rating
Injection pumps															
Gratec BMP 5	0.5-12	3	Worm	Fresh mix	25	15	?	1.15	230	3/4''	30	Mortars, grouts, susspensions	60k	No	2
Gratec BMP 6	0.5 – 14	3	Worm	Fresh mix	15-25	25	760/550/1010	1.8	230	3/4''	30	Mortars, grouts, susspensions	85k	No	2
Sanax DT	2-15	2.5	Worm	Fresh mix	25	40	950/530/820	1.8	230	25	30	Mortars, grouts, susspensions	104k	Yes	1
Sanax S8	0-8.5	2	Peristaltic	Fresh mix	15	55	930/530/880	0.55	230	25	30	Mortars, grouts, susspensions	85k	Yes	1
Pumps for fine materials															
PFT SWING M	0.9	3	Worm	Fresh mix	20	70	1100/460/500	1.5	230	19	76	Paints, grouts, coatings	195k	Yes	2
Strobot 406S	0-15	6	Worm	Fresh mix	30	65	1200/580/770	1.5	230	25	?	Paints, grouts, coatings	?	No	2
Graco RTX 1500	7.6		Peristaltic	Fresh mix	7	66	?	1.5	230	25	57	Paints, grouts, coatings	?	No	5
Graco T-Max	6.4	1.5	Piston	Fresh mix	50	64	?	?	?	25	?	Paints, grouts, coatings	?	No	5
Continous mixers															
Stromixer D 1000	15	5	Worm	Dry mix	2	95	980/700/950	1.5	230	-	30	Mortars, grouts, plasters	?	No	5
PFT Lotus XS	20	4	Worm	Dry mix	2	66	?	1.3	230	-	50	Mortars, grouts, plasters	52k	Yes	5
Filamos KM 40 Standard	40	5	Worm	Dry mix	2	72	?	7.5	400	-	25	Mortars, grouts, plasters	95k	Yes	5
Inline mixing stations															
PFT Ritmo M	1.5-15.4	3	Worm	Dry mix	20	103	750/600/1380	2.2	230	25	45	Mortars, grouts, addhesives	195k	Yes	2
PFT Bolero	0-11	4	Worm	Dry mix	20	112	800/700/1500	1.8	230	25	68	Mortars, composites, grouts	210k	Yes	2
Putzmeister P12 Sprayboy	6-12	4	Worm	Dry mix	25	125	714/696/1437	1.8	230	25	50	Mortars, grouts, addhesives	?	Yes	5
Putzmeister MP10	3.5-13.5	4	Worm	Dry mix	30	90	1500/620/1020	1.5	230	25	50	Mortars, composites, grouts	?	Yes	5
Putzmeister Duomix 2000	22 - 35	2	Worm	Dry mix	20	250	?	5.5	400	25	?	Mortars, grouts, addhesives	?	Yes	5
Filamos CM20	3-9	4	Worm	Dry mix	30	305	?	1.5	400	25	90	Mortars, grouts, plasters	208k	Yes	5
Filamos Mini	12	2	Worm	Dry mix	15	155	1410/590/1280	3	230	25	?	Mortars, grouts, addhesives	?	Yes	5

The market research [Tab. 26] showed that there were available solutions based on a screw pump, used for pumping fine-grained mortars and plasters, or grouting pumps based on the peristaltic principle. The specific pump type was then selected based on initial tests of the print material, as described further in the experimental section. The length of the supply hose will be chosen as short as possible to limit pressure losses and thus allow the pump to respond flexibly to pressure changes in the nozzle and also to pump stiffer materials. A shorter hose is also easier to clean in the event of a clogging.

5.3.3. Design of 3D printer

A key component of 3D printing technology is the 3D printer. At the time of writing this chapter, such a device was not available to the author of the thesis, so it was necessary to provide it. Due to the high price of industrial robots, exceeding the capabilities of the author's department, it was decided to outsource the manufacturing of the 3D printer to an external company. Due to the novelty and specifics of the 3DCP process, it was first necessary to establish a precise assignment in the form of a design specification. The basic parameters of the device were set out in chapter 5.1, for the purpose of the exact specification it was necessary to extend them further [Tab 27].

The external dimensions of the device were based on the size of the printing space and the limited spatial possibilities of the 3D printing laboratory. The maximum allowable payload of the end effector was determined as the sum of the expected weight of the print head and the 2 m long concrete supply hose. The supply voltage was matched to the capabilities of the laboratory. The equipment had to be robust, capable of operating in dusty and wet conditions. It had to be able to process data in Gcode format. Control was designed from an external laptop, connected by cable via a USB port. The device had to be fitted with emergency switches, allowing the

operator to switch off the printer at the touch of a button in the event of an emergency. In this case, the power supply to the stepper motor drives is disconnected via the contactor.

Tab.27. Design parameters of the 3D printer

Parameter	Printing volume	Dimensions	End effector speed XY	End effector speed Z	End effector accuracy	End effector max. load	Power supply
Unit	(mm)	(mm)	(mm/min)	(mm/min)	(mm)	(kg)	(V)
Scope of values	1000x1000x1000	1250x 1250x1250	0-6000	0-800	±1	15	230

Based on these parameters, a concept for the technical design of the machine was subsequently proposed in Autodesk Fusion 360 [Fig.16]. The device was designed to print horizontal or spiral layers with vertical or slanted travels with fixed size and orientation of the layer within a single print. This type of movement does not require a change in nozzle orientation and therefore does not require a change in the end-effector cap. For this reason, Cartesian kinematics with motion in three perpendicular XYZ axes was proposed. To ensure accuracy, a rigid frame structure made of 40x40 mm Jackel steel profiles was chosen. The main frame was designed from two welded rectangular frames, joined together at the corners by four cross members, for ease of assembly and transport anchored to the frames by bolted connections. This structure, forming a rigid block, was the support for the Z-axis linear guide. This was designed as a double, formed by two linear guides Z1 and Z2, on opposite sides of the block frame. These were designed as rails of Jackel profiles guided at the ends by two vertical support bearing rails of 20 mm diameter. The drive of the Z-axes was designed to be provided in each of the Z1 and Z2 guides by a trapezoidal bar connected to the rail at its centre by a bearing carriage. The trapezoidal bar is mounted at both ends in axial and radial bearings, ensuring the transmission of forces from the bar to the aluminium frame bed, bolted to the respective Z-axis frame cross member. Vertical movement along the trapezoidal bar is provided by a NEMA 34 two-phase phase stepper motor with torque 12.5Nm, mounted at the top of each guide and supported at the bottom by trapezoidal bear. The connection between the motor and the threaded rod was designed to eliminate misalignment and vibration transmission via a flexible coupling. The rails carried in this way formed the support for the Y-axis.

It was designed in the form of a travelling trolley, welded from two Jackels connected at the heads by flat cut-outs of 6 mm thick steel plate. The trolley was mounted on the Z-axis rails by two pairs of running wheels with bearings, custom designed in durable engineering plastic type PA6. The movement of the Y-axis was provided by a pair of NEMA 34 two-phase stepper motors with torque 12.5 Nm fitted with shepherds, custom-made by 3D printing in PETG material. The power from the motors is transmitted to the motion through the shepherds by connecting to a toothed belt stretched over one of the running rails in the range of motion of the Y-axis. The design of the X-axis was similar to that of a short carriage in the form of a

weldment of Jacks and cut-outs made of 6 mm thick steel plate. This was mounted on rails formed by the Y-axis frame over identical plastic running wheels with bearings. The travel was again provided by a NEMA 34 two-phase stepper motor with torque 12.5 Nm fitted with shepherds, custom-made by 3D printing in PETG material. It was moving on a toothed belt, tensioned in the range of motion of the X-axis over the transverse Jackel forming the travel rail on the side of the Y-axis carriage. The design of the linear guides with threaded rod and roller gears is chosen in this way for several reasons, namely the ability to operate in dusty and wet environments, minimisation of failure on impact of blasting material, relative simplicity and hence robustness, the possibility of repair without sophisticated technical equipment and affordability. A lever-operated mechanical limit switch has been designed at each end of each axis to ensure immediate stopping of the respective axis when its spatial limit is reached.

On one of the side frames, the control unit, power supplies and motor drivers and the relevant interfaces are housed in a plastic IP40-protected enclosure for operation in wet and dusty environments. The control unit, which provides the conversion of Gcode into signals to the individual motors, was designed as an 8-bit Arduino Mega 2560 control board [88], operated by Arduino 1.8.9 [89]. The bottom of the box contains the drivers for the four individual axis motors, one printhead motor and the corresponding power supplies. The equipment will be powered from the grid via a separate power supply, allowing connection to a standard 230V single-phase mains supply. In order to ensure operational safety and the possibility to deactivate the device at any time in case of emergency, a safety circuit with two emergency switches is designed to switch off the power part (stepper motor driver power supplies). The cables from the stepper motors, limit switches and power supply cable are fed into the box via panel connectors. The cabling is designed with flexible cables without shielding. DX12 and GX16 type cable connectors are included. The printer also includes a rectifiable printing plate in the form of a deck of welded profiles, fitted with a laminated printing plate on the top face, allowing printing of wet material and washing of the plate. The deck is anchored to the floor via rectifying screws.

Fig.16. Render of 3D printer design in Autodesk Fusion 360

Marlin 1.1 [90] is designed as the firmware of the control board. In the printer firmware it is set which logic output of the Arduino is assigned to which motor (there can be multiple motors for one axis), how many pulses the respective motor has to receive to cover a certain real distance and other settings are included, e.g. acceleration, deceleration speed during direction change and others. Before running the printer for the first time, the control system settings will need to be adjusted in the Marlin environment according to the needs of the printing technology and printer parameters, then compiled and uploaded to the Arduino control board. For each change to the printer settings this operation must be performed again, some changes can also be written directly to the control board using Gcode. The printer control is designed from an external personal computer using Pronterface [91], which is a fully featured GUI host interface for 3D printers and CNC. The Pronterface application sends commands in Gcode format to the control board via the printer's USB port, and the control board executes the commands without feedback according to the firmware settings. It also allows you to view the current printer status (e.g. current position, status of limit switches, etc.) For example, the expression G0 X100 F3200 is a command to move the X-axis to a coordinate system position of 100 in mm units, at a speed of 3.2 m/min (units are set in firmware). The abbreviations M114: Get Current Position and M119: Endstop States have been set on the bottom bar of the Pronterface for quick entry of common commands.

5.3.4. Design of printhead and extrusion nozzles

In order to ensure constant pressure and flexible control of the nozzle extrusion according to the needs of the Gcode controller, a special print head was designed to facilitate the extrusion of single component material. The printhead was also designed to enable easy nozzle changes to print layers of different profiles [Tab.28] and quick connection and disconnection from the supply hose and printer. The nozzle body was designed from 250 mm long DN25 thick-walled steel pipe. In the middle, an angled branch from the DN25 pipe was connected to the pipe at a 45° angle to connect the supply hose to the print material. The tap was fitted with a 20 mm long G1″ pipe thread at the end for fitting a GEKA female threaded coupling. It seemed impractical to regulate the extrusion by an extrusion auger driven by a stepper motor. For this reason, a square flange made of 4 mm thick strip metal with dimensions 50 x 50 mm and a hole in the flange axis of Ø 6 mm was welded on the top of the pipe [Fig.17]. This hole was used to run the shaft of the discharge auger of Ø 5 mm, which was designed as a 25/25 helix made of 3 mm thick strip metal with a pitch of 25 mm and an outer diameter of 25 mm for tightness reasons. The shaft of the auger mouthed into a 50x50x80 mm spacer designed as a 3D printed using CPEG filament. This was connected to the nozzle body flange by four screws. The shaft ran through a thrust bearing and rubber sealing ring, anchored into the house. At its end in the spacer it was connected to the stepper motor NEMA 23 two-phase phase stepper with torque 4.5 Nm via a flexible coupling to eliminate misalignment and vibration transmission. This was connected via a cable connector to the printer control unit. The tubular body of the head was fitted with a 30 mm long G1″ pipe thread on the underside to allow various extrusion nozzles to be screwed onto it. These were

designed as 3D printed of CPEG with different diameters of outlet to print layers of different W and L parameters and with a G1″ female thread on the connection to printhead.
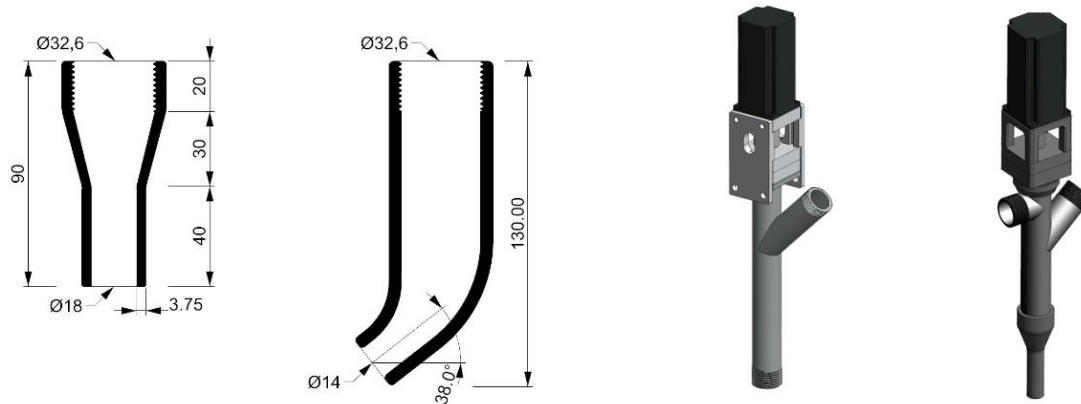
Fig.17. a) Nozzle TP-18 – Section b) Nozzle TP-14-38deg – Section c) Isometry of printhead PH1 in Autodesk Fusion 360 d) Printhead PH3

The author assumed that the pressure in the pump-hose-nozzle system would need to be equalized for the printhead to function properly. The solution offered was to equalize the pressure between the nozzle and the pump using a pressure sensor in the nozzle at the hose connection and an electronic speed control in the pump linked to it. Due to the complexity and cost of this solution, it was proposed to solve the pressure control by regulating the pump speed according to the visual control of the nozzle discharge outlet. This solution proved to be insufficient in the experimental part. During the experimental validation, the printhead PH1 was the basis for subsequent versions PH2, PH 3 and PH 4, which were better suited to the 3D printing technology, especially in terms of pressure balancing between the nozzle and the hose. As a part of 3D printing technology on an inclined board a curved interchangeable nozzle TP-14-38deg with an extrusion outlet inclination of 38° and a diameter of 14mm was developed and printed of CPEG [Fig. 17].

Tab.28. Proposed extrusion nozzle diameters

Nozzle type	TP-10	TP-15	TP-18	TP-22	TP-25
Inner diameter (mm)	10	15	18	22	25
Layer width (mm)	15-18	18-22	22-25	25-28	28-32

5.4. Modelling and programming of print scripts

One of the key tasks within the project was to design models and control scripts to convert them into physical form via a 3D printer. As described in Chapter 2, the conversion of 3D models into layers is provided by slicing, i.e. transforming surface of printed 3D object into a set of contour curves in order to represent layer-wise physical interpretation regarding given parameters. For these tasks it was first necessary to find suitable software. Due to the project's focus on design prefabricates, it was decided to take advantage of the possibilities offered by parametric modelling when creating the models. The CAD tool Rhinoceros was chosen as the most

advantageous tool in terms of price/performance ratio (the price of the student version was 150 EUR), within which the free parametric modelling plugin Grasshopper can be used. A suitable CAM tool, i.e. slicer, had to be found for pre-production preparation, simulation and print data preparation. Since the firmware of the available printer works with the Gcode format, it was necessary to find a slicer that can generate this format. A search of available solutions led to the selection of a slicer in the form of the Silkworm plug-in, which could be conveniently integrated into the Grasshopper environment to obtain two outputs in one step.

The 3D printed object models were ideally created as parametric geometry in the Grasshopper environment, allowing quick changes to the model parameters and easy generation of different variants. Where this was not possible or was too tedious, the geometry of the models was created as non-parametric geometry in the Rhinoceros environment and then imported as a surface from the 3dm file into Grasshopper. 3D objects were always modelled as open NURBS surfaces of zero thickness, and in some cases polysurface or mesh type solids were created for visualisation purposes. The basic parameters that influenced the form of the models and subsequent scripts were the thickness and height of the print layer. In this work, only horizontal layers with the same layer width and height were printed within a single printout, except when printing at an angle on a tilted plate, but where the layers are also parallel and equal. If the external dimensions of the geometry were known, then the area had to be offset by half the layer width, and the height of the whole geometry had to be in integer multiples of the layer height. In the case of the visualizations, the layers were modelled as a polygon with rounded ends in order to provide a realistic appearance [Fig.18].

The size of the models was limited by the size of the printer's print space. Within the scripts, it was therefore necessary to define the printer's print space for the sake of simulating the correspondence of the printed object with the printer's print space. In accordance with the print space of the physical printer, it was defined by a cube with dimensions 1000 x 1000 x 1000 mm. A print area of 850 x 600 mm was also modelled, corresponding to the print deck.
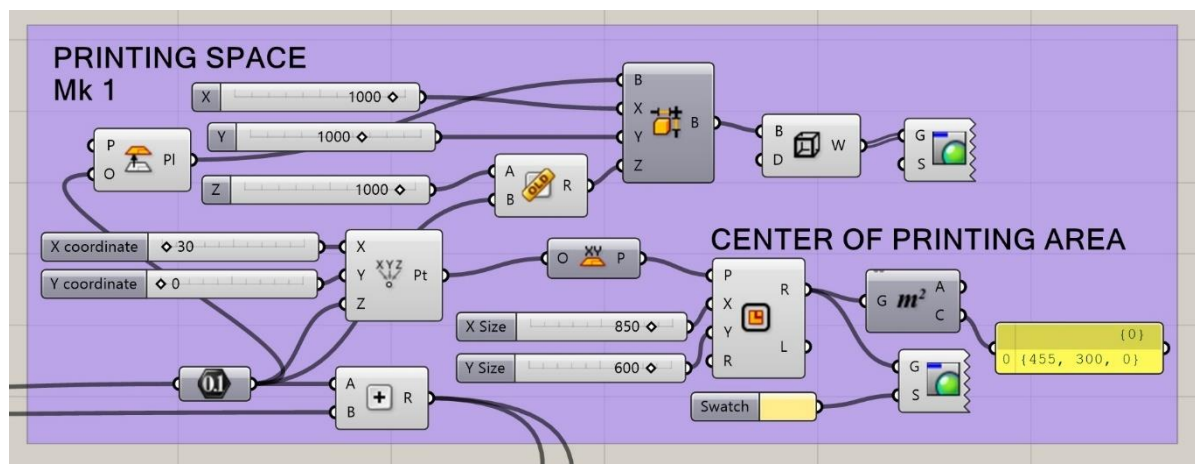
Fig.18. Part of Grasshopper script – Parametric definition of printing space for3D printer Mk 1

In some cases, the printing path was generated directly as a sequence of curves or as a single 3D curve without the need to create a 3D surface. In other cases,

the printing path was obtained by intersecting horizontal planes with the 3D model in the form of a surface and then modifying the resulting curves according to the type of printing path. The ramp length in continuous 3D printing of horizontal layers with ramps was chosen as three times the layer height.

If it was not necessary to parameterize the model, trajectories or surfaces were generated in Rhinoceros and then exported to Grasshopper. The output was then a 3dm CAD file with geometry and a parametric gh model with CAM settings. In case it was practical to parameterize the 3D model or printing path, it was more convenient to do the model creation and slicing in Grasshopper, everything was fully parameterized, and the complete job was saved only in gh format.

The printing path prepared in this way is then loaded in Grasshopper to the desired XYZ coordinate in the print space. The script enables to parametrically select the position of the printout within the print area, both in the XY plane and in the Z direction, by X, Y, Z-offset variables. Selectable printout position in the XY plane provides the possibility of printing multiple smaller objects within one print area. The Z-offset value enables increasing the Z coordinate of the printout by an additional underlay plate because of the possibility to remove the printout from the print area after the print is finished and to perform another print job in a short time, thus reducing the technological break for smaller prints. It also enabled to change the position of the printout in the Z-axis with respect to the length of the exchange nozzle.

The final fitted trajectory curve is subsequently cut into a sequence of segments in each separate horizontal curve or in the whole 3D curve, whose length was chosen to be 2 mm for the sake of accurate curve approximation. This sequence of lines is further processed through the Silkworm Movement plugin node, where the parameters of the nozzle movement velocity v and the nozzle extrusion coefficient f are assigned to it, which in the subsequent Gcode control the direction and number of pulses of the stepper motors that drive the XYZ axes and the extrusion screw in the print head. As part of the output from the node, the sequence is merged back into a single parameter and sent to the Merge node, where the different parts of the print job are merged into a single parameter. Within the print jobs, similar to the FFF method printers, a test trajectory with extrusion is inserted before the actual printing path, necessary to compare nozzle pressures, typically several tens of decimetres long. After the printing path, a passage of the print head without extrusion to a specified final position after the print is completed is then inserted [Fig.19].

In the case of printing with travels, the printing path is then divided into the appropriate number of print trajectories for individual layers, interspersed with travels without extrusion. This concatenated parameter is then connected to the Silkworm Generator node, which combines the print motion parameter, the printer settings from the Load Settings node, and the Sort. In the Load settings parameter, the printer settings from the external file 3D_Concrete_printer_Settings.ini are loaded. The Sort parameter handles input comparison, it is set to 1 by default, i.e. compare all. In the 3D_Concrete_printer_Settings.ini file, it was necessary to define default values for the variables providing the default printer settings. The file was created by modifying the ini file for the Průša Mk3 i3 printer settings.
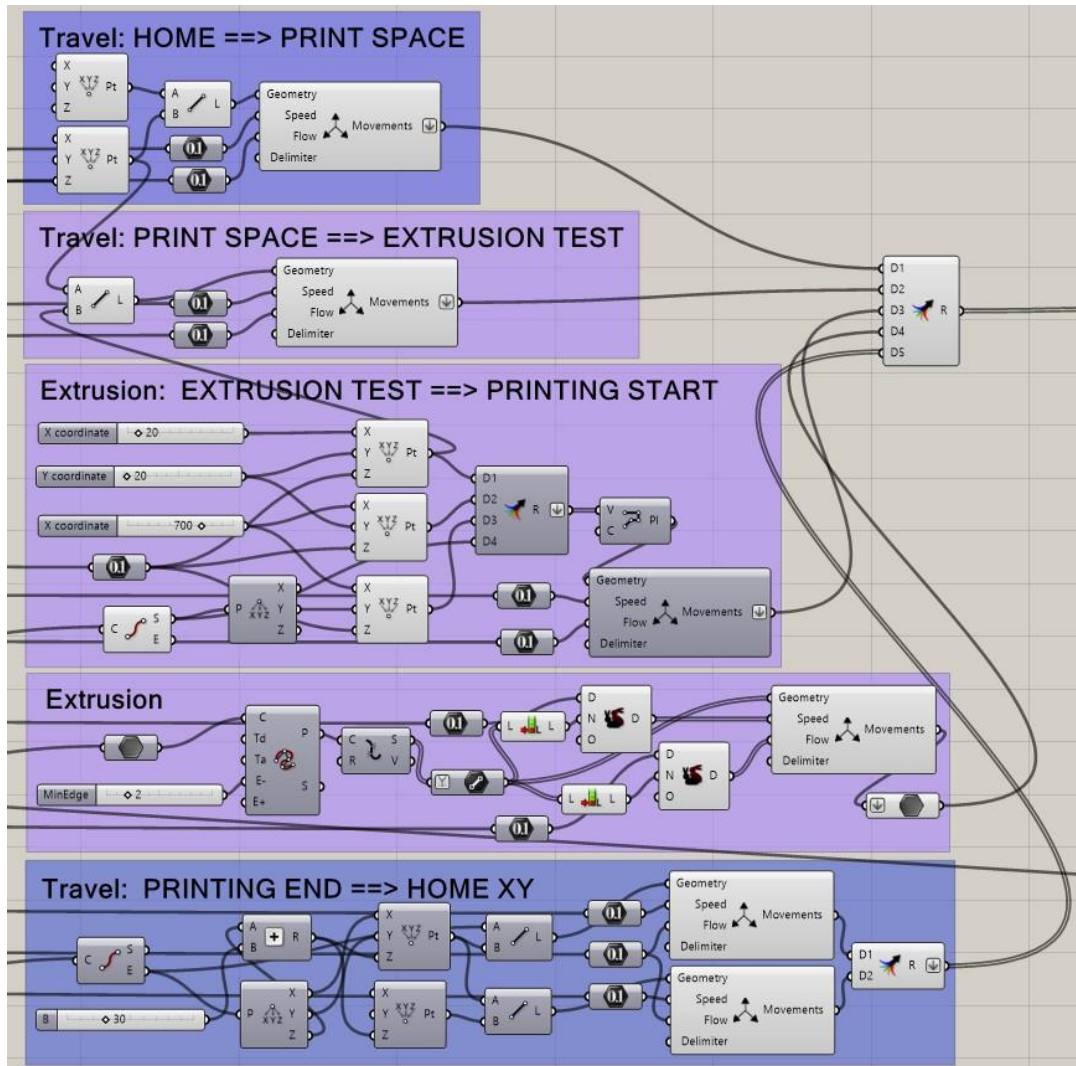
Fig.19. Part of Grasshopper script – Silkworm Movements definitions and merging

The Silkworm Model output from the Silkworm Generator node is then connected to the Silkworm Viewer node. Here, the parameters for displaying the output in the Rhinoceros environment are assigned. The print start, and end layer numbers, printing path visualization and printer view are handled. The Gcode output from the Silkworm Generator node generates a Gcode script to control the 3D printer. The Gcode is further modified by connecting it to a sub-script, modifying it according to the needs of the printing technology. The first 8 lines of the script are taken out, the part concerning the temperature settings for the FFF printer and the extruder settings is deleted. An automatically generated text summarizing the basic parameters of the print job is then inserted before the script itself for the purpose of script analysis. After this, a section of previously extracted text is inserted containing the new extruder settings, the Home command, the unit settings, followed by the print script itself [Fig.20]. The finished Gcode can be visually inspected in the Panel window and then exported to an optional directory.
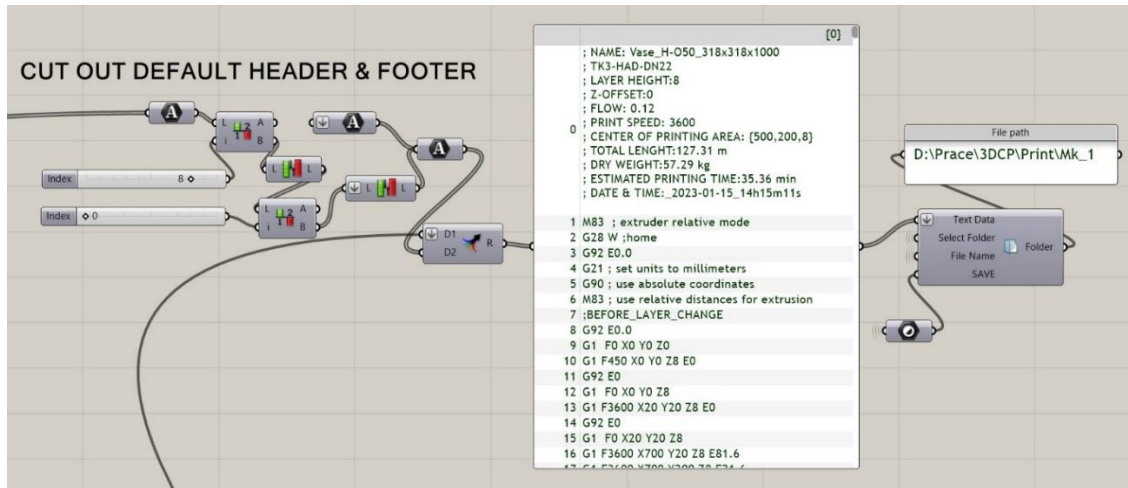
Fig.20. Part of Grasshopper script – Parametric Gcode text adjustments and export

Parameters that allow the parametric script to optionally define layer parameters, slicing settings and print jobs in real time in addition to model dimensions and placement are summarized in the Tab. 29.

The script also automatically generates the calculation of technological data necessary for print job planning and material preparation, such as the external dimensions of the printed element, calculation of the estimated printing time or calculation of material consumption in kg of dry mix [Fig.21].

Tab.29. CAD+CAM model parameters

Parameter	Object height	Print position X	Print position Y	Print position Z	Layer width	Nozzle velocity XY	Nozzle velocity Z	Extrusion flow
Unit	(mm)	(mm)	(mm)	(mm)	(mm)	(mm/min)	(mm/min)	(-)
Abbreviation	h	X-offset	Y-offset	Z-offset	w	v	v-z	f
Scope of values	0-1000	0-1000	0-1000	0-30	18-32	800-4500	800	0.05-0.20
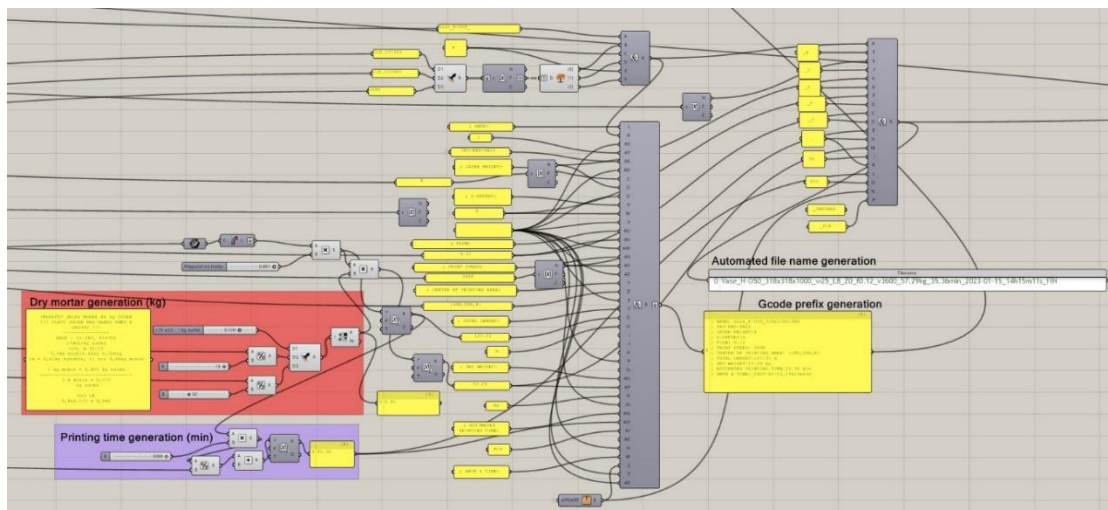
Fig.21. Part of Grasshopper script – Generators of speed, mass, file name and Gcode prefix

As part of the development of the control scripts, the question was how to verify the stability of the elements during printing in the modelling and slicing process. In Chapter 2, Grasshopper plugins were described to assess stability via Mohr-Coulomb material model based on selected material parameters derived from fresh mix properties. The influence of the flow mechanism or process parameters, such as nozzle rotation or corner build-up, is not considered. Furthermore, no information on the final mechanical performance, visual appearance, influence of environmental factors or sustainability can be derived within the described process [45]. Technological parameters and their variations were also not considered. In this case study, a continuous mixer was used to prepare the print material, a different type and length of hose was used, and a print head and nozzles of unknown design were used. On the basis of these facts, the author assumed that the material properties at the nozzle end would be affected by the different nature of the mixing and pumping equipment and the print head, compared to the properties determined by the 1 kg measurement in the laboratory, and that their values would be affected by a significant error. The simulation input values will therefore not be accurately determined and the model on which the stability calculation is based in these tools will not provide relevant results in conjunction with the technology. In addition, the above tools only address stress, print stability and strain and do not describe the quality of the layers, i.e. deformations such as cracks or cross-profiling of the layers. Thus, they do not consider the quality requirements and without addressing them, it is not possible to print design elements in the visual quality that is the focus of this work. For these reasons, the author decided not to use the tools to simulate the result of the printing process. The shape of the models in terms of ensuring stability was solved for the first scripts by estimation and later based on the experience gained during the first 3D printing jobs. In addition to model parameters such as slenderness and eccentricity in the direction of the wall normal, the overhang of the layers, the length of single layer, technological parameters such as v, f and the type of print path, and material properties such as buildability and open-time played a role.
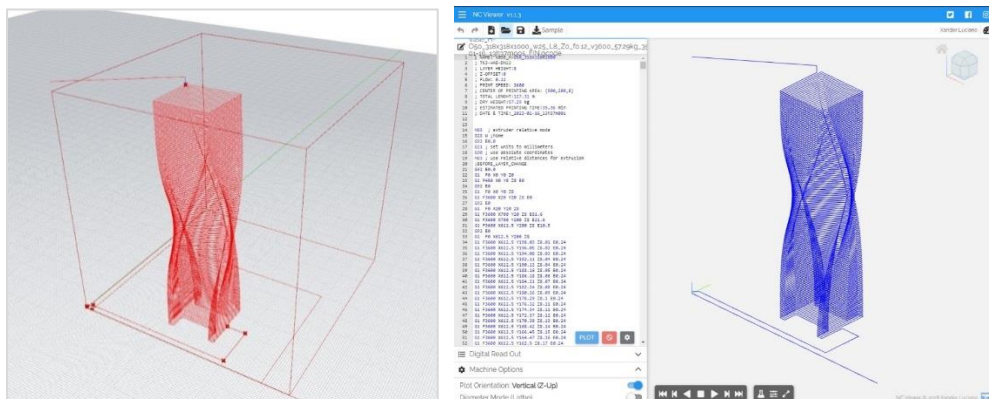
Fig.22. a) Window of the perspective view of the parametric model in Rhinoceros 7 displaying the print space, print area, printing trajectory of the H-O50 object, nozzle pressure equalization test trajectory and end travel. b) View of the print script in NC Viewer

After setting all the design parameters of the model, the Gcode could be generated. To avoid errors in the Gcode script, the finished script had to be checked

before running the print job. Unfortunately, unlike many other CAM solutions, Silkworm does not allow checking the correctness of real-time print job simulation scripts; the task has to be performed in external tools. The functionality check of the Gcode scripts was first performed in Pronterface, which was also used within the project as an environment for printer control and print job management. In the Pronterface window [Fig.23], the printing path is shown with a red curve, the crossings with a grey curve. Unfortunately, viewing trajectory models generated from Gcode scripts in Pronterface was not found by the author to be user-efficient, mainly due to the difficulty of rotating the model in the 3D environment. Easier inspection of the Gcode scripts could have been performed in the more user-friendly online Gcode viewer NC Viewer [Fig.22b] [92].

As part of the testing methodology developed by the author in Chapter 5.5.2, it was necessary to develop test scripts to verify the basic parameters of the print jobs. The Testing v-f script was designed as a sequence of contiguous straight trajectories of length 790 mm, differing in/f. It allowed verification of the values of the print parameters v and f and the layer parameters L and W for a given nozzle and a given material [Fig.23b].
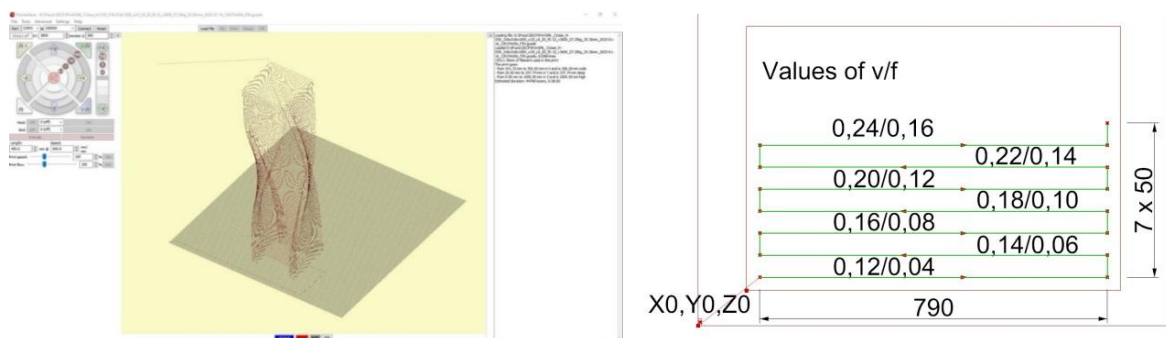
Fig.23. a) Pronterface interface displaying the print space, print area, printing trajectory of the H-O50 object, nozzle pressure equalization test trajectory and end travel.
b) Testing v-f script. Trajectories for testing of v/f parameters of extrusion in Rhino

5.5.   Testing methodology

In order to define fresh state properties of materials, the author of the thesis, taking into account the research and the unique nature of 3DCP, developed his own methodology, combining conventional standard methods for testing concrete and mortar, methods used in the literature and his own procedures. During the development of the project, as the author's knowledge of material and technology behaviour deepened, the methods for describing their behaviour were gradually refined and the number of quantities monitored was increased. This is captured in the final version of the test report on page 89. The consistency and resulting strength were tested by conventional methods. Verification of pumpability, extrudability and buildability of mixtures and printability of objects was carried out by in-house developed methods. For this reason, it was necessary within the framework of this thesis to develop not only the actual testing methodology but also the testing apparatus. The author of the thesis assumed that the behaviour of the materials would be influenced by the size of the samples as well as the type and size of the

apparatus on which the preparation and testing of the material takes place, therefore it was decided to perform a basic design of the parameters of the mixtures on a small scale in quantities up to 1 kg and then refine it in quantities of 8 to 12 kg on a 3D printer in full scale. Since the author assumed that the tensile strength would be more critical than the compressive strength, the properties of the materials in the hardened state were tested only by the concrete bending test (three-point load test).

5.5.1. Small scale testing

Material preparation

The preparation of the custom made mixes was based on the European Guidelines for Self-Compacting Concrete [93]. The sample preparation procedure took into account the full-scale material preparation technology. The weighing of the components for the individual mixtures was carried out on a Kern EW scale with an accuracy of 2 decimal places. The small-scale mixtures were mixed on a standard laboratory mixer [Fig.24a,b]. Dry mix preparation was designed as mixing the components first in the mixer for 5 minutes in order from coarsest to finest. The original idea for preparation of fresh mix was based on standard methods, i.e. first adding the whole amount of dry mixture into the vessel and then gradually adding mixture of water with PCA and VMA during 5 minute long mixing. As described in the experimental part, this method turned not to be workable due to the forming the dry consistence that resisted to be mixed to more liquid one. Subsequently, testing of the various parameters of the mixture was proceeded. The preparation of ready-made industrial dry mixes was simplified compared to those mixed from single ingredients. Whole amount of water was placed into the mixer vessel, mixing was initiated and the dry mixture was gradually added. The wet mixture was stirred for 5 min to fully blend. If the consistency of the fresh mixture was still too dry, additional water was added. The resulting mixture was left at rest for 5 minutes to relax.

Fig.24. Small scale testing equipment a), b) Standard lab mixers c) Flow test apparatus

Flow

Based on a review of the state of the art, the author assumed that the more fluid the consistency, the better the pumpability, so it was decided to verify the initial consistency by slump testing the mixtures on a shaking table [Fig.24c]. The target consistency was assumed to be in the range of 130 to 150mm

Extrudability / Buildability

In order to determine the extrudability of the mixtures, due to the ambiguous methodology and the unavailability of suitable test equipment, it was decided to simulate machine printing by extrusion from a hand-held extrusion gun used for the application of single-component sealants. Two variants of the extruder guns were available, the SKIL Masters F0152055MA Drench gun 2055 MA [Fig. 25a] with extrusion provided electrically and manually powered sealant gun Powerfix Profi for standard cartridges 300 or 310 ml [Fig. 25b].

Fig.25. a) Electric sealant gun SKIL Masters F0152055MA Drench gun 2055 MA
b) Manual sealant gun Powerfix Profi

For extrusion, it was proposed to use conical plastic nozzles with a circular nozzle profile with a diameter of 15 mm, which were an accessory of the extruder gun. The test consisted of depositing a layer of material by extrusion with a hand-held extruder gun from a circular nozzle of a given diameter and trajectory onto a flat plate [Fig.27]. The extrusion was carried out continuously along a line of length of 200 to 300 mm, with the nozzle inclined at 45° to the plate, the horizontal component of the velocity of the gun movement was in the opposite direction to the horizontal component of the extrusion vector. The nozzle rested on the bottom edge of the base plate during extrusion. The value of the extrusion force and the velocity of the nozzle along a given trajectory are not completely controllable in the manual operation of the gun, so this test provides only indicative results, but nevertheless provides usable results. The ability of the material to be extruded and the subsequent quality of the layers so extruded were assessed. If the first layer was successfully applied, the buildability was tested by depositing multiple layers on top of each other, as is the case with 3D printing by mortar extrusion [Fig.26]. The quality parameters of the layers monitored were the spread, the number and width of cracks and the deformation of the lower layer due to the overloading of the upper layers.

In this dissertation, a sample evaluation system based on subjective observations was developed to evaluate the tests [Tab.30-32]. This method of evaluation was resorted to because of the difficulty of any quantifiable measurement in manually operated apparatus. Since all evaluations were performed by one person, the author of this thesis, it can be assumed that all evaluations are burdened with the same systematic error. It is then possible to objectify this established subjective evaluation system after introducing some calibration conversion.
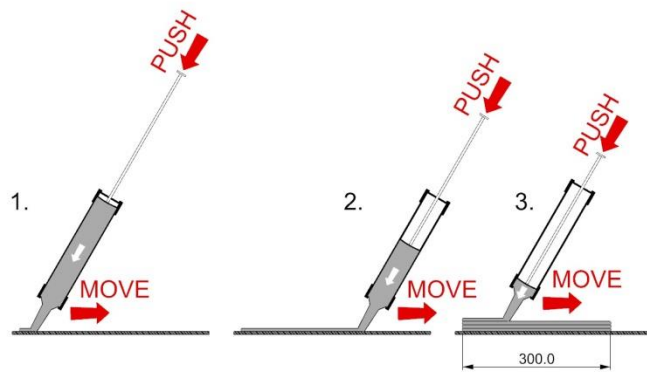
Fig.26. a) The extrudability/buildability testing procedure in a small scale using the sealant gun b) The author using pistol Skillmaster for testing of extrudability of mortar

The author assumed that the extrusion testing would refine the desired spread value for further mixture designs. During extrusion testing, the additive and water content was subsequently refined to improve extrudability and the ability to support additional layers without deformation. The mixtures with the best parameters were then selected from the materials so modified and these were further subjected to large-scale testing.

Tab.30. Summary of criteria monitored during small scale testing

Property	Mixing time	Relaxing time	Spread (Flow test)	Extrudability	Buildability	Setting time
Unit	(min)	(min)	(mm)	(-)	(-)	(min)
Best	-	-	-	1	1	-
Worst	-	-	-	5	5	-

As part of the thesis, it was also necessary to determine the values of workability and open-time of mixtures. The key property affecting workability and also open-time is the rate of onset of solidification of the mixture. This quantity is normally tested for cement mortars by the penetration test on the Vicat apparatus. The test method consists of measuring the value of the penetration of the needle into the test body over time, from which the degree of setting of the mixture is then derived. The start is in the range of 3-4 hours for CEM I 42,5 R, depending on the manufacturer. In the case of a single component mix without a setting accelerator, the author requires a setting time of about 20-30 minutes, which cannot be achieved in such a short time by hydrating the cement without a setting accelerator or by rapid heating of the mix. The initial setting and hence the consistency of the mix are primarily based on thixotropy, so that they can be reversed over a period of time by mixing. It is the author's opinion that the onset of solidification in these mixtures consists of irreversible, slow solidification and reversible, rapid solidification due to the thixotropic nature of the material. To determine the consistency of the material in the pump, it is essential to consider the technology of material preparation. In the case of the batch printing technology developed by the author, this is done in such a way that from the batch of material mixed in the vessel, after a short relaxation, the mixture is dosed into the pump hopper in batches, where the material is being

compacted during filling in the pump hopper and thus mechanically stressed and, in the case of manual filling, also heated. The remaining part of the mixture is relaxing in the vessel and needs to be restored to consistency by mixing before being transferred to the pump hopper.

The thixotropic component of the solidification is therefore disturbed in part of the material by repeated mixing at different intervals in the case of the technology used. This, according to the author, results in a very complex solidification process in the pumped material, whose time-varying reversible and irreversible components cannot be separated, and it is very difficult to simulate the behaviour of the material in 1 kg quantities in the laboratory. The author believes that the onset and progression of solidification of 3D printing mortar is very difficult to simulate in batch mixing technology of this type. Determining solidification values by measuring needle penetration is not considered by the author of the paper to be conclusive, even in an indicative range. It has only been used as a control test in the development of Sorfix-based material (Chapter 6.3.6). Considering the expected maximum printing time of 60 minutes, the author considers the values of the onset of setting times given by the binder manufacturers in the technical data sheets to be sufficient for workability and open-time purposes. Therefore, in the small-scale testing, only an indicative time was recorded as to when the open time of the mixture ended without the possibility of extending it by additional mixing. The actual workability and open-time of the mixture will only be verified on a large scale on the final apparatus and considering real conditions. The achievement of the relevant results described in Chapter 6 proves that the chosen procedure without measuring the onset time was correct.

After verifying workability and also open-time, it was necessary to determine how to measure the buildability of the mixture. The author assumed that the buildability depends on the same variables used to assess workability and open-time, in addition to a number of other variables and boundary conditions that would not be possible to verify on a small scale. The effect of the printing apparatus will need to be considered, i.e. its effect on the material in the pumping system and in the print head, where the heating of the motors results in heating of the compound and shear stress within the system, which affects both the hydration of the binder and the thixotropy of the compound. The influence of ambient boundary conditions will also play a role, where due to the wet nature of the printing process, the heating of the machines and computers and the presence of physically working people, the temperature and humidity of the air will dynamically change during the printing process and their effect on the mixture and the printed layers. The author therefore assumed that buildability values would result from large scale testing and it can be assumed that the ability to set the correct values for this variable will affect the resulting printability of the models.

Testing on Viscotester iQ

To determine static and dynamic yield stress and thixotropy it was suggested to perform additional testing of CM450 on Viscotester iQ (Thermo Fisher Scientific, HAAKE).

Although the result of a viscosity measurement is information about the viscosity in the appropriate physical dimensions (Pas), it must be remembered that

the measurement result is always relative and strongly related not only to the geometry of the testing apparatus, but also to the loading protocol, i.e., the history of mixture handling, loading rate and loading method. For this reason, the currently applied protocol for cement paste enriched with additives was chosen for the measurements. A coaxial grooved cylinder was selected for viscosity measurements [Fig.27].

It is desirable to load the mixture according to two different protocols to determine the static yield strength, the degree of thixotropy and the dynamic yield strength. Static yield strength and thixotropy are measured on the mixture without mixing. The rotor has a total of three cycles of operation starting with a prescribed increasing shear rate from 0 1/s to about 10 1/s. This increase lasts for 60 s. The maximum shear strain is then held constant for 30 s when the shear surface formation in the material is enhanced and then comes the last segment where the rotor slows down for one minute from 10 1/s to a complete stop. This creates a loop whose surface area represents thixotropy. This measurement is repeated for selected times, always with a newly inserted mixture in the cylinder. Immediately after the protocol described above, the mixture is loaded with a protocol to determine the dynamic yield strength. The mixture is additionally agitated for 30s, then allowed to stabilize (read torque drops to zero) and loaded with a total of three cycles of rotor acceleration and deceleration. The dynamic viscosity can then be read from each segment.
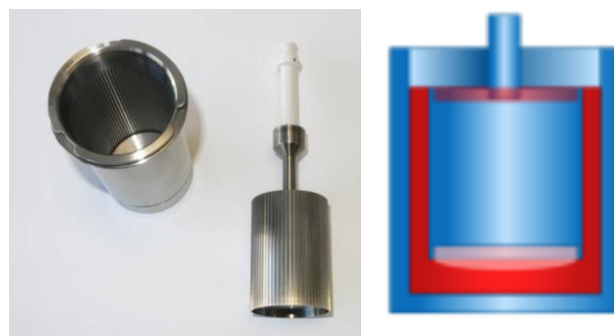
Fig.27. a) Coaxial cylinder b) Section of cylinder with rotor and tested mixture in red.

5.5.2. Full scale testing

The aim of the large-scale testing was to verify the real buildability of the material, as well as the printability in combination with a specific script and the subsequent quality of the prints. Each print job was a test in its own way due to the complexity of the 3D printing process and changing boundary conditions. The author of this thesis anticipated that the behaviour of the materials would be influenced by the size of the samples as well as the type and size of the apparatus on which the material was being prepared and tested. After verification of the mixture by testing in quantities up to 1kg on the extrusion gun, testing and subsequent adjustment of the formulation on the final apparatus [Fig.30] in quantities of several kg was proceeded with. Similar to small scale testing, the original idea of preparation of fresh mix was based on standard methods, i.e. first adding the whole amount of dry mixture into the vessel and then gradually adding mixture of water with PCA and VMA during 5-

minute-long mixing. As described in the experimental part, this method turned not to be workable due to the forming the dry consistence that resisted to be mixed to more liquid one. Mixing was planned to be carried out on a RUBI Rubimix 50 N forced circulation mixer. For a stiff consistency check prior to the pumpability test, it was proposed to perform an indicative consistency test by measuring flow on a handheld flow test kit [Fig.28].

Fig.28. Simplified test apparatus and demonstration of the flow test for an indicative check of the consistency of the mixture before printing

Subsequently, a pumpability test will be carried out by pumping fresh material by pump S8 via 3m long hose DN25. The aim is to verify the pumping performance, its reserve and controllability. It will be carried out by pumping fresh material for about 2 minutes back to the mortar pump while increasing the pump power to the maximum level. Pumpability in this case corresponds not only to the ability of the material to be displaced, but also to respond flexibly to changes in pump power and to provide a reserve of pumping power at the highest pump power level. This is necessary to maintain the pumping rate at the end of the hose during 30-60 minutes of pumping, when the consistency of the material will decrease due to solidification and the need to continuously increase the pump output. The result will be evaluated visually by subjective assessment - a successful test will demonstrate the ability of the material to be forced out of the hose at varying rates corresponding to the pump rate. Should the difference between the lowest and highest pumping rates be minimal, the consistency will need to be adjusted to a more fluid consistency by adding PCA.

*Fig.29. a) Test print to find the optimum extrusion coefficient f with the resulting miniprotocol
b) Testing trajectories for testing of v/f parameters according to v-f script*

After verifying the pumpability, it was proposed to perform the extrudability test by extruding the material from the nozzle on a printer without moving the axes. This test will be carried out by pumping material into the nozzle at pump power level 1 at a static position of the print head at a height of approximately 250 mm above the substrate, while simultaneously extruding the nozzle at f 0.15 for 30 seconds. This test extrusion will be set up in the Pronterface environment. A successful test will verify the ability of the material to be extruded from a given nozzle at a sufficient rate and will indicate the quality of the material in the loose layers and its possible defects i.e. cracks. In the case of a nozzle with pressure control, the nozzle bypass through the control outlet will also be checked. If this test passes, the final printability test can proceed. These will be ensured by running print jobs according to the given scripts. Execution of the print job will be ensured by continuously pumping material into the print head at the appropriate pump speed while running the print GCode script in Pronterface. This will ensure the movement of the print head and extrusion from the nozzle according to the parameters given by the script. In the case of material testing, it will first be necessary to verify the v/f printing parameters for a given mixture, layer parameters l/w and nozzle diameter. This will be ensured by printing the Testing v-f script, which is designed in (Chapter 5.4) as a sequence of 790 mm long straight trajectories differing in the v/f parameters [Fig.29].

After finding the optimal v/f parameters, it will be possible to proceed to testing the buildability of the material and the printability of the script. In case of insufficient buildability, the inherent weight of the layers and the insufficient strength of the partially hydrated material will lead to the depletion of this strength and subsequent visible deformations of the printout, possibly leading to loss of stability and collapse, before the print job is finished [Fig.30].

The author assumed that a combination of material properties, surrounding environment properties, technological parameters, and model geometry would have an effect. On the material properties side, the main issues were the consistency of the mixture, the initial strength and the rate of ramp-up. The environment affects the hydration and thus buildability by temperature and humidity. Among the process parameters, layer height, nozzle travel speed, extrusion coefficient, printing time, material batch size and type of printing trajectory of the model will affect printability. Testing will be therefore required for each model and material combination.

Fig.30. Collapse of TAM geometry during printing process due to an error of printer, causing unexpected layer eccentricities on top

In terms of model geometry, the slenderness and eccentricity of the walls in the direction of the wall normal, the maximum overhang of the layers or the length of the shortest layer played a role. In the case of loss of stability, the priority was to preserve the geometry of the object, unfortunately any collapse of stability led to a time delay and thus in most cases to a progression in the hydration of the material and thus its deterioration without the possibility of further use. The first modification to increase buildability was a modification to the technology, consisting of extending the print time by reducing the speed v. This meant in some cases extending the print time beyond the value of the open-time material. Because of this, it was necessary to reduce the material batch size and increase the number of batches. This procedure led to the risk of changing the pumping performance between batches with different consistencies and therefore to a change in the width of the layers and associated layer quality defects. This was solved by smoothly feeding successive batches of material by gradually mixing the fresh batch into the previous one in the pump hopper with the help of the pump operator. This activity required considerable experience and was very mentally and physically demanding. In case this procedure did not lead to improved buildability, it was possible to increase the printing time by reducing the layer height, which affected the physical appearance of the print compared to the original visualisation and made it necessary to match the layer height in the case of objects composed of multiple smaller prints. If increasing the print time did not ensure the stability of the printout, the situation could be addressed by increasing the layer width. This modification required offsetting the trajectory axis by half the difference in layer widths to maintain the outer envelope of the object, while at the same time entailing higher material consumption and higher weight of the prints. Such intervention in the object geometry meant additional work for the programmer if the script was not fully parameterized.

In the case that even after increasing the layer width, collapse occurred during printing, it was necessary to modify the geometry of the object by changing the external shape and reducing the eccentricities of the walls, or by inserting reinforcement elements. In order to monitor the printing parameters and evaluate the quality of the prints, a system based on subjective observations has been developed, similar to small-scale testing. This system has been summarised in the Chapter 6 in an original test report. On the basis of the tests carried out in this dissertation, it was therefore possible to determine precisely those properties that significantly affect the buildability, printability and quality of prints.

Tab.31. System for monitoring of printing parameters and evaluation of print quality

Recipe

Mortar No.	Dose (kg)	CEM (g/1kg)	GLS (g/1kg)	ST06/12 (g/1kg)	ST53 (g/1kg)	ST06 (g/1kg)	Water (ml/1kg)	GL (g/1 kg)	MM (g/1kg)	MF6 (g/1kg)
1										

Printing environment conditions and fresh mix properties

Mortar No.	T $_{air}$ (°C)	Φ $_{air}$ (%)	Time of mixing	Time of relaxing	Pumpability	Fastening
1						

Gcode parameters

GCode name						
L		w		v		f	

Printing process parameters and quality criteria

Printing task No.	1
Mortar No.	
GCode	
Print head + Nozzle	
Final printing start	
Final printing end	
Pumping degree	
Pumping surges	
Nozzle bypass flow	
Print height (mm)	
Layer width (mm)	
Layer profiling	
Layer discontinuities	
Layer cracks	
Layer thinning	
Surface deformation	
OVERALL QUALITY	

Tab.32. Rating scale in the system for monitoring printing parameters and evaluating print quality

Monitored value	1	5
Pumpability	Full	No
Fastening	Full	No
Pumping degree	0	6
Pumping surges	No	Strong
Nozzle bypass flow	Full	No
Layer profiling	No	Strong
Layer discontinuities	No	Strong
Layer cracks	No	Strong
Layer thinning	No	Strong
Surface deformation	No	Strong

54

6. RESULTS

6.1. Machinery equipment
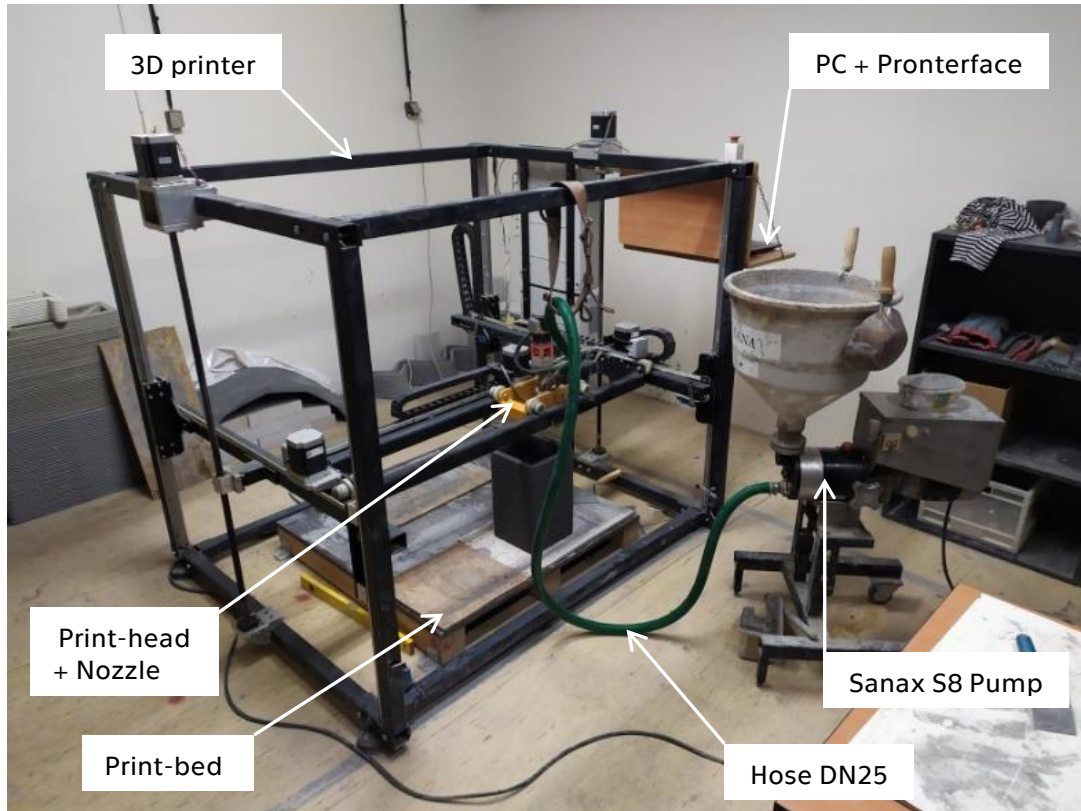
Fig.30. Final printing apparatus

6.1.1. Material preparation equipment

The weighing of dry mix and liquid additives and water up to a volume of 14 kg was carried out on a scale DS608 with a weighing accuracy of 2 g. [Fig.31a] For weighing between 14-80 kg, a CAS DB2 bridge scale [Fig.31b] with an accuracy of 20 g (up to 60 kg) and 50 g (up to 150 kg) was used. During the process of testing the materials in large volume, it was found that the performance of both the DWT BM-720 M mixer and the RUBI Rubimix 50 N mixing station was not sufficient for mixing the stiff thixotropic mixture. The DWT mixer with one whisk was not able to mix the mixture at all, while the Rubimix mixer was only able to effectively mix quantities of up to 12 kg, in addition to a time of 20 minutes, which reduced the workability time of the mixture to an unreasonable limit. In order to increase the mixing capacity and the quantity of the mixture up to 70 kg, an original mixing station [Fig.31c,d], with one speed and a mixing vessel capacity of 60 litres with an output of 2.5 kW and a supply voltage of 400 V was manufactured by an external supplier based on the experience with the RUBI mixer. The mixing volume was sufficient, but it took up to 25 minutes to mix 50 kg of CM276 with this machine for a stiffer consistency, which disproportionately increased the working time and reduced the workability/open time of the mixture. This mixer, as shown further in the practical section of the thesis, was found to be underperforming for mixing stiff thixotropic mortars during the

course of the project and was henceforth designed for mixing dry ingredients only. For the mixing of fresh mixtures, the following was acquired gear stirrer FESTOOL MX 1600/2 EQ DUO with double rods, which shall be able to mix up to 90l of mortar [Fig. XX]. The stirrer allowed changing the mixing performance between stages 0-6. This was already found to be fully sufficient for the purpose of preparing the wet mix. Mixing of both dry and wet mixtures was carried out in plastic masonry buckets and mortar buckets of 30 and 60 litres capacity.

Fig.31. a) DS608 scale b) CAS DB2 bridge scale c) Bespoke mixing station- Fresh mixing setup d) Dry mixing setup

6.1.2. Material supply system

Based on the design of the supply equipment parameters in Section 5.4.2, it was necessary to find a pump that would be able to pump thixotropic consistency. After consultation with Sanax chemical construction, two pumps were provided - the Sanax S8 with a peristaltic pumping unit [Fig. 32a] and the Sanax DT, fitted with a screw pump [Fig. 32d]. The S8 pump is designed by the manufacturer for grout and fine-grained mortars, whose pasty consistency should, according to the consultation with the supplier, allow flowing from the trowel. The DT pump is designed for pumping medium flowing fine grain mortars, adhesives and paints. Both pumps have been tested by pumping 6 to 12 kg of wet mix of a given consistency several times. Both machines allowed the pumping power to be regulated down to zero. The upper power value allowed, even with a reserve, to pump out the mortar at a rate of about 8 l/min.

Testing of both pumps was carried out on C276 cement mortar with a flow of 140 to 160 mm (see Chapter 6.3.2 for more details). The peristaltic pump, operating as a cyclic machine, exhibited pressure surges, causing slight pressure fluctuations of approximately 0-10%, which affected the quality of the layers when printing from the tube. Its maintenance was very easy due to its simple design and cleaning time took a maximum of 5 minutes. The spindle pump, operating as a continuous machine, did not exhibit surges, but its maintenance proved too demanding. The design of the pump itself includes a cylindrical chamber used to feed material from the hopper to the spindle, which is sandwiched between the motor and the spindle. In this chamber, after approximately 20 minutes of pumping, the print mortar settled and subsequently solidified in the space between the chamber shell and the working area of the screw feed vanes. Cleaning of such deposited material was very difficult even after disassembly and took over 45 minutes beyond cleaning of the remaining parts

of the pump, moreover, the mortar deposited in the chamber was unusable and increased the amount of waste. Based on this testing, the S8 peristaltic pump was subsequently purchased.

The pumping part using peristalsis works on the principle of material moving in a circular motion through a protrusion. This movement is ensured in the mechanical part of the pump by sliding the metal pins out of the circular ring by a rotating motor-driven eccentric. Pumping performance is ensured by regulating the maximum degree of pin extension by means of a rotary wheel on the side of the pump, allowing 0-6 revolutions. The pins press against plastic or aluminium slats (depending on the pump version), which ensure that the material in the pumping space, formed by an aluminium ring, is moved into the outlet opening. The pumping area where wet material or water flows is separated from the mechanical part with the slats by two silicone sealing membranes in the shape of intermediate rings. The pumping compartment is enclosed at the front of the pump by a solid circular steel face, with an inlet connected via a quick coupling to a plastic hopper in the upper part and an outlet to a hose in the lower part. The face is attached to the pump body by a bolt in the axis of the face, which passes through a sealing rubber profiled liner and the pumping and mechanical parts.

An important part of the operation of the transport system was the preparation and final washing. Before each use of the pump it was necessary to pump approximately 2 litres of water through the pump, hose and print head and nozzle to flush out any deposits, cover the system with a water film to facilitate pumping of the mortar and ensure that the inside of the system did not take the water from the mortar during printing. As part of the preparation of the printing apparatus, the first approximately 2 litres of material were then removed at the start of the pumping process to collect the water trapped in the system during the flushing process. When the printing was finished, or if the printing was interrupted for longer than the set-up time of the mortar, the apparatus had to be flushed with about 10 litres of water to prevent the material from setting. During testing, it was found that the volume of the internal part of the pump was about 0.5 litres. The volume of the inner space of 1 metre of DN25 hose is approx. 0.5 litres, so with a hose length of 3 m, 2 litres, i.e. approx. 4.5 kg of extra dry mix, had to be used each time to prepare the material. This volume of material, together with the 2 litres of material mixed with the water in the system at the beginning of the press, was waste at the end of the press.

The Sanax S8 pump and accessories were adapted to the needs of the 3D printing technology based on the needs that arose during the project. The hose included in the original delivery of the S8 pump was not suitable due to its excessive stiffness and the type of end connections to the printer, so it was experimentally replaced with a standard DN25 garden plastic water hose fitted with GEKA couplings at the ends. For the purposes of the printing technology used, this solution has proved to be perfectly satisfactory, with two lengths of 3 and 4 m being used during the 3 years of printing and only three failures due to wear and tear. The existing bayonet outlet on the pump was replaced with a GEKA coupling to connect to the new hose. The supplied pump chassis with two running wheels proved to be too low and unstable for refilling purposes during 3D printing. Therefore, it was supplemented with the original jack-welded chassis, mounted on two mandrels and two mini casters

[Fig. 32b]. The pump motor experienced three failures during print jobs over 1 hour due to the triggering of the built-in thermal protection, so it was fitted with a digital thermometer for temperature control [Fig. 33c]. In the event of a temperature rise above 60°C, it was possible to cool the motor casing and avoid a key equipment failure during printing.

Fig.32. a) *Pump S8 b) Upgraded pump S8 c) Thermometer on S8 motor d) Pump DT*

The consistency of the material required the presence of an operator during the pumping process to ensure the filling of the hopper and, above all, the permanent compression of the solid material into the pumping compartment. The operator used a circular rod, a fan, to fill the pump, and in the case of the most rigid consistency it was necessary to push the material into the pump with rubber gloved hands. The operator also monitored the amount of material at the discharge outlet of the print head and the quality of the printed layers and adjusted the pumping power of the pump and thus the pressure value in the hose accordingly. In the event of an increase in the stiffness of the material, it was then necessary in some cases to moisten the material with a spray gun. The operator's work was very demanding, filling required considerable physical strength, pressure regulation required considerable experience and foresight, and coordination of all activities required coolness.

An important characteristic of the pumping system, which significantly affects the printing technology and the resulting print quality, is the pressure rigidity of the selected pumping system. The system is not able to react flexibly enough to changes in pump performance due to leaky joints, frictional pressure losses and hose flexibility. Thus, a rapid change in material consistency due to the onset of material solidification or the subsequent pumping of material from multiple batches of different consistency results in a delayed response at the end of the system, i.e. in the print head and thus the nozzle. This makes it very difficult to ensure a uniform supply of material to the nozzle and to control it by varying the pump output without the risk of pressure fluctuations in the nozzle and consequent variations in the layer profile.

The pump was used for pumping all the materials mentioned in this thesis for a total of about 1200 machine hours. After about 400 hours, due to the excessive stress on the pumping chamber, the pins of the pumping chamber were worn out, bent, or their ends were widened and one or more pins in the ring were subsequently straightened [Fig.33]. The wear was apparently related to the material consistency, which in used single component 3D printing mortars was due to thixotropic behaviour stiffer than in mortars prescribed by the pump manufacturer. In one case, the pins were straightened during pump operation, resulting in the peristaltic unit being

destroyed and having to be completely replaced. After approximately 1200 hours of operation, the aluminium ring forming the pump body was worn out and due to leaks causing pressure losses, the pumping performance dropped dramatically, making it impossible to pump the material efficiently.

Fig.33. a) Peristaltic lamellas of S8 pump b) Pins of S8 pump, worn out after 400 machine-hours. c) Internal worn-out front cover and sealing rings.

Further applicability of the S8 pump will be addressed in follow-up research after the defending of this thesis. In addition to replacing the worn-out ring, the author proposes to solve the situation by changing the printing technology and switching to a two-component material. The advantage of such a solution is, besides the rapid onset of solidification of the layers and the resulting dramatic increase in buildability, also the prolongation of the workability of the material. The material can be significantly more fluid, allowing the pump to be filled by gravity and saving one person. It will also be necessary to address the pressure control between the printhead and pump by automatically synchronizing them so that the presence of the pump and nozzle operator can be reduced. For this purpose, it is envisaged to acquire a MAI pump specifically designed for 3D printing.

6.1.3. 3D printer

Based on the specification in chapter 5.3.3, an original 3D printer was fabricated with significant contribution of the author and delivered in 2019 [Fig. 34]. Details of specific parts of the printer are shown at Fig. 35-38.

Fig.34. a) 3D printer parts before assembly b) Assembled 3D printer, carrying PH5
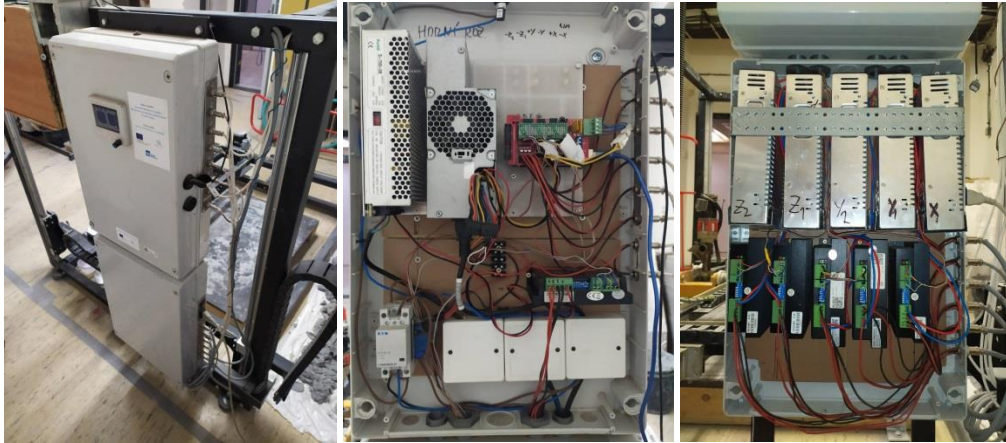
Fig.35. a) Control unit boxes b) Detail of upper box- extruder power supply unit, Arduino power supply unit, Arduino PLC, extruder driver, contactor c) Detail of lower box- power supply units and drivers for stepper motors X, Y1, Y2, Z1, Z2.
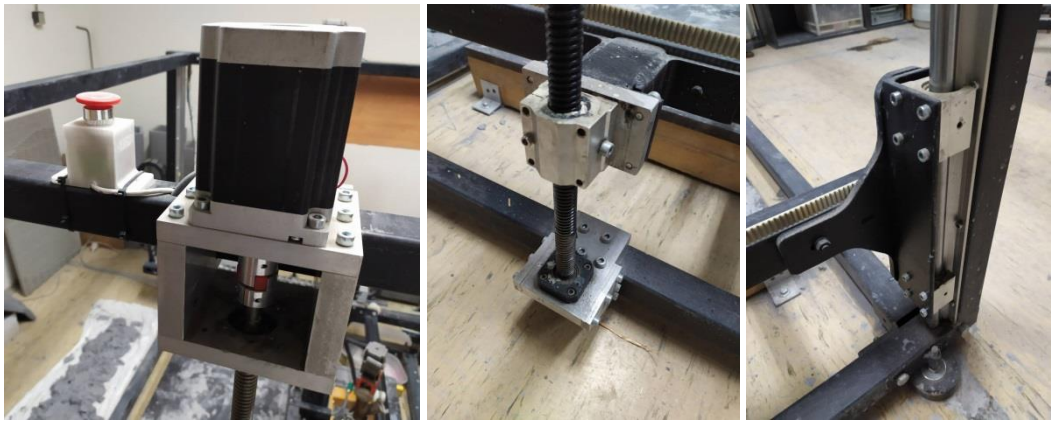
Fig.36. a) Detail of Z axis upper fit with step and emergency stop button
b) Detail of the Z axis lower fit with torque bar and ball bearing
c) Detail of the Z axis linear motion slide guide rail with pair of ball bearings sliding blocks
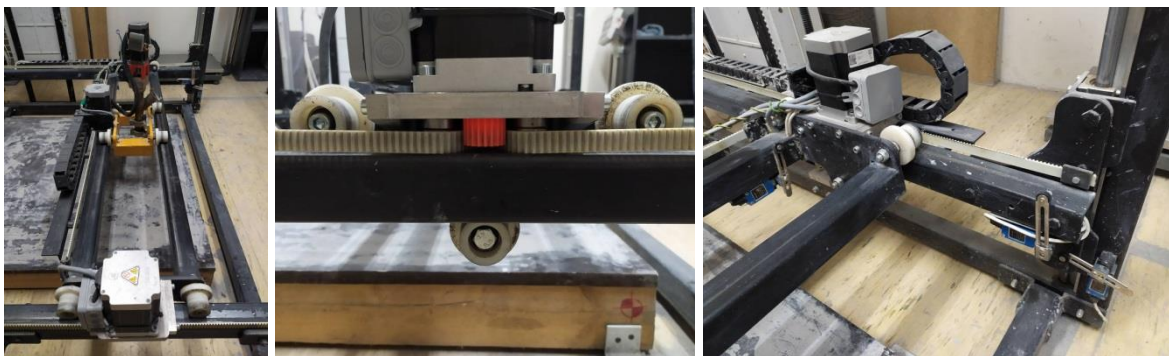
Fig.37. a) Y axis cart, carrying X axis cart b) Detail of 3D printed shepherd on Y axis motor c) Detail of the XYZ axis corners with end stop

Its acquisition was made possible within the framework of the project Innovated Laboratory and Testing Infrastructure for the Doctoral Programme in Civil Engineering under the subsidy programme Operational Programme Research, Development and Education. The printer was located in room CS134 as the basis of

the author's thesis of the newly built 3D Printing Laboratory in Civil Engineering. The printer was mounted on the floor over rubber targets with height rectification. Its structure was aligned using a laser gauge and rectification so that the Z axis was vertical, and the Y axis of the printer formed a horizontal plane, all to an accuracy of ±1 mm. A pallet was placed in the corner of the print space corresponding to the 0, 0, 0 coordinate and after rough alignment with the laser gauge to the horizontal plane with an accuracy of ±1 mm, it was anchored to the floor with chemical anchors. The top corner of the pallet board was then aligned to a point corresponding to the printer coordinates 0, 0, 0. The print head with the corresponding extrusion nozzle must be anchored into the X-axis carriage and fixed so that the nozzle mouth axis is at position 0, 0, 0. The head must be connected to the control unit via a cable connector. The head should then be connected via the GEKA coupling to the hose connected to the mortar pump. The printer must now be connected via USB cable to the PC running Pronterface. After pressing the network connection switch in Pronterface, the printer must be connected via the appropriate port.

Fig.38. a) X axis cart, carrying PH5 b) X axis cart from bellow, with nozzle TP11 c) Detail of 3D printed shepherd on X axis motor

After connection to the pump with the material of final consistency, the nozzle must be raised to a position that allows the extrudability test. This is done by simultaneously starting the pump and the E command with the appropriate numerical value corresponding to the length of the extrusion interval in seconds, e.g. E300. In Pronterface, the Speed value must be set beforehand, which sets the extrusion coefficient f. The execution of commands can be interrupted by the Pause button or terminated by the Off button. After the extrudability has been verified, the HOME command must be executed, and the printer will align itself via the limit switches to the position 0, 0, 0. From the HOME position it is possible to start the print job with the Print button after loading the appropriate GCode script. For most print jobs in this thesis, the HOME command is given at the beginning of the script and therefore does not need to be entered separately. G01 Z150F500 and G01Z250F500 shortcuts have been added to the bottom bar of the Pronterface for quick entry of common commands to test the extrudability of the material into buckets 150 and 250 mm above the worktop.

This printer was further modified during the elaboration of this thesis according to the needs of technology development. The X-axis trolley was equipped with various attachments, allowing quick assembly and disassembly of the DN 20 tube and several different types of print head. The supply hose from the pump was flexibly anchored to the printer frame in order to reduce the load on the X-axis and to avoid collision between the hose and the print, which was crucial especially for prints of 400 mm or more. Print jobs, where multiple prints up to approximately 30 kg in size were required, were run on 18 or 24 mm thick backing plates, stacked on a print pallet, with the option to move the print from the print area to the curing area on the plate after the print job was completed and to run another print. It was then necessary to change the value of the Z-offset parameter in the control script by the value of the thickness of this plate.

While testing the printer, an unexpected problem with the execution of the HOME command occurred. When the printer tried to set itself to the Z=0 GCode position using the HOME command, in some cases the control system ignored the Z-axis limit position signal from the limit switches and the Z-axis travel collided with the printer frame. The functionality of the switches was verified in Pronterface by an existing signal after the M119 command was entered. As a consequence, a height difference in the position of the carriage on the trapezoidal bars Z1 and Z2 was sometimes created and the Y-axis was subsequently deflected out of the horizontal plane. This problem had to be solved by aligning the trapeze bar on the deflected axis using manual rotation and checking with a spirit level. In some cases, the control system also ignores the Y-axis value setting and adjusts to the last known position. The author assumes it was caused by overflowing the controller memory as it was solvable by turning the printer off and on, disconnecting it in Pronterface, and sometimes restarting this application.

6.1.4. Printhead

The author first tested the possibility of using a 300 mm long DN20 pipe, carried by a trolley on the X-axis and directly connected by a hose to the S8 pump, as an extrusion nozzle for 3D printing [Fig.40a]. During the printing process, it became apparent that this solution was unable to eliminate the pressure fluctuations from the cyclic peristaltic pump S8, resulting in undesirable fluctuations in the width of the layers or layer breaks [Fig.39b,c]. This solution did not allow for constant pressure or flexible control of the extrusion output according to the needs of the GCode controller.

The pipe solution was therefore abandoned and the PH1 print head was fabricated, allowing the GCode to control the pumping power by means of a motor with a screw and to be fitted with interchangeable extrusion nozzles of different diameters and material solutions [Fig.40a]. During the testing of the PH1 printhead, it proved to be very difficult to balance the nozzle pressure with the material pressure supplied by the pump without pressure sensors. The solution offered was to balance the pressure between the nozzle and the pump using a pressure sensor in the nozzle and an electronic speed control in the pump linked to it. Due to the complexity and cost of this solution, it was chosen to address the pressure control in a simpler way.

Fig.39. Printing by extrusion of DN20 pipe a) Set-up b) The first successful print of CM276 mixture c) Fluctuations in pressure and layer appearance when printing from a pipe without an auger and pressure control

The body of the printhead was provided with a second opening opposite the material inlet, allowing material not removed by the screw to leave the printhead space and not increase the pressure in the body and subsequently in the nozzle. This solution had the advantage of being able to visually control the pressure in the head body based on the amount of material leaving the print head body space and increase the pump output accordingly. Excess material was to be hosed off into the pump hopper and reused. In order to test this assumption, a print head PH2 was fabricated by 3D printing from CPEG [Fig.40b].. It addressed the material control by expanding the inner nozzle body and supplying and removing material from the auger in the direction of the auger shaft normal. Subsequent testing of the PH2 confirmed the concept's ability to regulate pressure by bypassing material. The translucent discharge hose did indicate the volumetric flow rate at the discharge outlet of the PH2 body, but after pressure tuning, the amount of material being diverted was in the order of millilitres per second, so that there was no continuous discharge of material to the pump hopper.

Fig.40. a) PH1 with interchangeable nozzles b) PH 2 with pressure control by material discharge

Subsequently, a PH3 printhead was manufactured using DN30 elbows and crossovers, which had a drain hose only about 300 mm long [Fig. 41a]. The hose was to be used only for visual pressure control and a place where excess material could be stored without the possibility of further use. This solution was used for about 1 year,

then due to the need to test different material consistencies and different nozzle sizes [Tab.33], [Fig.42b] it was no longer usable.

Tab.33. Interchangeable nozzles used

Nozzle	TP-10	TP-10-120	TP-11	TK-12	TP-16	TK-18	TP-22	TK-25
Material	CPEG	CPEG	Metal	Metal	CPEG	Metal	CPEG	Metal
Diameter (mm)	10	10	11	12	16	18	22	25
Length (mm)	60	120	55	55	80	55	80	55
Layer width (mm)	15-18	15-18	15-18	18-20	20-24	21-25	25-32	30-36

Therefore, a PH4 head was manufactured in which the excess material fell freely through a perpendicular, continuously closed discharge outlet from the body into a plastic hopper, from which it was manually transferred to the pump hopper after filling and reused. This action required an extra worker in the event of higher material flow at the discharge outlet due to a more fluid consistency or small nozzle profile but proved to be the most effective in terms of pressure control and achieved layer quality and was used for the remainder of the project. In order to better coordinate the material inlet and outlet, a PH5 head was subsequently fabricated where the inlet and discharge outlet of the nozzle body are perpendicular to each other [Fig. 41c].

Fig.41. a) *PH3 with material discharge without pressure control b) PH4 with infinitely adjustable material discharge for nozzle pressure control c) PH5 with discharge perpendicular to the side*
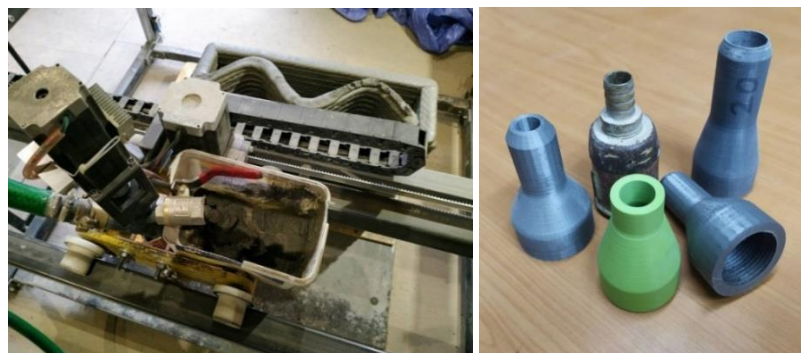
Fig.42. a) *Pressure control in PH4 - discharge of excess material into the vessel c) Demonstration of different nozzle designs*

6.2.   Modelling and programming of print scripts

During the implementation of the project, it was found that in Grasshopper, if a print trajectory is composed of multiple sections, some sections of an otherwise continuous trajectory may result in an incorrect assignment of the directional vector of the curves and subsequently generate a script where trajectories with the opposite direction of the velocity vector are superimposed. This results in errors being transferred to the generated GCode script (sample part of the GCode script on the page 76. When such a script is loaded into Pronterface, the necessary travels are then automatically generated by the system as part of the trajectory alignment, which are then inserted between the print sections, so that the print trajectory is interrupted by unwanted travels instead of a continuous flow. Unfortunately, the Silkworm plug-in does not allow visual simulation of the print trajectory, so the author solved this problem by extending the script with a part [Fig 43a] that enabless to display the directional vectors of all trajectory sections via arrows [Fig 43b].
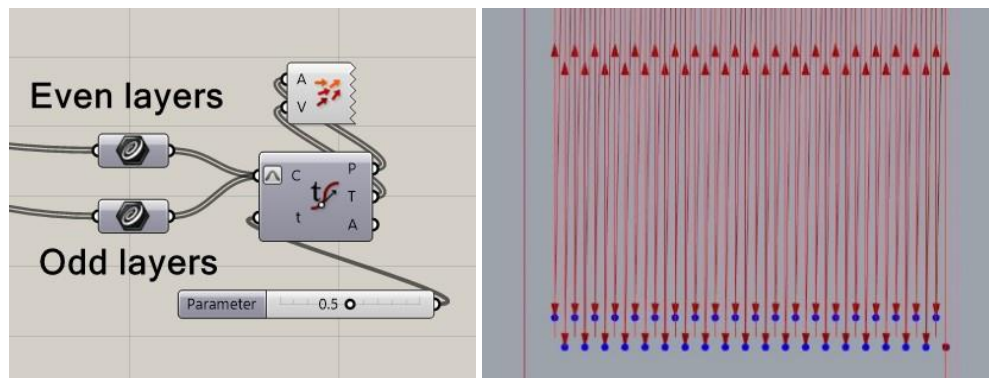
Fig 43 a) Grasshopper script to display directions of trajectory curves b) Directions of trajectory curves displayed in Rhino as arrows

Even after this problem was solved, it was desirable to check the GCode scripts on the printer before printing according to the methodology described in Chapter 5.4.

After the script was found to be error-free in the virtual tools, its functionality was then checked by dry testing on the printer. Dry testing consisted of running the script on the printer via Pronterface without connecting to the pump. If the printer executed the script flawlessly, it was possible to perform a wet test by printing, i.e. running the script with the printer connected to the pump supplying the print material. During this test, the parameters of the print job could be further adjusted within the script in order to achieve the maximum ratio of print quality to print efficiency. The shape of the models in terms of the constraints imposed by buildability was solved for the first scripts by estimation and later based on the experience gained during the first 3D printing jobs.

In the experimental part of the thesis, dozens of scripts were developed by the author for different types of objects and print trajectories, examples are included in the case studies.

Sample part of the GCode script (Total length is 63 829 lines)
Vase__H-O50__318x318x1000__w25__L8__Z0__f0.08__v2700__57.29kg__47.15min

; NAME: Vase__H-O50__318x318x1000
; TK3-HAD-DN16
; LAYER HEIGHT:8
; Z-OFFSET:0
; FLOW: 0.08
; PRINT SPEED: 2700
; CENTER OF PRINTING AREA: {500,200,8}
; TOTAL LENGHT:127.31 m
; DRY WEIGHT:57.29 kg
; ESTIMATED PRINTING TIME:47.15 min
; DATE & TIME:__2021-09-01__10h07m40s
M83 ; extruder relative mode
G92 E0.0
G21 ; set units to millimetres
G90 ; use absolute coordinates
M83 ; use relative distances for extrusion
;BEFORE__LAYER__CHANGE
G92 E0.0
G1 F0 X0 Y0 Z0
G1 F800 X0 Y0 Z8 E0
G92 E0
G1 F0 X0 Y0 Z8
G1 F4000 X20 Y20 Z8 E0
G92 E0
G1 F0 X20 Y20 Z8
G1 F2700 X700 Y20 Z8 E54.4
G1 F2700 X700 Y200 Z8 E14.4
G1 F2700 X612.5 Y200 Z8 E7
G92 E0
G1 F0 X612.5 Y200 Z8
G1 F2700 X612.5 Y198.03 Z8.01 E0.16
G1 F2700 X612.5 Y196.05 Z8.02 E0.16
G1 F2700 X612.5 Y194.08 Z8.03 E0.16
G1 F2700 X612.5 Y192.11 Z8.04 E0.16
G1 F2700 X612.5 Y190.13 Z8.04 E0.16
G1 F2700 X612.5 Y188.16 Z8.05 E0.16

...abbreviated list of lines 37-63 280

G1 F2700 X387.63 Y283.54 Z1006.48 E0.16
G1 F2700 X387.63 Y287.51 Z1006.5 E0.32
G92 E0
G1 F0 X387.63 Y287.51 Z1006.5
G1 F800 X387.63 Y287.51 Z1036.5 E0
G92 E0
G1 F0 X387.63 Y287.51 Z1036.5
G1 F4000 X0 Y0 Z1036.5 E0
G92 E0 ; reset extrusion distance

6.3.   Material

6.3.1. Redrock printing mixture

As described in Chapter 5.2.2, three 25 kg samples of original cement-based 3D printing mortar F1, R1and P1, differing in recipes, rheological properties and water content, were delivered to be tested. As neither a pump nor a 3D printer was yet available at the time of delivery of the mortar samples, testing was carried out only on a small scale by hand extrusion and standard test methods as suggested in Chapter 5.5.1.

The first task was to find the water content that would ensure the best consistency of the mixture. Regarding that, three batches (I, II, III) of 500g of each material were prepared. Batch I was prepared with the water content at the lower limit of the recommended dose, Batch II with the water content at the upper limit of the recommended amount, and Batch II was prepared with the average of the two values. The weighing of the respective batches was carried out on a Kern EW scale with an accuracy of 2 decimal places. Fresh mixtures were prepared on a standard laboratory mixer. Whole amount of water was placed into the mixer vessel, mixing was initiated, and the dry mixture was gradually added. The wet mixture was stirred for 5 min to fully blend. If the consistency of the fresh mixture was still too dry, additional water was added. The resulting mixture was left at rest for 5 minutes to relax. After the material was relaxed, the cartridge gun was filled with it and the extrusion test was performed as described on the page 57. Tests were performed using an electrically powered sealant gun SKIL Masters F0152055MA Drench gun 2055 MA. Consistency of materials P1-I, P1-II and R1 didn't enable extrusion on SKIL Masters so it was extruded with a manually powered sealant gun Powerfix Profi.

Fig.44. The result of Redrock mixture extrusion test by sealant gun Powerfix Profi
a) Batches F1/II and F1/III b) R1-III c) d) P1-II

Tests demonstrated different properties of tested mixtures [Fig.44], [Tab.34]. Mixture F1 displayed near-to-zero extrudability on both of extrusion guns even after the water amount was increased above the recommended dose; it was extrudable only manually from the open cartridge without the nozzle. Mixture R1 displayed good extrudability on both extrusion guns but its flow was too high, so the buildability seemed to be limited. The best performance was reported on mixture P1-II; it displayed very good extrudability and enabled deposition in stacked layers as shown

on Fig. 45d. The quality of layer texture was also very good as they were smooth and displayed no cracks. However, usability of this mixture is limited as it had open time only around 10-15 minutes, which is too short to be used for big scale printing. As the recipe of the mixtures was unknown, it didn't allow adjustments to improve its performance. Considering the high price (30 CZK/kg) and the inability to flexibly adjust the recipe, the author decided to abandon the cooperation with Redrock and develop the printing material on its own.

Tab.34. Fresh properties of Redrock mixtures F1, P1 and R1

Material	dmax	Water content recommended (ml/kg)	Water content adjusted (ml/kg)	Extrudability	Buildability	Open-time
R1	1	120-130	154	0.5	0.1	25min
F1	0.5	124-130	130	0.1	Not tested	20min
P1	1	148-155	155	1.0	1.0	10min

6.3.2. Cement-based printing mixture

The aim of this chapter is to find the optimal recipe of the fresh cement mixture and to verify its applicability for the fabrication of high-quality architectural elements by two-phase testing with regard to the given printing technology. The first task was to find the ideal content of water and admixtures in order to obtain favourable values of workability, pumpability, extrudability, buildability and printability of the fresh mix. Further, the formulation and technology were tuned to maximize the quality of prints of a wide range of geometries. Following the research-based process described in Chapter 5.2.2., two dry mixtures of cementitious printing mortar were designed (CM276, CM450). Further in this chapter, fresh mixture preparation, properties and performance is described together with selected case studies for both mixtures. Preparation and testing of mixtures were conducted in two steps using methods and equipment described in Chapter 5.

CM276 mixture

Based on the dry mixture recipe, six types of fresh mixtures were designed to be tested varying in admixtures and water content. The aim was to reach the lowest possible content of water, i.e. maximizing strength and minimizing set up time while maintaining workable consistency by the high PCA content similarly to the SCC. The buildability was planned to be controlled by VMA. During first tests, it turned out the original idea of mixing process is not workable due to the low water content. When the whole amount of dry mixture was put in into the mixing vessel, mixer was turned on and water with PCA was gradually added, the mixture formed balls of material, which were almost impossible to break off even if the time of mixing was extended up to 20 minutes. So the process had to be reversed. To maintain workability, the whole amount of water and PCA was placed into the mixer vessel first, mixing was initiated, and the dry mixture was gradually added. The wet mixture was stirred for 5 min to fully blend. When the mixture gained liquidity, the VMA was gradually added till the consistency seemed to be workable. Its content was increased during mixing

of 2 minutes to maximize the viscosity and therefore the buildability of the resulting mixture. After 5 minutes of relaxing, testing of CM276 mixture started according to methods outlined in Chapter 5.5, The flow test was conducted the first. Subsequently, an extrusion test was performed [Fig.45]. The consistency of all mixtures was too stiff to be extruded by the electrically powered sealant gun SKIL Masters so all tests were facilitated on a manually powered sealant gun Powerfix Profi. As shown in Tab. 35, the best results were achieved by the mixture CM276, which was further tested and modified by full scale testing.

After determining the ratios of the components of the fresh mixture on a small scale in quantities up to 1 kg, testing on a full-scale apparatus in quantities of several kg was proceeded with. The author assumed that when testing on a full-scale apparatus, due to the multiply higher quantity of the mixture and the different mixing technology, there would be differences in the results and the recipe verified on a laboratory scale would have to be adjusted. Mixing of the dry mix in batches of 8-12kg was carried out using a DWT BM-720 M mixer with a single mortar whisk in a 20 litre bucket for 5 minutes, where the ingredients were added sequentially from coarsest to finest [Fig.46].

Fig.45.a) b) c) The results of extrusion tests using sealant gun Powerfix Profi

Tab.35. Options of CM276 mixture according to water and additive content

CM276	A	B	C	D	E	F	G	H	I
Component	m (g)	m (g)	m (g)	m (g)	m (g)	m (g)	m (g)	m (g)	m (g)
CEM ČM	276.0								
MS	31.0								
ST06/12	255.0								
ST53	255.0								
ST6	183.0								
Water	150.0	125	125	125	125	120	115	115	110
PCA	3.0	6	3	3	3	3	5	4	6
VMA	3.0	3	6	5	3	3	4	4	3
w/c	0.49	0.41	0.41	0.41	0.41	0.39	0.37	0.37	0.36
Spread (Flow) (mm)	180	185	135	140	145	130	147	137	150
Extrudability	1	1	3	2	1	4	1	3	2
Buildability	4	5	1	1	1	1	2	1	2
Workability (min)	35-40	35-40	20-25	25-30	25-30	20-25	25-30	25-30	25-30
Rating	7	8	6	2	1	9	5	3	4

The preparation of the wet mixture was first tested on an 8kg sample. Adding water with PCA to the full batch of dry mixture proved to be inoperative when stirred with a DWT BM-720 M stirrer in a 20 litre bucket, the material formed a ball that could not be stirred [Fig.47a]. Further, the mixing was done as dry to wet only, i.e., first the whole mixing batch of water with PCA was put into the bucket, then the dry component with fibres was gradually added while stirring, and after reaching a liquid consistency, VMA was added. In the case where the VMA was added all at once, solid balls were formed in the mixture, which were very difficult to stir, so it was necessary to modify the procedure and add the VMA gradually [Fig.47b]. The DWT BM-720 M mixer was subsequently replaced by a RUBI Rubimix 50 N mixing station due to the low mixing efficiency of the mixture with VMA.

Fig.46. a) Mixing of dry components in custom-built mixing station b) Mixing of 018 kg of fresh mortar with MX 1600 DUO 2 gear stirrer with double whisks

Fig.47. a) Consequence of inappropriate mixing procedure - adding water with plasticizer to the whole batch of dry mixture leads to the formation of dry mixture with lumps.
b) Temporary change in consistency after addition of VMA - formation of spherical lumps

After a five-minute relaxation of the material, the consistency of the mixture was verified by an indicative flow test on a simplified test apparatus [Fig.48]. The flow rate was measured at an acceptable value of 145 mm, so the pumping test could follow [Fig.49]. It was performed on peristalsis pump S8. Prior to mixture, 2 litres of water were used to cover the inner surfaces within the pump and the hose by water film, so the fresh material can easily flow through the system. After all recessive water was drained the fresh mixture was placed into the hopper. It was too stiff to penetrate into the peristalsis unit naturally by gravity, so it was pressed by the wooden stick. The pumping started with the flow rate set on level 1 of 6. The mixture enabled

pumping in a full range of 0 to 6, so the pumpability was the pumpability was assessed as satisfactory.

After verifying the pumpability, it was proposed to perform the extrudability test by extruding the material using a printer without moving the nozzle as proposed in 5.5.2. Full scale printing tests started in the end of December 2018 following the successful dry testing of the recently developed 3D printer. As there was no printhead developed yet, the extrudability test of CM276 was provided using a DN20 pipe [Fig.40]. Extrusion was facilitated solely by pump S8, directly connected to the extrusion pipe. This solution didn't allow controlling the extrusion in terms of stable extrusion rate as did the printhead, where the extrusion was controlled via auger. The aim of extrudability test was to verify the ability of the material to be extruded from a given nozzle at a sufficient rate and indicating the quality of the material in the loose layers and its possible defects, i.e. cracks. Testing displayed good extrudability in full range of pump power, so the final printing tests could be started. The first print was conducted according to a simple script with the path consisting of circular 18mm high horizontal layers of d=280mm, connected by vertical travels.

Fig.48. Simplified flow test of CM276-123-3-5-0.6-0.8 (modified by admixtures:123 g W, 3g MG, 5gMM, 0.6gHCA, 0.8g MF6). Flow value 150 mm.
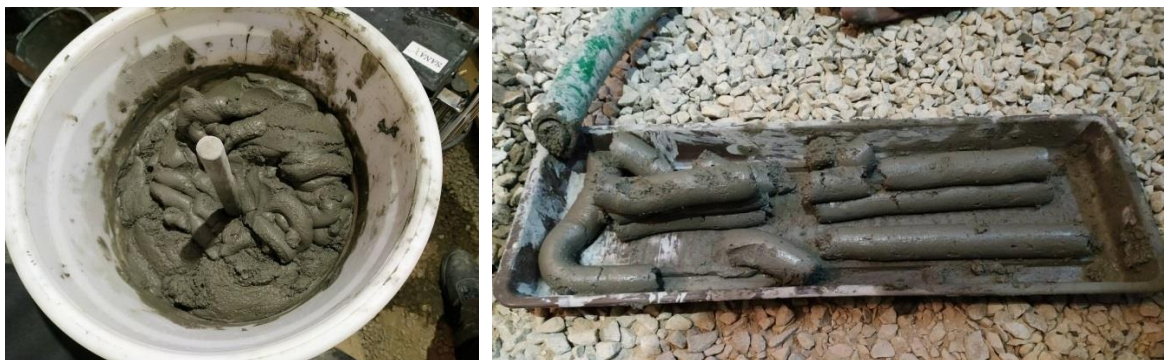
Fig.49 a) Consistency of material in the pump hopper before pumping test with manual filling with wooden rod b) Unsatisfactory result of the mixture pumpability test – material is too stiff

During January and February 2019, the tube printing technology was gradually adopted. Different extrusion combinations and speeds were tested, and experimentation was also conducted with the CM276 recipe. Initially, due to unfamiliarity with the technology and material behaviour, the result was printing with massive layers [Fig.51a], as know-how increased with time; the layer profile was reduced to L8/W24 [Fig.51b,c]. Gradually, printing of smooth layers without cracks was

also mastered. During January and February 2019, the tube printing technology was gradually adopted. Different extrusion combinations and speeds were tested, and experimentation was also conducted with the CM276 recipe [Fig.50a]. Initially, due to unfamiliarity with the technology and material behaviour, the result was printing with massive layers, as know-how increased with time, the layer profile was reduced to H8/W24. Gradually, printing of smooth layers without cracks was also mastered. Size of printed geometries was still limited to 300mm height by insufficient buildability. The solution to the problem of insufficient buildability encountered the technological problem of limited extrusion control and the resulting layer fluctuations. The control of extrusion was possible only by adjusting the power of pump, but as the pumping system was elastic, it displayed delays in time and pressure when adjusted. To solve this problem, it was decided to extrude continuously without pumping stops during travels. It worked well for smaller prints made of one continuous layer generated using spiral slicing, but for horizontal slicing with travels it affected layers in seams, where bulks of deposited material were created. When printing objects over 10 minutes, due to imperfections in the manual pump filling, material supply failures occurred, which were transmitted to the extrusion pipe and caused variations in the layer profile.

These observations demonstrated that it was impossible to achieve print quality without controlling extrusion. For this reason, the first PH1 printhead with auger and interchangeable nozzles was developed. To link it to parametric print scripts, the values of v and f had to be determined. To verify them, the Testing v-f print script was used to verify v-f and to assign layers l and w to the given parameters. During the testing of PH1, it was found that it was difficult to maintain the pressure balance between the screw and the pump. This problem was solved by designing a plastic print head PH2 and then a metal PH3 with pressure regulation by a discharge outlet. Further testing revealed that the speed of rotation of the screw, i.e. the extrusion coefficient f, has a key influence on the shape of the layers. Decreasing this coefficient below 0.08 caused excessive layer profiling and cracking. For layers without cracks and profiling, it was necessary to keep the extrusion coefficient f above this level.

Fig.50. a) v-f script test with CM276 b) Improving buildability and quality by adjustments of recipe

Fig.51. Printing with mixture CM276 by its extrusion from a pipe a) First print – thick layer b) Thin layers after 1 month of development c) Print examples

In order to ensure higher buildability, the VMA content was increased in some formulations up to 6-7g/1kg, or the water content was reduced to 116 ml. In order to increase buildability and reduce crack formation, MF6 fibres were added at 0.6g/kg. The result was a stiffer consistency with a spread of approximately 120-125 mm, with mixing times extended to 25 minutes, which substantially reduced open time. To extend the open-time, the formulation was enriched with the addition of HCA solidification retarder at a dose of 0.5-0.6 g/kg. The resulting formulation, due to the balanced ratio of extrudability and buildability, allowed the printing of design elements up to 800mm in height with L8/W22 layers in high quality without cracks and layer profiling [Fig.50b,c].

Bulks above 15 kg of fresh mix had to be mixed on a custom-built mixing station with a capacity of 62l. The stiffer consistency of the materials caused the mixing time to be extended to 25 minutes, which reduced the open time. In order to reduce the mixing time and thus increase the open time, the MX 1600 DUO 2 gear stirrer with double whisks was used solely for the preparation of fresh mixtures, with which the mixing time dropped to 5-10 minutes depending on the batch size. The change in mixing technology led to a different behaviour of the fresh mix, whose recipe had to be adjusted with each change in technology. The assumption was confirmed that not only is there a difference between laboratory mixing and full-scale mixing, but also that the properties of the mixture depend on the type of apparatus used.

During repeated print tests, it became apparent that consistency verification by the orientation flow test yielded inconsistent results in terms of buildability. A mixture with the same flow rate showed different buildability values for the same print scripts. Therefore, further consistency testing of the fresh mix was performed by visual and haptic assessment of the mix.

As it was more and more obvious how complex were the technology and printing process and how sensitive was the material, more sophisticated methods have been implemented. From the first successful print, a record was kept of each print job to describe the technology, environmental and material parameters for process analysis and repeatability. In the beginning simple logs were used [Fig.52]. The content and appearance of the 3D printing logs was gradually updated over time according to the experience gained, the spectrum of measured quantities was increased, and the graphical form of the records was modified. After 10 months, in response to a sudden change in material behaviour and the need to interpret this

change, comprehensive 3DCP logs were introduced [Fig.53a,b]. The measurement and recording of quantities during the printing process by two to three personnel was very challenging because, due to the material solidification rate of 20-30 minutes, each measurement and recording of values in the logs meant a delay of minutes and thus a reduction in open time. Therefore, it was not always possible to record all the values in the log, nor was it practical in the case of repeating the same values in multiple tasks.

Fig.52. Evolution of printing log a) 01-16-2019 b) c) 01-16-2019

From December 2018 till December 2019 about 85 printing tests were performed using CM276, varying in scripts, admixture and water content, nozzles, surrounding environment and other parameters. Regarding these tests, it was found that other previously unforeseen variables have an influence on the course and outcome of the printing process. During the experimental part, in one case, due to the temporary unavailability of the original cement CEM I 42,5 R produced by Českomoravský cement, a.s. (Závod Radotín, it was replaced by cement of the same type produced by CEMEX Prachovice). However, this change of the input raw material seemingly meeting the same quality requirements of the standard had a significant effect on the final properties of the mixture. The consistency of the mixture was significantly worse, with a spillage of 130 mm during the test. The material showed impaired extrudability during printing and caused tearing of the layers, the recipe could not be repeated with this type of cement therefore only cement from the manufacturer Českomoravský cement was used in the CM276 mixture. Variations in the properties of the mix ingredients also had a large effect on the material behaviour and the quality of printing [Fig.53c]. Their properties varied even when different batches of an identical product from the same supplier were used, as was the case for PCA and VMA. Storage conditions also played a role, with the temperature in the storage area fluctuating between 18-28°C. Technological parameters such as, among others, the heating of the pumping system by the motors and the environment during printing, causing acceleration of hydration, or wear of the pump and auger in the print head, causing pressure losses during pumping and extrusion of the mixture, were also influential.
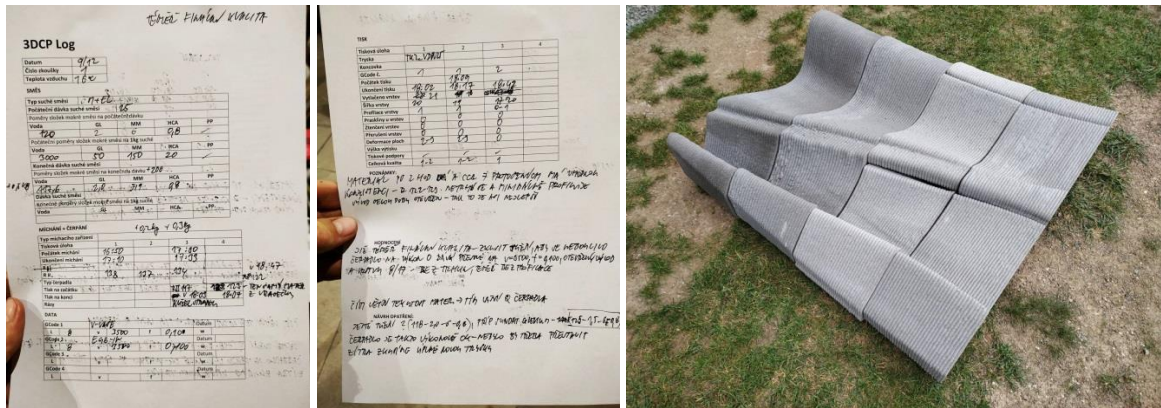
Fig.53. a, b) An early version of complex 3DCP log with handwritten notes c) Varying quality of printing due to variations in the properties of the mix ingredients

Within the project, tests were carried out to determine the flexural tensile strength of the resulting material and to map the effect of orthotropy on this property. For this purpose, a test body was printed from L10/W32 layers with dimensions 250 x 500 x 200 mm [Fig. 54a]. Nineteen test solids were subsequently cut from the solid with dimensions of 40 x 40 x 160 mm. Thirteen specimens were cut in the direction perpendicular to the layers, six specimens parallel to the layers [Fig. 54b]. The surfaces of the specimens were ground locally for better interaction with the test apparatus. The solids were then subjected to a 3-point bending test to complete rupture [Fig.54c]. Seven specimens with the orientation of the cut perpendicular to the layers were loaded as row A with the force applied parallel to the layers, the other six were loaded as row B also parallel to the layers but perpendicular to the direction of the force from the previous test. The remaining six bodies were loaded perpendicular to the layers as row C [Fig. 54b].
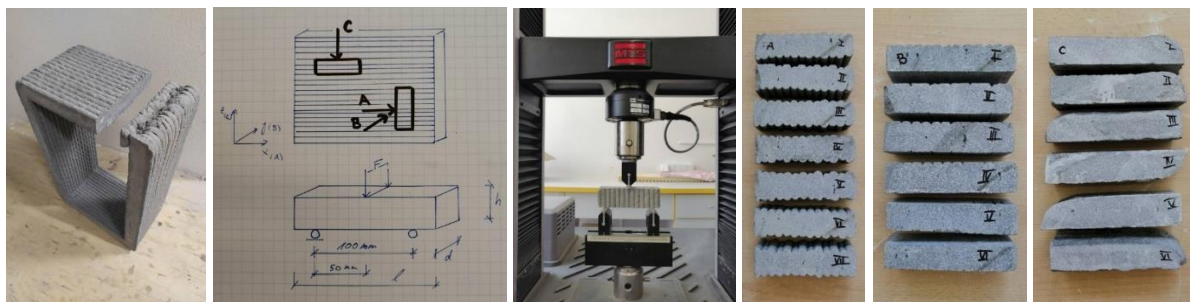
Fig.54. a) Printout for specimen cutting b) Diagram of the position of the specimens and the direction of the applied force for the test of the effect of orthotropy on the flexural tensile strength c) Flexural tensile strength test of CM276 (photo Lukáš Jogl), c), d) Ruptured test bodies as the result of the test of the influence of orthotropy on the flexural tensile strength of CEM276 (photo Lukáš Jogl)

Specimen A achieved a strength range of between 3.4-5.2 MPa. Specimen B had a strength range between 3.9-10.6 MPa. Specimens in row C achieved a strength range between 7.7-16.0 MPa [Tab.36]. The test shows that specimen C, where the applied force was oriented perpendicular to the layers and thus no stress was applied to the joint between the layers, achieved a minimum flexural tensile strength of 7.7 MPa, which is approximately 97% higher than the same value for specimen A and 85%

higher than specimen B. The weakening in specimens A and B can be attributed to the weakening of the material due to imperfect cohesion of the printed layers. It can be assumed the material is therefore orthotropic in nature.

Tab.36. Results of flexural tensile strength test a) Group A b) Group B c) Group C

Group A

	Height [mm]	Weight [g]	F_{flex} [kN]	σ_{flex} [MPa]
1	40,2	375,0	1,1	3,5
2	39,9	390,8	1,6	5,3
3	40,8	390,3	1,6	5,0
4	40,8	385,6	1,6	5,1
5	40,2	387,7	1,6	5,2
6	39,6	372,5	1,0	3,4
7	40,3	380,4	1,0	3,5

Group B

	Height [mm]	Weight [g]	F_{flex} [kN]	σ_{flex} [MPa]
1	39,2	322,9	0,889	4,0
2	39,4	345,6	1,209	4,6
3	39,6	348,5	1,023	3,9
4	40,9	353,6	1,701	6,5
5	39,4	321,7	2,212	10,6
6	39,4	301,9	1,243	6,4

Group C

	Height [mm]	Weight [g]	F_{flex} [kN]	σ_{flex} [MPa]
1	40,5	420,5	2,529	7,7
2	41,1	429,4	4,637	13,7
3	40,1	420,8	4,276	13,3
4	39,5	444,3	4,984	16,0
5	38,7	413,7	3,869	12,9
6	42,2	434,7	3,170	8,9

Case study 1 - Vase V with inclined walls

This study demonstrates possible technological solutions to increase buildability, i.e. the temporary support during printing by sand backfill, reduction of layer thickness and extension of printing time. Model of V vase was designed with walls slanted under 82°, top layer was offset 100 mm from the base [Fig.55]. First Gcode of the 750mm high model was generated with 94 layers of L8/W25. Total weight was 63 kg. Slicing was made as one 114.6m long layer with ramps. Deposition parameters were v3500/f0.18, so the total printing time for was 35 minutes. Material preparation was divided into two doses of 33 kg of dry mix (66 kg for model, 3 kg reserve for the pumping system). Second dose of dry mix was mixed with water 10 minutes after the printing started. There were 3 persons involved, one in charge of the printer, second in charge of the S8 pump and the third in charge of second material dose preparation and as a team support. First printing task ended by collapse after 70% of geometry was printed due to insufficient buildability. It was decided to address buildability by supporting the print during printing by sand fill. Additional labour was necessary to provide sand fill and temporary shuttering made of bricks. It was built to support only bottom 400 mm of print [Fig.56a]. Second printing task was successful, but the surface quality was not sufficient [Fig.56b]. To eliminate additional labour and to address both buildability and the quality, new Gcode was generated with L5/W25 and printing time extended to 55 minutes. Third printing task was successful; the printout had almost perfect quality. The curing of the printout was provided by spraying of water in two following days. After 7 days of hardening, white spots appeared on the vase [Fig.56c]. It was not possible to wash it down by pressure washing. Author assumes it was calcium hydroxide efflorescence caused by inefficient curing. The key parameters of the selected printing task are summarised in the printing log [Tab.37].
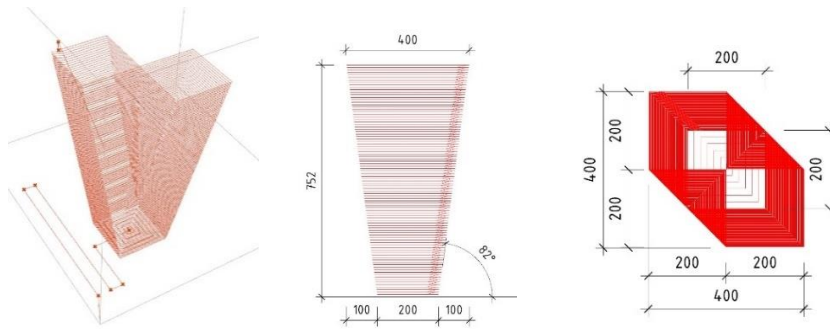
Fig.55. Printing path of V vase in Rhino a) Axonometry b) Elevation c) Top view

Fig.56. a) Printout of V vase L8/W25 with layers supported during printing by sand backfill b) Hardened printout after 2 weeks c) Hardened V vase L5/W25

Tab.37. Case study 1: Log of print tasks for vase V (problem values in yellow)

CM276-F	Dose (kg)	Water (g/kg)	MG (g/kg)	MM (g/kg)	HCA (g/kg)
1	33	120	3	3	1
2	33	120	3	3	1
3	38	120	3	3	1
4	28	120	3	3	1
5	38	120	3	3	1
6	28	120	3	3	1

Mortar No.	t_{air} (°C)	Φ_{air} (%)	End of mixing	End of relaxing	Pumpability	Fastening
1	22	42	+10	+15	2	3
2	23	46	+10	+15	2	3
3	24	50	+10	+15	2	3
4	24	50	+10	+15	2	3
5	20	36	+10	+15	2	3
6	21	38	+10	+15	2	3

GCode1	Vase-V_425x425x752_w25_L8_Z0_f0.18_v3500_63kg_33.35min_2019-06-25						
L	8	w	25	v	3500	f	0.18
GCode2	Vase-V_425x425x752_w25_L5_Z0_f0.12_v2100_63kg_55.45min_2019-06-28						
L	5	w	25	v	2100	f	0.12

Printing task No.	1	2	3
Mortar No.	1+2	3+4	5+6
GCode	1	1	2
Print head + Nozzle	PH3+TP12	PH3+ TP12	PH3+ TP12
Final printing start	+20	+22	+20
Final printing end	+55	+57	+1:15
Pumping degree	2-3	2-3	0-1
Pumping surges	1	1	2
Nozzle bypass flow	4	4	5
QUALITY			
Print height (mm)	632	750	750
Layer width (mm)	25	25	25
Layer profiling	2	3	1
Layer discontinuities	2	3	1
Layer cracks	2	3	1
Layer thinning	1	2	1
Surface deformation	4	1	1
Printing supports	0	Sand	0
OVERALL QUALITY	COLLAPS	3	1

Case study 2 – Panels for prefabrication of organically shaped reception desk

The aim was to demonstrate the ability to produce large design objects from smaller prefabricated panels with the finest possible detail.

Fig.57. a) Visualisation of the reception desk (by Dominik Císař) b) Model section and layer incl. reinforcements c) Reception desk panelization showing division into four panels

The reception desk was designed by designer Dominik Císař as a surface in Rhinoceros [Fig.58]. The author of the work provided the design of production technology and fabrication of sample panels using 3D printing technology. The desk model was vertically sliced into 250mm wide sections with an estimated weight of approx. 50 kg to facilitate manual handling of the panels [Fig.59]. Four panels were designed to create a sample of a typical 1 m wide reception desk section. These panels were designed to be suspended onto the desk support frame via anchors. The envelope of each panel was reinforced internally with additional stiffeners to reduce the risk of collapse during printing and to increase the stiffness of the panel. The panels were sliced onto an L8/W18 layer with a total filament length of approximately 150m [Fig.59a,b] and a dry mix weight of approximately 45 kg. Subsequently, panels 3 and 4 were printed. During printing, stainless-steel anchors in the form of threaded rods or L profiles were inserted between the layers. Panels 1 and 2 could not be printed due to buildability exhaustion and subsequent collapse, so it was decided to split each of these panels into 3 smaller sections A-B-C and print these separately [Fig.60a]. These six panels were eventually printed, some of which had to be supported by sand fill during printing [Fig.59c].
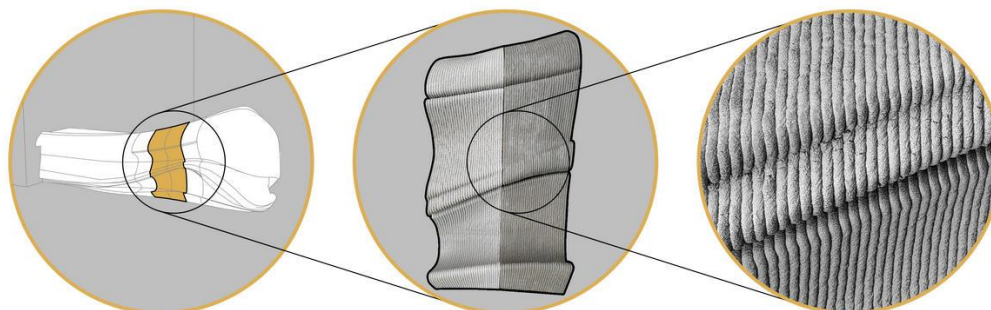
Fig.58. Reception desk panelization scheme (by Dominik Císař)

This case study has shown that with such a fine layer profile, maintaining the uniform quality and width of the layers is a major issue. Layer widths are difficult to measure and adjust during the printing process. As a result, the width of the printed panels varied by 2-5 millimetres, which affected the subsequent accuracy and made it

impossible to align the panels accurately. Variations in material properties in print jobs were also a major problem. This caused a difference in the appearance of the layers and thus the panels [Fig.60b,c]. The printing technology and material CM276 used appears to be unusable for such high-quality requirements, for commercial implementation it would be necessary to achieve a uniform quality of material and layers so that the appearance of the panels would not differ from each other. It would also be advisable to increase the buildability and therefore the width of the panels to 500 mm, reducing the number of joints on the resulting reception desk. This modification would also allow for increased efficiency of the technology by reducing the unit labour of printing and assembling the panels. Regarding Case study 1 to improve quality and buildability, decreasing layer height to 5 mm and resulting extended printing time would be an option. Unfortunately, due to continuous problems with fluctuating material properties, starting in September 2019, this solution could not be adopted. The key parameters of the printing task are summarised in the printing log [Tab.38].
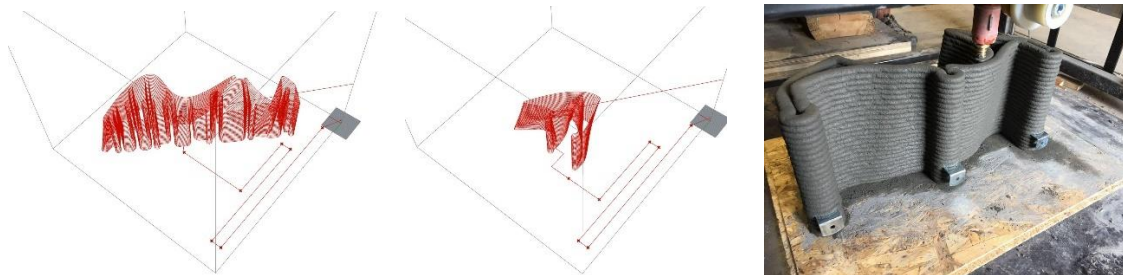
Fig.59. a) Panel 3 printing path b) Panel 2-A printing path c) Printing of panel 2-C

Fig.60. a) Panel 2 assembled of smaller parts 2A, 2B, 2C b) c) Set of printed panels 1(A+B+C)+2(A+B+C)+3+4, displaying various quality

Tab.38. Case study 2: Log of print tasks for reception panels (problem values in yellow)

CM276-F	Dose (kg)	Water (g/kg)	MG (g/kg)	MM (g/kg)	HCA (g/kg)
1	18	120	3	5	0.8
2	16	121	3	5	0.8
3	50.5	122+	3	5	0.8
4	48	120	3	5.2	0.8

Mortar No.	t_{air} (°C)	Φ_{air} (%)	End of mixing	End of relaxing	Pumpability	Fastening
1	24	55	+15	+20	2	2
2	24	54	+15	+21	2	2
4	23	51	+20	+26	2	2
5	21	54	+24	+30	2	2

GCode 1	RECP__P2C__TK10__L8__v2500__f0,10__DW 13.14kg__FIN					
L	8	w	18	v	3500	f	0.15
GCode 2	RECP__P2A__TK10__L8__v3200__f0,10__DW 12.42__FIN					
L	8	w	18	v	3500	f	0.15
GCode 3	RECP__P4__TK10__L8__v3500__f0,15__DW 43.85kg__FIN					
L	8	w	18	v	3500	f	0.15
GCode 4	RECP__P3__TK10__L8__v3500__f0,15__DW 41.24kg__FIN					
L	8	w	18	v	3500	f	0.15

Printing task No.	1	2	3	4
Mortar No.	1	2	3	4
GCode	1	2	3	4
Print head + Nozzle	PH3+TK10			
Final printing start	+25	+30	+32	+26
Final printing end	+40	+42	+1:15	+1:05
Pumping degree	1	1	1-3	1-4
Pumping surges	1	1	2	2-3
Nozzle bypass flow	1	1	1-2	2-4
QUALITY				
Print height (mm)	250	250	250	250
Layer width (mm)	18	18	18	18
Layer profiling	1	3	2	2
Layer discontinuities	1	1	1	2
Layer cracks	1-2	2	1	2-3
Layer thinning	1	1	1	2
Surface deformation	1	1	1	1
Printing supports	-	-	-	-
OVERALL QUALITY	1-2	2	1	2-3

Case study 3 – Fencing/partition panels MinSurf

The aim was to demonstrate the ability to address limits of buildability in organically shaped panels made of fine layers. This case study was inspired by 3D printed ceramic bricks, developed by Brian Peters as a part of the project Building Bytes [Fig.61a] [94]. It was intended to be used in two possible directions as a panel-brick for assembly of fence panels or partitions. First design of panel MinSurf, based on minimal surfaces had to be adjusted due to insufficient buildability [Fig.61b]. Inclination of walls has been increased from 47° to 70° in MinSurf Mk.2 and first Gcode was generated with layer L8/W18 [Fig.61c]. During printing it became obvious that 8mm height is too thick to address fine details in such an organic surface so new Gcode with layer L5/W18 was generated [Fig.61d]. This adjustment was proven to be printable in excellent quality of layers [Fig.62a]. As a result of stress in bottom layers and maybe also decreasing pumpability during hydration of material, sides of panels were not vertical, but inclined about 85° [Fig.62b]. An option to compensate decreasing layer width along Z could be gradual widening of the model or gradual increasing the flow parameter in the Z direction. Four panels were printed in high-quality, enabling two different assembly settings [Fig. 62c,d]. Unfortunately, due to continuous problems with fluctuating material properties, starting in September 2019, this solution could not be adopted. The key parameters of the printing task are summarised in the printing log [Tab.39].
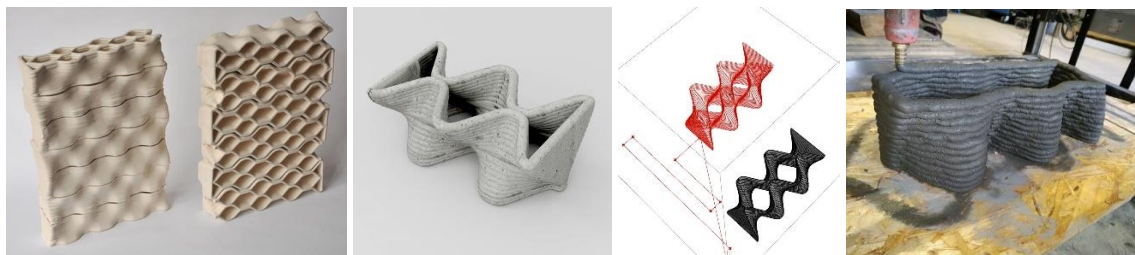
Fig.61. a) Panels of 3D printed ceramic bricks, Brian Peters [94] b) Visualisation of panel MinSurf c) Panel MinSurf 2 L8W18 printing path + source 3D surface in Rhino d) Printing of panel MinSurf 2 using L8W18 layer

Fig.62. a) High-quality layers of panel MinSurf using L5W18 layer b) Widening gap between two panels, caused by inclined walls c) Set of four panels d) Second option of panel assembly

Tab.39. Case study 3: Log of print tasks for MinSurf panels (problem values in yellow)

CM276-F	Dose (kg)	Water (g/kg)	MG (g/kg)	MM (g/kg)	HCA (g/kg)
1	16	125	3.2	5	0.8
2	16	125	3.2	5	0.8
3	16	125	3.2	5	0.8
4	16	125	3.2	5	0.8

Mortar No.	t_{air} (°C)	Φ_{air} (%)	End of mixing	End of relaxing	Pumpability	Fastening
1	24	52	+15	+20	2	2
2	26	54	+15	+20	2	2
3	25	58	+15	+20	2	2
4	24	48	+16	+21	2	2

GCode 1	MinSurf__47deg__355x175x250__L8__W18__v3500__f0.15						
L	8	w	18	v	3500	f	0.15
GCode 2	MinSurf__70deg __355x175x250__L8__W18__v2500__f0.12						
L	8	w	18	v	2500	f	0.12
GCode 2	MinSurf__70deg __355x175x250__L5__W18__v2500__f0.08						
L	5	w	18	v	2500	f	0.08

Printing task No.	1	2	3	4
Mortar No.	1	2	3	4
GCode	1	2	3	3
Print head + Nozzle	PH3+TK10			
Final printing start	+25	+35	+28	+25
Final printing end	+		+48	+45
Pumping degree	2	2	1	1
Pumping surges	2	2	1	1
Nozzle bypass flow	2	2	1	1
QUALITY				
Print height (mm)	96	250	250	250
Layer width (mm)	18	18	18	18
Layer profiling	3	3	1	1
Layer discontinuities	2	2	1	1
Layer cracks	2-3	2-3	2	2
Layer thinning	2	2	1	1
Surface deformation	Collapse	2	2	2
OVERALL QUALITY	Collapse	3	1	1

Various sample prints using CM276 not involved in Case studies

Fig.63. a) b) Vase Twisted c) Stool d) H-O vase (all designed by Dominik Císař)

Fig.64. Examples of prints from CM276 mixture a) High-quality prints b) Illustrative set of prints

CX450 mixture

Based on the mixture recipe designed in Chapter 5.2.2, fresh mixture was developed and tested to determine the content of admixtures and water content. Due to know-how gained during development of CM276, development was conducted solely in full scale. To determine viscosity and thixotropy, additional small-scale tests were facilitated ex post.

Testing of CX450 on a viscometer

In order to verify the viscosity and thixotropic properties of the CX450 mixture, measurements were carried out on a Viscotester iQ, type HAAKE. The tested mixture had a significantly higher viscosity compared to the reference cement paste (w/c = 0.4) and due to the type of sand used, the mixture showed resistance to the insertion of the test rotor. In some measurement cycles, the rotor was completely stuck in the cylinder and the analysis could not be evaluated. Thus, this geometry of the measuring instrument is not suitable for the tested mixture.

The mixture was stressed according to two different protocols to determine the static yield strength, the degree of thixotropy and the dynamic yield strength. Due to the significantly higher viscosity of the mixture, the achieved thixotropy is one order of magnitude higher than the reference cement mixtures. The mix was tested at a total of 4 times, ranging from 15 minutes of mix age to 60 minutes. The mixture did not change significantly during the measurement period. Due to the significantly

different viscosities of the reference cement pastes and the CX450 mix, a reliable comparison between them in terms of thixotropic properties according to the additives added cannot be made. Thus, the results presented below are for the tested mixture alone.

Fig.65a shows the thixotropic loop record for the mixture at different ages. At one hour of age (green), a significant slip layer between the cylinder and the rotor has probably formed and the stress has thus dropped significantly. It can be seen that the thixotropy of the mixture remains almost unchanged after one hour. The thixotropic loop changes with time especially in the low shear rate region where it increases to the static yield stress. The rest of the envelope curve does not experience as pronounced a change as compared to the pure cement paste, where a pronounced envelope area is formed even after the drop from the static yield strength, see Fig.65b. This indicates just the desired nature of the mixture for 3D printing, where the mixture gains in shear resistance (flowability) with time but does not change significantly when printing where flowability is required. The increasing static yield strength can be seen in Fig.66b. Fig.67 shows a record of dynamic loading and unloading. There is a significant increase in shear stress not only during loading but also during unloading of the material when the strain rate is close to zero.
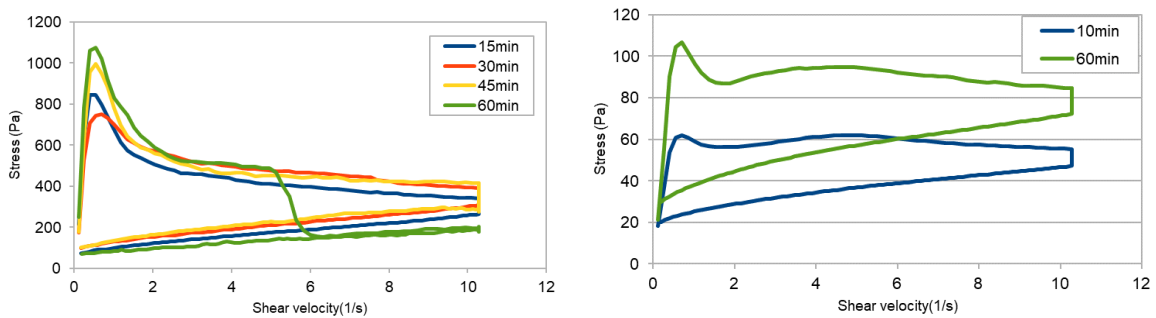
Fig.65. Thixotropic loops a) CX450 b) Pure cement paste w/c=0.4
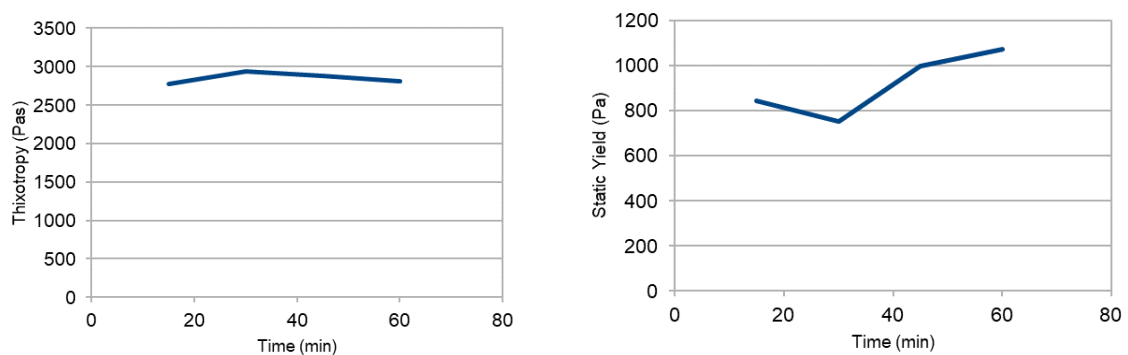
Fig.66. a) Thixotropy b) Static yield stress
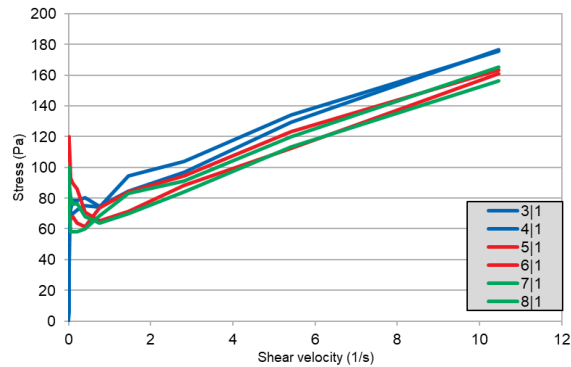
Fig.67. Dynamic load cycles at a mixture age of 60 minutes, unloading in dashed lines.

It is more appropriate to use other test geometries for the mixture, such as a rotor with blades. It would be appropriate to further test the mixture based on the expected age from the start of the print to the end of the print. It can be assumed that from the thixotropic loop, the desired mixture property for the 3D mixture can be observed. However, this still needs to be confirmed or refuted by further testing on a more suitable geometry. The inappropriate shape of the rotor was trapping small aggregates and further separation may have occurred and the tested mixture was not properly homogeneous in the cylinder.

Case study 4 - Technology for the production of cladding panels by planar 3D printing on an inclined board

The aim of this project was to develop technology for the fabrication of 3D printed cladding panels. The panels were intended for a commercial project, i.e. cladding a wall in the existing staircase of a historic house with a solarium. The size of the tiling with relief was 2450 x 1400 mm, it was divided into 4 panels with dimensions 600/1400 mm [Fig.68a]. Due to the manual installation the weight was limited to 75 kg per panel. Thickness of resulting panels was 27 mm. The panels together formed a relief, so it was essential to maintain the uniform appearance of the individual panels. The slenderness and length of such panels precluded the possibility of using existing 3D printing technology and also the printer whose space did not allow fitting such a panel horizontally. To overcome these limitations, the author developed a 2D printing technology on an inclined board where buildability is ensured by supporting the layers onto the board. The technology consists of depositing the layers from a curved nozzle along the inclined board, allowing a pattern protruding from the plane of the panel to create a relief on its surface. The diagonal orientation of the inclined plate then made it possible to fit a 1400 mm long panel into the print space [Fig.68b].

The thickness of the panel without reinforcement and therefore the width of the layer is only 25 mm, the height of the layer was 8 mm, the printing width was 670mm and the length 1400 mm. Printing was done at an angle of 38°, the inclination of the printing board and the angle of the nozzle outlet corresponded to the same angle. The nozzle was custom made using FFF 3D printing technology from CPEG plastic. CX450 material with modified additive and water content was used for the fabrication. Due to the significantly longer open time of the CX450 mixture, it was

possible to batch up to 75kg. Prior to printing the final versions of the panels, 4 print jobs were performed to verify the feasibility of the technology and to determine the optimum v/f printing parameters and recipe [Fig.69a,b]. Finally 4 panels were printed in high-quality with the average printing time 60 minutes [Fig.69c].
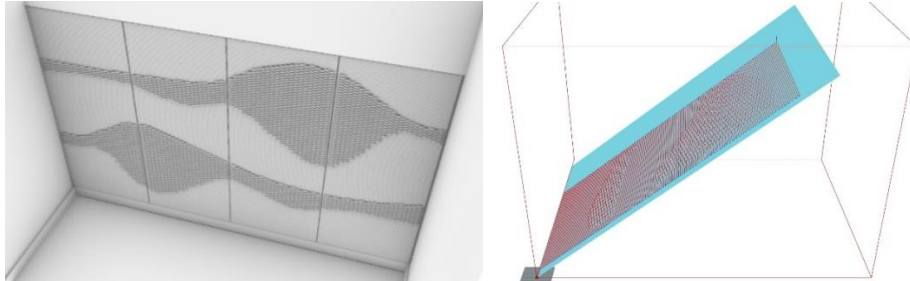
Fig.68 a) Visualisation of a cladding wall made of 3D printed panels
b) Printing path of P3 panel in Rhinoceros

Fig.69. a) Test of 3D printing on inclined board using angled nozzle b) Detail of the panel end showing the change in layer thickness due to the increase in pump pressure c) Printout of panel 3

The printed panels were covered with PE film as part of the treatment. Unfortunately, during the maturation process, despite the foil covering, a slight bend occurred, where the free ends lifted off the printing plate by about 4 mm apparently due to the different shrinkage on the bottom and top face of the panel [Fig.70].

Fig.70. a) Panel end lifting due to different shrinkage 24 hours after printing

After a week of curing, the panels were fitted with PP reinforcement fabric on the reverse side, pressed into a 2 mm cement screed [Fig.73a]. After 3 days, the panels were cut on the sides to a final width of 600 mm using a diamond blade saw.

To verify the flexural strength, indicative flexural tensile stress tests were subsequently carried out on the reference specimens. Specimens were made of panel cut-outs with dimensions of 325 x 1400 mm. The loading for a span of 1340 mm was provided by sand-lime bricks [Fig.71, 72]. 25 mm thick unreinforced panel displayed

tensile strength of 3.63 MPa. Tensile strength of 27 mm thick panel reinforced by PP fabric was determined to 4.20 MPa. These values are only indicative and would need to be confirmed by testing according to the applicable standard as for CM276.

Fig.71. a) Indicative flexural tensile strength test a) Loading of unreinforced panel b) Maximum load of unreinforced panel at failure c) Detail of failure of unreinforced panel

Fig.72. a) Indicative flexural tensile strength test a) Loading of reinforced panel b) Maximum load of reinforced panel at failure c) Detail of failure of reinforced panel

An anchoring system consisting of stainless steel L profiles glued to the panel with epoxy adhesive was developed for the panel mounting [Fig.73b]. The reliability of the anchors was verified by a pull-off test [Fig.73c,d]. After one week curing of all 4 panel, they were pressure washed and, after drying, sprayed with MasterProtect H 321 protective coating [Fig.73e]. Finished panels were finally delivered to the final destination, where they were installed using a steel frame anchoring system [Fig.74].

Fig.73. a) Panel reverse side with reinforcing mesh and 2mm squeegee b) Anchor profiles glued to the reverse of the panel c) Indicative test of the pull-off force perpendicular to the panel d) Indicative test of the pull-off force along the panel e) Set of finished panels coated with MasterProtect H 321 prior to the final delivery

Tab.40. Case study 4 (Part1): Log of print tasks of cladding panel print jobs

CX450	Dose (kg)	MF6 (g/kg)	Water (g/kg)	MG (g/kg)	MM (g/kg)
1	60+10	0.5	132	2.5	4.5
2	74	0.5	132	2.5	5.0
3	70	0.5	132	2.5	5.0
4	70	0.5	135	2.5	4.2
5	72	0.5	133	2.5	4.3
6	66	0.5	125	4.2	2.7

Mortar No.	t_{air} (°C)	Φ_{air} (%)	End of mixing	End of relaxing	Pumpability	Spread (mm)	Fastening
1	13	46	+21	+26	1-2	155	4
2	19.5	42	+25	+33	1	160	4
3	20	44	+24	+30	1-2	158	4
4	15	42	+21	+27	1-2	162	4
5	18	49	+30	+36	1-2	159	4
6	16	51	+27	+33	1-2	162	4

GCode 1	PAL_P1_REV_650x1500x25_L8_W25_38deg					
L	8	w	25	v	3200	f	0.10
GCode 2	PAL_P2_REV_650x1500x25_L8_W25_38deg					
L	8	w	25	v	3200	f	0.10
GCode 3	PAL_P3_REV_650x1500x25_L8_W25_38deg					
L	8	w	25	v	3200	f	0.10
GCode 4	PAL_P4_REV_650x1500x25_L8_W25_38deg					
L	8	w	25	v	3200	f	0.10

Printing task No.	1	2	3	4	5	6
Mortar No.	1	2	3	4	5	6
GCode	1	2	1	1	3	4
Print head + Nozzle	PH4+TP15-38deg					
Final printing start	+45	+51	+58	+1:05	+58	+50
Final printing end	+1:40	+1:55	+1:56	+2:00	+1:52	+1:45
Pumping degree	1-2	1-2	1-2	1-2	1-2	1-2
Pumping surges	1	1	1	1	1	1
Nozzle bypass flow	1	1	1	1	1	1

As part of the testing of the CX450 material, 12 print jobs were performed. The key parameters of the selected printing task are summarised in the printing log [Tab.40].The project demonstrated the feasibility of the proposed slant plate printing technology and its applicability in the production of custom-designed embossed panels of minimal thickness and weight. It also demonstrated the functionality of the author's proposed CX450 compound. Thanks to the appropriate choice of technology

and material, a uniform appearance of the panels was achieved with minimal aesthetic defects, giving the product a unified impression. The resulting architectural element achieves top fabrication quality and high aesthetic value. A similar panel could only be produced by casting into custom-made moulds, which are redundant in the case of 3D printing; moreover, the proposed production technology produces a minimum of waste.

Tab.41. Case study 4 (Part2): Log of print tasks of cladding panel print jobs (problem values in yellow)

QUALITY						
Print height (mm)	1500	1500	1450	1500	1500	1500
Layer width (mm)	25-32	25-26	25-27	25-26	25-26	25-26
Layer profiling	2	2	2	1	1	1
Layer discontinuities	1	1	1	1	1	1
Layer cracks	2	1-2	1-2	1-2	1-2	1-2
Layer thinning	3	1	1	1	1	1
Surface deformation	0	0	0	0	0	0
Printing supports	Board	Board	Board	Board	Board	Board
Notes	-	-	Pump collapsed	-	-	-
OVERALL QUALITY	2	1	1-2	1	1	1
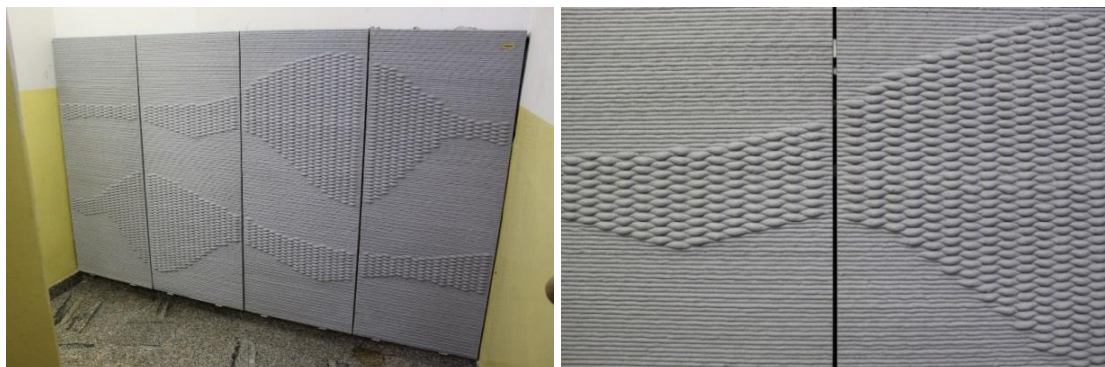
Fig.74. a) Final installation of the relief cladding panels in the staircase b) Detail of the relief in the connection of the cladding panels and demonstration of the quality of the layers

6.3.3. Flow 3D 100 printing mixture

In order to obtain a reliable printing material with constant properties and higher buildability, it was decided to test the applicability of the industrially produced 3D printing mortar Flow 3D 100, developed in 2020 by the company. Master Builders. Designed primarily for printing buildings with continuous mixing technology, this mortar is a one-component dry mix with buildability based on a combination of thixotropy and a setting accelerator with a workability of 20-25 minutes. (See Chapter 5.2.1) The use of this mix promised a number of advantages, including stable quality due to the industrial background of the supplier, as well as time savings when using a ready-mix, requiring only the addition of water. As part of the testing of Flow 3D 100, the material supplier and construction equipment rental company TONSTAV servis

were consulted about the possibility of using continuous wet mix preparation in a plastering machine. This consultation showed that continuous material preparation causes slight pressure fluctuations due to bubbles and imperfect dry mix supply to the mixing chamber, which is not a problem in machine plastering, but that a 100% guarantee of uniform quality and volume flow of material for 3D printing is difficult to achieve. This assumption was further confirmed by studying the quality of the layers on the Prvok project tested at the same time at the Experimental Centre of FCE, CTU by the Scoolpt studio using M-TEC in-line mixing station and continuous pumps [95]. The risk of print quality variation was found to be unacceptable for 3D printing of design elements and it was decided to stick with batch mixing technology.

Since the mortar was designed by the manufacturer for 3D printing and its parameters seemed to be compatible with the printing apparatus, testing was carried out directly on a full scale by testing the pumpability and subsequent printing of the mixture with the water content recommended by the manufacturer of 176 ml/kg. Mixing was carried out with a FESTOOL twin rotor mixer in a plastic mortar pot. First, all the mortar water was poured into the pot, then the remaining material was gradually added while stirring at grades 3-6. Mixing took 3-6 minutes depending on the batch size. After mixing, the material was left at rest for 3-5 minutes for relaxation. The fresh mixture was then transferred to the hopper of pump S8 and pumped to the printer. For batches larger than 6 kg, the material was dispensed into the hopper in batches of about 6 kg; the remaining material in the mortar was always mixed by machine after about 5 minutes. After checking the consistency, a flow test was carried out. A water content of 176 ml corresponded to a spread of 150 mm. A PH4 print head with metal nozzle attachments was used for printing. First, the extrudability and v/f ratio were tested by printing the Testing v-f test script. This determined the respective v/f ratios and nozzle type for the l/w layer parameters.

Fig.75. Various print tests using Flow 3D 100

Next, full-scale printing testing was carried out using the EGG and ORG vase scripts to test the buildability of the material when printing an object with overhangs and a subtle L8/W18 spiral layer. Eight printing jobs were performed with batches of 7 to 8 kg, the results of which are summarized in Table 42. The material proved to be too fluid at the given water content, reaching acceptable print quality only after repeating the print job three times, during which time hydration progressed by about 15 minutes, and thus reaching the correct consistency. The water content was therefore

progressively reduced from 176 ml to 162 ml in subsequent jobs. A layer width of 17mm was achieved, which is the smallest size achieved in the project [Fig.75].

In the following part, the aim of the project was to investigate the 3DF100 behaviour when printing larger objects from batches of 18 kg or more. A model of a table base TAM with a spiral path and a L10/W32 layer was selected as the test script. Material mixed from 36 kg of dry mix in one batch was used. Mixing and relaxing the material and preparing the print of such a large batch took about 15 minutes. Subsequently, after 5 minutes of printing, the consistency and pumpability of the material deteriorated dramatically due to the rapid onset of hardening. In order to continue printing without interrupting the layers, it was necessary to raise the pump power to the highest level, but unfortunately, due to the characteristics of the pumping system, the pressure in the nozzle fluctuated and thus the profile of the layers also fluctuated. Over the next 5 minutes or so, the material then became so stiff that pumping was not possible at all and it was subsequently difficult to get the material out of the hose. It was therefore decided to try mixing in two batches of 18 kg each. The TAM script was therefore reprinted, with the second batch of material being ready after about 10 minutes from the start of mixing the first batch. During the printing process, due to the different setting times and thus consistency of the batches, there was again a pressure fluctuation which the equipment operator failed to compensate for and consequently a fluctuation in the layer profile [Fig.76a,b]. Flow 3D 100 with a set time of 20-25 minutes proved to be unusable for our batch mixing technology and for printing objects with a print time of more than 15 minutes.

Fig.76. a) On the left, layer variation of a print of TAM model from Flow 3D 100, on the right the same model from Flow 3D 100 with HCA, treated with Kure 220WB - uniform layers, but spots b) Print log of TAM script using 2x18kg batch c) 1x36kg batch of Flow 3D 100

After consultation with the mix supplier, it was decided to extend the workability time of F3D100 with HCA hardening retardant in a volume of 1g/kg dry mix. This was added to the mix together with the premixed water. To save time, testing was again carried out directly at full scale. Subsequent tests showed that the HCA content would need to be raised to 10 g/kg to have the required effect of retarding setting. The amount of water was reduced to 146 ml to maintain consistency due to the plasticizing effect of HCA. The material was again tested on the TAM script [Fig-76c]. After several test prints, a high print quality was achieved, unfortunately the change in formulation led to the formation of rust spots on the surface of the cured prints [Fig.76d]. After consultation with the supplier, a protective spraying with Master Kure

was carried out on subsequent prints. This measure, as well as wrapping with PE foil, had no effect and the stains were still visible.

The result of the print jobs demonstrated the ability of the material without HCA to print small design objects up to 18 kg in weight and open time of 15 minutes in high quality. The workability of the fresh mixture was exhausted with longer printing times. The addition of HCA hardening retarder extended the open time to 40 minutes while maintaining the quality of the layers, unfortunately the change in formulation led to the formation of rust spots on the surface of the prints, which could not be removed even by applying different print curing procedures. The material was therefore unusable for the purpose of printing design prefabricates.

Case study 5 – Panel SIN

The aim of this study was to demonstrate the applicability of the F3D100 compound for printing in multiple batches of around 55 kg with a print time of 1 hour. In order to test, a panel object with an organically shaped PAN__SIN front wall with dimensions 800 x 144 x 800 mm was designed [Fig.77a]. GCode was generated with a continuous L8/W25 layer of 217.44 m length with ramps [Fig.77b]. The material was mixed from two 55 kg batches of 3DF100 with 10 g/kg HCA addition. By mixing the two batches sequentially during printing, the same extrudability was achieved and both batches were bonded without visible layer blending. Unfortunately, the material batch was not sufficient to print the last layer. The 55-minute print job showed that the addition of a retarder would extend the open time to a sufficient duration while maintaining high print quality and printing from the batches. This was the largest object printed by the author to date, weighing approximately 124 kg [Fig.77c, 78a].

Unfortunately, during the curing of the material, it became apparent that the high addition of retarder influenced the surface quality of the prints. Within 24 hours of printing, the material began to show brownish red spots on the surface of the layers, which became more pronounced within 2 weeks and reached a level that was not acceptable for use in design elements [Fig.78b]. The supplier recommended that the solution was to treat the surface with MB Kure 220WB protective spray at a concentration of 200 g/m^2 to reduce evaporation of surface water. Test prints were made and the product was sprayed on immediately after printing, unfortunately its effect on stain formation proved negligible. The subsequent advice to wrap the print in protective PE film to slow the transport of water to the surface did not solve the problem. It was therefore decided to abandon the modification of the cure retarder and the author decided to try to extend the cure time by creating a mixture of Flow 3D 100 with CX450 material. The key parameters of the selected printing task are summarised in the printing log [Tab.42].

Tab.42. Log of Flow 3D 100 print tasks incl. Case study 5 (problem values in yellow)

Mortar No.	Dose (kg)	Water (g/kg)	HCA (g/kg)	t_{air} (°C)	Φ_{air} (%)	End of mixing	End of relaxing	Spread (mm)	Pumpa bility	Fastening
1	6	177	0	26	52	+3	+9	160+	1	3
2	6	172	0	26	54	+3	+9	158	1	2
3	18	162	0	20	48	+5	+12	145	4	1
4	33	164	0	22	57	+5	+10	155	4	1
5	33	167	2.7	22.9	60	+5	+10	150	1	1
6	55+55	146	10	17.8	46	+6	+18	160+	1-3	1

GCode 1	EGG-IN_S_d215x250_L8_w18_f0.18_v3500_10,28kg_5.65min					
L	8	w	18	v	3000	f	0.15
GCode 2	TAM_S _d368x800_L10_w32_f0.18_v4200_29.01kg_12.33min					
L	10	w	32	v	4200	f	0.18
GCode 3	TAM_S _d368x800_L10_w32_f0.18_v4200_29.01kg_12.33min					
L	10	w	32	v	4200	f	0.16
GCode 4	PAN_Sin_HS_775x119x792_w32_L8_f0.14_v4000_93.93kg_54.36min					
L	8	w	32	v	4200	f	0.14

Printing task No.	1	2	3	4	5	Case st.5
Mortar No.	1	2	3	4	5	6
GCode	1	1	2	3	3	4
Print head + Nozzle	PH4+TP12-120		PH4+TK-24			
Final printing start	+12	+12	+18	+15	+13	+23
Final printing end	+15	+18	+32	+47	+45	+1:18
Pumping degree	1	1	1-6+	1-5	2-3	1.5-3
Pumping surges	1	1	1-3	1-3	1-2	1
Nozzle bypass flow	1	1	1-5	1-3	1-3	1-3
QUALITY						
Print height (mm)	180	210	488/800	800	800	792/800
Layer width (mm)	18-24	17	32-30	32-28	32-30	32
Layer profiling	3	2	2	2	2	1
Layer discontinuities	3	1	3	3	1	1
Layer cracks	1	1	2	2-3	1	1
Layer thinning	2	1-2	2	2	1	2
Surface deformation	1	1	1	1	1	1
OVERALL QUALITY	3	1	3	2-3	1	1
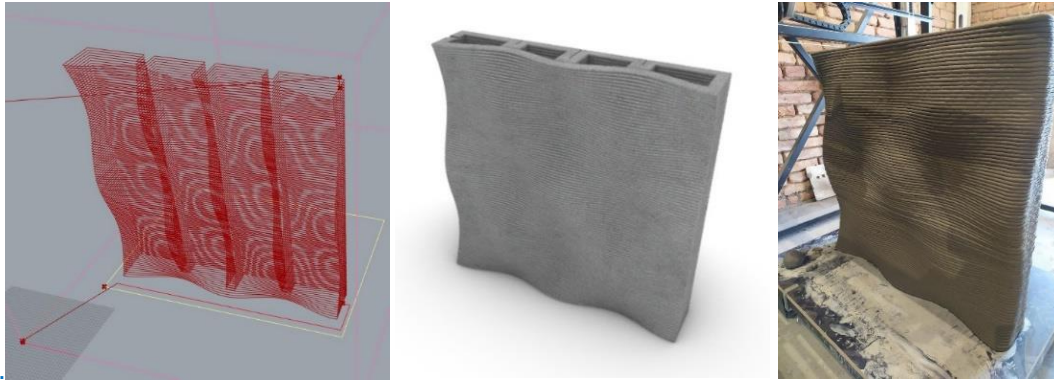
Fig.77. PAN SIN_HS_ 775x119x792 a) Printing path b) Visualisation c) Printout front
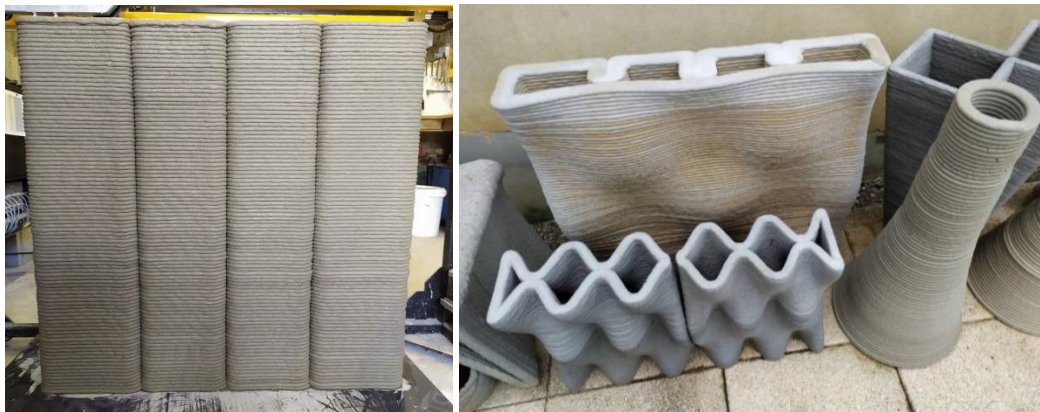
Fig.78. PAN SIN_HS_ 775x119x792 a) Printout back b) Brownish spots on SIN_HS printout of 3DF100 with HCA comparing to clean surface of MinSurf (CM276) without spots in the front

6.3.4. Print mixture based on Flow 3D 100 and CX450

The material mixture was developed with the aim to address problems of the industrial mixture Flow 3D 100 as described in Chapter 6.3.3. Main goal was to extend the open time and to maintain quality during curing, but cost reduction was also a benefit. According to F3D100 supplier, it contained 50% of CEM I 42,5 R Cemex Prachovice, similar to previously tested CX450 mixture. Based on this compatibility, the author decided to blend both mixtures in a ratio of 1:1 and to test the behaviour of the resulting material. The wet mix of 1kg blend was design with 145 ml of water, 1.75 g of PCA and 1.0 g of VMA. As the author was familiar with properties of both materials in the blend, it was decided to skip small scale testing and full-scale printing tests were carried out directly. As shown in following Case studies, mixture F3D100-CX450 seemed to be a perfect solution for a given technology that enabled superior quality printing with sufficient workability and buildability in terms of 1K mortar possibilities. As demonstrated in Case studies, new mixture allowed increasing of one batch to 76 kg while maintaining workability. On top of that, by reducing the content of the cost intense commercial F3D100 mixture to half, it also enabled the cost of the material to be significantly reduced. With the F3D100-CX450 blend using two 1-tonne batches of F3D100, dozens of print jobs were facilitated, including the successful completion of several commercial projects.

Unfortunately, the Flow 3D 100 mixture in the third batch, delivered in July 2021 exhibited different behaviour while using the same procedure, the mixture displayed cracks and workability was exhausted after 15 minutes. The primary reason, according to the supplier, was the delivery of the batch just before expiry and the degradation of the material due to the ingress of air moisture into the packaging. Three additional test batches were subsequently supplied by the supplier as part of the claim, but only the second of these displayed the behaviour of the original mixture. As there was no change in the ingredients of CX450, it is the author's estimation that there was probably a change in the recipe by the supplier of F3D100 or variation in the properties of the components. Due to the absence of reference samples from the first two functional batches of the mixture, the author of the thesis was unable to prove the assumption in a measurable way. As the supplier was unable to resolve this problem despite the author's cooperation, and the material could not be tuned to acceptable properties by other means, the further use of Flow 3D 100 had to be discontinued in November 2021. Moreover, after about 6 months of exposure of the prints to the external environment, it became apparent that this material also develops rust stains on the surface due to the effect of rainwater, which, similarly to F3D100 enriched with HCA, substantially degraded the aesthetic quality of the products. F3D100 has therefore proved unsuitable for the technology and for the production of exterior elements with high quality requirements when modified by the additional additives.

Case study 6 – Body for electric car charger Olife

The aim of this study was demonstrating the properties of F3D100-CX450 mixture and its ability to print geometries sensitive to buckling while sustaining high-end quality of printing. As the part of cooperation with Olife, who is a manufacturer of electric car rechargers, the 3D printed box for the charging station was designed by the author. It was designed with curved walls with the dimensions of 278/1400/360mm [Fig.79a,b]. GCode was generated with a continuous L8/W25 layer of 138 m length with ramps [Fig.79c]. The fresh mortar was mixed from one 76kg batch of 3DF100-CX450 with water and additives. Printing was made with v/f = 3600/0.12. During printing, printing supports of bricks were used but the buckling progressed to a collapse of one wall when 72% of model was printed [Fig.81a]. As the quality of printing was good, it didn't make sense to decrease the consistency. As the weight of the box had to be sustained the width of layer had to be kept. The only possible solution seemed to be adjusting the model, i.e. changing walls to vertical and inserting additional bracing in the middle of the long, slender walls [Fig.80]. Dimensions of the adjusted option were 250 x 1400 x 360 mm. To improve the quality of printing, water content was increased by 2 ml/kg comparing to first print. In order to support buildability and to balance the higher water content, printing speed was decreased to 3200 m/min. Based on these adjustments the model was subsequently printed in high-quality without the collapse, deformation or cracks within one hour [Fig.81b,c]. Successful printing of the original geometry which tends to buckling would not be possible with the given technology and 1K material, which is limiting design freedom by buildability but it still enables printing workable models.
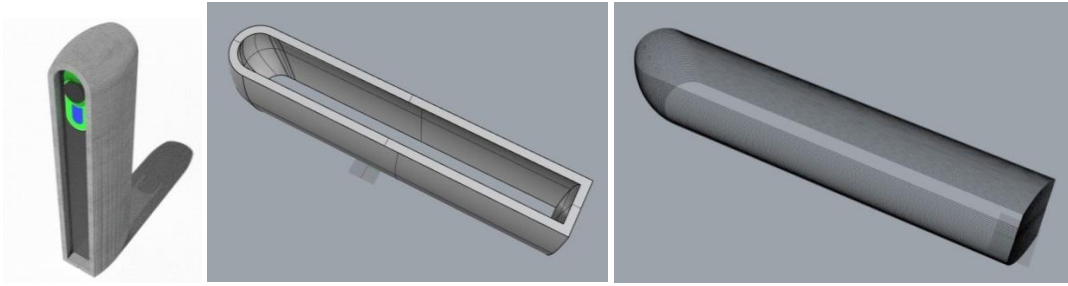
Fig.79. 3D model of the electric car charger body a) Option A b) Option B
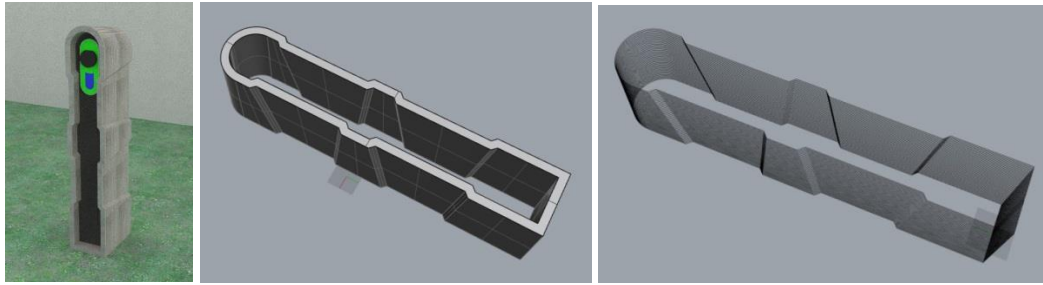
Fig.80. Printing path of the electric car charger body a) Option A b) Option B

Fig.81. a) Collapse of the wall of charger version A printout during printing due to buckling b) Successfully completed printing of the charger body version B after modification of the model and insertion of stiffening elements

Case study 7 – Vase H-O

The aim of this study was demonstrating the properties of F3D100-CX450 mixture and its ability to print 1m tall geometries sensitive to strength depletion while sustaining high-end quality of printing. As the testing object it was used the H-O vase, designed by Dominik Císař. The bottom perimeter of this object is only 1450mm long; its height is 1 m, which corresponds to 125 horizontal layers. The twisted shape is designed with overlaps that would make object sensitive to collapsing. For the purpose of quick modifications, it was redesigned by the author, who also created fully parametric script in Grasshopper [Fig.22a]. The dimensions of the option 1 were 353 x 353 x 1000 mm. It was sliced using spiral layer L8/W25, that was 152 m long, Parameters v/f were set as 3600/0.12, estimated printing time was 48 min. The fresh mortar was mixed from one 68 kg batch of 3DF100-CX450 with water and additives. The printing of H-O vase No.1 completing whole task, that resulted in high-quality layers [Fig.83a,b]. Unfortunately, when printing reached 850 mm of 1000 mm, shear cracks started developing at the inner edge of the vase where the stress was concentrated. The resulting width of cracks was 3-4 mm [Fig.83c]. To facilitate rapid setting time and higher shear strength, new printing task was conducted using pure

F3D100 material mixed in four batches of 18 kg. Similar to the task No.1, cracks started developing after 880 m of 1000 mm was printed and the geometry collapsed [Fig.83]. Third printing task was organized using 3 batches of 3DF100-CX450 (36+24+12 kg). To address higher buildability the printing speed v was decreased to 2100 m/min. It resulted in the printing without collapse, but the quality was not satisfying as layer profile varied due to the mixing of different batches [Fig.82d]. As there the width of layers varied, the batch of 66 kg of material was not enough and the printing was not completed. To maintain both quality and buildability, the author finally decided to adjust the model. It was resized in footprint from 353 x 353 mm to 318 x 318 mm and in the bottom part, overlapping was decreased by widening the central brace. This model was successfully printed of two 34 kg batches with superior quality without cracks [Fig.82e]. To verify this option, printing task with identical parameters followed 10 minutes later. At the very end of printing, the pump temperature reached 65 °C so the printing time, that the thermal protection of the motor has shut down the pump before the finishing the printing process. Similarly to Case study 6 this study demonstrated limits of technology using 1K materials prepared in batches for printing of geometries with slender walls. The final score for 1 successful vase H-O in high quality was 5 printing tasks, so the prototyping process makes sustainability of freeform geometries like H-O vase questionable; especially considering the number of products is limited to one or two pieces. The key parameters of the selected printing task are summarised in the printing log [Tab.43].

Fig.82. H-O vase printouts a) No.1 - side without cracks b) No.1 - Side with shear crack. c) No.2 – Layer profiling due to mixing of small batches d) No.4 - High-quality print of adjusted model e) Hardened H-O vase No.1 – Detail of cracks

Fig.83. Collapse of the H-O vase No.3 during printing due to depletion of shear strength

F3D100-CX450	Dose (kg)	Water (g/kg)	MG (g/kg)	MM (g/kg)	t_{air} (°C)	Φ_{air} (%)	End of mixing	End of relaxing	Pump ability	Spread (mm)	Fastening
1	76	140+	1.5	1	18	52	+15	+21	2	-	2
2	76	142	1.5	1	25.5	58	+11	+16	1	-	2
3	68	138+	1.5	1	24	54	+17	+23	1-3	-	2
4	4x18	138	F3D100 only		21.8	55	+3	+8	1	-	1
5	36+24+12	138	1.6	1	22	61	+8	+14	1-2	-	1-2
6	30+34	138	1.8	1	21	62	+8	+14	1-3	-	2
7	30+34	138	1.8	1	24	65	+7	+14	1-3	-	2

GCode 1	Wallbox__278x1400x360__w32__L8__f0.12__v3600__63.52kg__38.35min										
L	8	w	32	v		3600		f		0.12	

GCode 2	Wallbox__B__250x1400x360__w32__L8 __f0.12__v3200__63.92kg__43.42min										
L	8	w	32	v		3200		f		0.12	

GCode 3	Vase__H-O__353x353x1000__w25__L8__ f0.08__v3200__54.72kg__47.58min										
L	8	w	25	v		3200		f		0.08	

GCode 4	Vase__H-O__353x353x1000__w25__L8__ f0.08__v2100__54.72kg__72.5min										
L	8	w	25	v		2100		f		0.08	

Gcode 5	Vase__H-O50__318x318x1000__w25__L8__ f0.08__v2700__57.29kg__47.15min										
L	8	w	25	v		2700		f		0.08	

Printing task No.	1	2	3	4	5	6	7
Mortar No.	1	2	3	4	5	6	7
GCode	1	2	3	3	3	4	5
Print head + Nozzle	PH5+TK22			PH5+TK16			
Final printing start	+32	+20	+49	+21	+18	+22	+19
Final printing end	1:08	+1:08	+1:37	+1:09	+1:44	+1:17	+49
Pumping degree	2	2	1-3	1-2	1-3	1-3	1-5
Pumping surges	2	1	2	1	2-3	1-2	1-5
Nozzle bypass flow	2	1	1-2	1	1-2	1-2	1-5
QUALITY							
Print height (mm)	192/300	360	1000	880/1000	970/1000	1000	540
Layer width (mm)	32	30	25	25	25	25	25
Layer profiling	2	1	1	1	2-3	1	1
Layer discontinuities	1	1	1	1	2	1	1
Layer cracks	2	1-2	1-4	1	2	1	1
Layer thinning	1	1	1	1	2-3	1	1
Surface deformation		1	2-3	COLLAPS	1	1	1
Printing supports	Brick	-	-	-	-	-	-
OVERALL QUALITY	COLLAPS	1	1-3	COLLAPS	2-3	1	Pump collaps

Various sample prints using F3D100-CX450 not involved in Case studies

Fig.84. a) PAN__SIN, corner element (180kg) b) Various vases with L8/W18-22 in high-quality

Fig.85. a) Set of coloured planters with L8/W18 b) Big planters with L8/W25, d=600mm, batch 60kg, four prints in four tasks, uniform appearance, high-quality

6.3.5. Printing material Sikacrete 751 3D

In order to find a reliable material alternative for the continuation of the project, newly launched Sikacrete 751 3D printing mortar of the company SIKA was used in January 2022. This mortar is a one-component mix with buildability based on a combination of thixotropy and a setting accelerator with a set-up time of 20 minutes. The 600 kg samples delivered were tested in the 3D printing laboratory during February 2021. The material was designed for 3D printing with continuous mixing technology primarily for the purpose of printing design elements, which proved to be a challenge. Small-scale testing of the material was not performed due to the certification of the material for 3D printing and the assumption of achieving a suitable consistency based on the manufacturer's recommended water content. Five mortar samples were tested in turn.

Mixing was performed for 6 minutes on a two-rotor mixer, and the material was relaxed for 6 minutes after mixing. The water content of the first sample was set at 160 ml / 1 kg of dry mix in consultation with the supplier the rate was gradually reduced to 149 ml during testing of subsequent samples. The consistency prior to the pumpability test was found to be sufficient visually and by hand mixing, with the first sample apparently allowing pumpability. The material showed a markedly different behaviour compared to the previously tested mixtures and took some getting used

to. It was very easy to mix, showed higher flowability after relaxation, and adhered to tools and container walls, making it difficult to work with. The setting time was gradual. Its light colour, unlike previous mixes, seems to be ideal for colour tinting, according to the manufacturer it allows to achieve otherwise difficult to achieve white colour. The key parameters of the selected printing task are summarised in the printing log [Tab.44].

Tab.44. Log of selected print tasks using Sikacrete 751 3D (problem values in yellow)

Mortar No.	Dose (kg)	Water (ml/1 kg)	t_{air} (°C)	Φ_{air} (%)	End of mixing	End of relaxing	Pumpability	Fastening
1	8	160	14.9	48	+6:00	+12:00	1	0.2
2	10	155	15.6	51	+6:00	+12:00	0.8	0.3
3	25	150	16.1	57	+6:00	+12:00	0.8	0.3
4	28	150	13.5	42	+6:00	+12:00	0.6	0.5
5	28	149	14.2	45	+6:00	+12:00	0.2	0.8

GCode 1	V-EGG-OUT_259x252x258_w18_L8_Z0_f0.08_v3200_5.45kg_6.76min						
L	8	w	18	v	3200	f	0,08
GCode 2	Vase_H-O50_318x318x1000_w25_L8_Z0_f0.08_v2700_57.29kg_47.15min						
L	8	w	25	v	2700	f	0,08

Printing task No.	1	2	3	4	5	6
Mortar No.	1	1	2	3	4	5
GCode	1	2	2	2	2	2
Print head + Nozzle	PH5+TK16					
Final printing start	+20:00	+46:00	+20:00	+35:00	+20:00	+20:00
Final printing end	+2:00	+50:00	+24:00	+42:00	+6:00	+6:00
Pumping degree	0.2	0.4	0.4	0.4	0.4	0.4
Pumping surges	0	0.2	0.4	0.4	0.4	0.8
Nozzle bypass flow	1.00	1.00	0.80	0.60	0.60	0.20
QUALITY						
Print height (mm)	64	88	126	400	448	456
Layer width (mm)	-	25	25	25	25	25
Layer profiling	-	0.00	0.00	0.00	0.00	0.00
Layer discontinuities	-	0.00	0.00	0.50	0.30	0.60
Layer cracks	-	0.00	0.00	0.00	0.40	0.30
Layer thinning	-	0.00	0.00	0.60	0.00	0.60
Surface deformation	1	0.00	0.00	0.00	0.00	0.20
OVERALL QUALITY	COLLAPS	1	1	1-	2	3

With the given printing technology, the material was not able to achieve sufficient buildability when printing the V-EGG-OUT test object with 18 mm wide layers and collapsed after about 8 layers were printed [Fig.86a]. When printing 25 mm wide layers, the H-O test object achieved top quality layers after three test prints,

unfortunately, when printing over 400 mm, cracks formed at the bottom of the print due to the slow strength build-up of the material [Fig.86b,c,d]. When the water dose was reduced to 149 ml / 1 kg dry mix, in order to solve this problem, the pumpability of the mix was reduced and consequently the Sanax S8 pump failed. A Sanax DT pump with a larger pumping chamber and the expectation of higher performance was therefore rented. Unfortunately, during the subsequent printing process, some of the material in the pumping chamber solidified and the subsequent pressure fluctuations had a negative impact on the uniformity of the layers and thus the overall print quality. From the tests carried out it was clear that the material, despite its undeniable qualities, is not compatible with the 3D printing technology and especially with the preparation of the material in batches and its use for further purposes of this project was thus excluded.

Fig.86. a) Sikacrete 751 3D printing test result No. 1 – Collapsed V-EGG-OUT object
b) Sikacrete 751 3D printing test result No. 4, Sanax DT pump behind
c) Sikacrete 751 3D printing test result No. 3 and No. 4 – top quality of H-O_050 objects
d) Sikacrete 751 3D printing test result No. 4 - Detail of cracks within the bottom part of H-O_050

6.3.6. Sorfix-based printing mixture

Following the design of the printing mixture based on cement-free binder Sorfix, small-scale and then full-scale tests were conducted in February 2022. For purpose of determining the water and additive content in small-scale testing, recipes with higher binder content and expected the shorter setting time were selected from the proposed mixtures. Their parameters are summarised in Tab. 25. Similarly to CM276, the consistency was first verified on a small scale by a flow test, extrudability by extrusion using a manually controlled sealant gun Powerfix Profi. Testing was performed on 1.000 g samples of the dry mixture, enriched with water and additives as shown in Table 45. The water content was fixed and the PCA and VMA content were determined by successive iterations to ensure ideal consistency. The material preparation procedure and laboratory equipment were similar to CM276 (see Chapter 6.3.2). Extrusion test was made in 200 mm long filaments as it was regarded sufficient to determine key properties [Fig.87-95]. Based on the multi-criteria analysis, three options with best performance were selected to maintain full scale testing. Testing aimed on printing quality in the first phase, in the second phase buildability was tested. Quality testing was conveyed by printing one 12 kg batch of fresh mortar enriched by the respective water and additives content. It was performed by printing the script Test_R_200x200x976. Respective GCode was generated with a continuous

L8/W25 layer of 96 m length with ramps. Printing was made with v/f = 3000/0.10 parameters.

Tab.45. Composition, properties and rating of Sorfix-based mixes by small-scale testing

Mixture type		SF350			SF450			SF550		
Option		a	b	c	a	b	c	a	b	c
Sorfix (g)		350			450			550		
ST06/12 (g)		250			250			250		
ST53 (g)		100			150			150		
ST06 (g)		150			100			-		
Limestone (g)		50			50			50		
MF006 (g)		0.5	0.5	0.5	0.5	0.5	0.5	0.5	0.5	0.5
Water (g)		140	160	175	180	200	225	220	250	275
v/c		0,40	0,45	0,50	0,40	0,45	0,50	0,40	0,45	0,50
PCA (g)		25	17	16	14	8	6	8	5	5
VMA (g)		3	9	12	5	6	3	3	5	5
Properties	**Rating**	a	b	c	a	b	c	a	b	c
Flow / Spread (mm)	-	125	190	160	180	160	170	138	138	148
Workability (min)	-	0	25	20	40	4	20	25	40	40
Flowing	0,20	4	1	1	1	1	1	3	3	2
Extrudability 0min	0,25	5	4	2	4	1	1	2	4	3
Extrudability+30min	0,10	5	3	5	1	1	5	5	1	1
Buildability	0,15	5	3	2	4	1	3	1	2	4
Cracks	0,10	5	1	4	1	1	1	2	2	1
Workability	0,20	5	3	4	1	1	3	3	1	1
Overall score		9	7	8	4	1	2	6	5	3

Fig.87. Results of small-scale testing of SF350a a) Consistence at the end of mixing b) Flow

Fig.88. Results of small-scale testing of SF350b a) Extrusion test

Fig.89. Results of small-scale testing of SF350c a) Flow b) Extrusion test

Fig.90. Results of small-scale testing of SF450a a) Flow b) Extrusion test

Fig.91. Results of small-scale testing of SF450b a) Flow b) Extrusion test

Fig.92. Results of small-scale testing of SF450c a) Flow b) Extrusion test

Fig.93. Results of small-scale testing of SF550a a) Flow b) Extrusion test

Fig.94. Results of small-scale testing of SF550b a) Flow b) Extrusion test

Fig.95. Results of small-scale testing of SF550c a) Flow b) Extrusion test

All of three material options allowed successful printing of 12 kg [Fig.96-98]. Comparing quality of printing, option SF550c was rated as the most promising. In the successive buildability testing, it displayed the ability to print 750 mm tall prismatic specimen, thought the quality would need additional test [Fig.99a]. Then it was used to print 400 mm tall H-O vase in high quality [Fig.99b,c]. These results were also used in the bachelor thesis of Martin Hunčík, supervised by the author [95]. Due to the time limited scope of the project; tests of hardened properties were not facilitated. It would be necessary to provide compressive and flexural strength testing of hardened mixtures; shrinkage tests would be also beneficial. Hardened pieces of mixtures display fragile behaviour, they can be torn by hand, so significantly lower values of strength can be expected than for cement based mixes. Sorfix has displayed properties that can facilitate behaviour necessary for 3D printing mortars. It can be considered as the cement supplement due to its low CO_2 footprint and its origin as the industrial waste. The cost of Sorfix is lower the high grade cement and it is lower even comparing to fine aggregates. However, mechanical properties of the hardened state have to be studied to verify its applicability as a cement substitute. The key parameters of the selected printing task are summarised in the printing log [Tab.46].

Fig.96. Mixture SF450b a) View of the individual layers of the specimen b) Detail of the layers at the bottom of the specimen c) Detail of the shape of the layers of the print specimen from above

Fig.97. Mixture SF450c a) View of the individual layers of the specimen b) Detail of the layers at the bottom of the specimen c) Detail of the shape of the layers of the print specimen from above

Fig.98. Mixture SF550c a) View of the individual layers of the specimen b) Detail of the layers at the bottom of the specimen c) Detail of the layers of the print specimen from above

Fig.99. a) Test of buildability − printing of SF550c up to the height 750mm b) c) High quality print of H-O_050 vase with the height 440mm − SF450b

Tab.46. Log of print tasks using SF450b and SF550c (problem values in yellow)

	Dose (kg)	Mix	MF6 (g/kg)	Water (g/kg)	MG (g/kg)	MM (g/kg)
1	12	SF450b	0.5	200	8	6
2	12	SF450c	0.5	225	6	3
3	12	SF550c	0.5	275	5	5
4	30	SF550c	0.5	250	5.8	3
5	15	SF450b	0.5	200	8	2.7

Mortar No.	t_{air} (°C)	Φ_{air} (%)	End of mixing	End of relaxing	Pumpability	Fastening
1	25	55	+8	+14	1	2
2	25	52	+8	+14	2	1
3	26	53	+8	+14	1	2
4	25	55	+12	+18	2-4	1
5	25	52	+10	+17	2	2

GCode 1	Test__R__200x200x976__HS__225x225x984__w25__L8__Z0__f0.1__v3000__44,16kg__32.12min						
L	8	w	25	v	3000	f	0.12
GCode 2	Vase__H-O50__181x181x440__w22__L8__Z0__f0.12__v3000__11.58kg__9.75min						
L	5	w	22	v	3000	f	0.12

Printing task No.	1	2	3	4	5
Mortar No.	1	2	3	4	5
GCode	1	1	1	1	2
Print head + Nozzle	P5+TP12				
Final printing start	+20	+21	+18	+30	+25
Final printing end	+32	+31	+32	+56	+35
Pumping degree	1-2	1-2	1-2	1-5	1
Pumping surges	1	2	1	2-3	1
Nozzle bypass flow	1	1-2	1	1-3	1
QUALITY					
Print height (mm)	344/950	320/950	424/950	752/950	440/440
Layer width (mm)	22-24	22-26	22-23	22-25	18-20
Layer profiling	1	1	1	1-3	1
Layer discontinuities	1	1	1	1-2	1
Layer cracks	1-2	1-2	1	4-5	1
Layer thinning	1	1	1	2	1
Surface deformation	1	1	1	1	1
OVERALL QUALITY	1-2	2	1	3-4	1

7. DISCUSSION

The review conducted in the introduction of this thesis has shown that the process of 3D printing from concrete is a very complex engineering problem, requiring mastery of a wide range of skills. The cited studies mainly focus on printing strategies, material behaviour in fresh and mature state in terms of print job feasibility and strength characteristics. The results obtained in this work have provided a wide range of knowledge describing the behaviour of printing materials, the specifics of the technology used and outlined the internal and external variables and boundary conditions affecting the outcome of the printing process. Due to their comprehensiveness, they provided the author of the thesis with his own perspective on the issue of 3D printing by extrusion of single-component mortars. A broad discussion is necessary to evaluate these results. In the experimental part carried out, the author, in addition to the areas described in the research, also focused on the issue of print quality control, which is essential for commercial application in the field of architectural prefabricates.

The first area of application was printing materials on a single-component basis. In the experimental part, the author designed and tested four individually designed mixtures and also tested three commercially available premixes. In the tests conducted, the author traced the specifics of the 3D printing technology and materials used and focused on the risks associated with achieving high quality printing of thin layers. These risks stem mainly from deviations from the prescribed values in terms of technology and materials used. In the case of materials, the risks increase when products designed for use in conventional construction are involved.

To understand these risks, it is necessary to understand the differences in robustness of technologies and materials for 3D printing and for conventional technologies. Conventional technologies such as monolithic concreting, cement screeds, plastering or masonry are by their nature relatively robust technologies, allowing standard quality to be achieved even with slight variations within the manufacturer's or standard's procedure. Conventional building materials are therefore also inherently robust and allow, in combination with commonly used technologies, the correction of any slight variations in formulation or technology and flexible quality control during their processing into the final product.

The properties and behaviour of 3D printing mixtures are greatly influenced by conflicting requirements for the behaviour of the mixtures and also by the specifics of the technology for which they are designed. Another important technological factor appears to be that it is essentially impossible to modify the quality of the final product retrospectively once the material is deposited. The desired properties of 1K mixtures are achieved by a specific grain size curve, a high proportion of highly effective additives and fine admixtures, which, according to the author of the paper, causes an order of magnitude higher sensitivity of the formulations to changes in composition compared to conventional materials. Thus, according to the author, the variance of acceptable deviations in material and process properties is significantly lower compared to the standard requirements for conventional materials. Because of this, the requirement to achieve a very precise quantity, quality and homogeneity of input raw materials is essential in their production and processing. As the

experimental part has shown, this requirement is very difficult to achieve in the long term with the materials offered in retail sales.

In order to accurately describe the properties of the tested mixtures, a proprietary test methodology based on multi-stage small- and full-scale testing was developed as part of the work. During testing, the assumption that the properties of fresh mixtures are influenced by batch size and type of mixing equipment was confirmed. Recipes achieved in quantities of 1 kg on a laboratory mixer then had to be adjusted for batches of tens of kg, prepared on a 1-4 kW mixer.

In order to address all the necessary process parameters, a sample evaluation system based on subjective observations was developed within this thesis to evaluate the tests. This method of evaluation was resorted to because of the difficulty of any quantifiable measurement in manually operated apparatus. Since all evaluations were performed by one person, the author of this thesis, it can be assumed that all evaluations are burdened with the same systematic error. It is then possible to objectify this established subjective evaluation system after introducing some calibration conversion. The described evaluation system proved to be valid in the experimental part and yielded applicable results in the context of this thesis. The testing methodology, the number of monitored parameters and test logs were augmented as the experiments progressed and enabled a detailed description of material behaviour and technological parameters to provide a sufficient knowledge base necessary for mastering the 3D printing technology designed by the author.

The author's mixes CM276 and CX450 differ significantly in cement content and type, while SF450b and SF550c use Sorfix binder instead of cement. All mixtures contain fine admixtures either in the form of microsilica or ground limestone. Thixotropic behaviour is achieved by a combination of fines, PCA and VMA. The thixotropy was verified for all mixtures by printing and for CX450 by measuring on a viscometer. The w/c ratio of the mixtures varies from 0.30 for CX450, to 0.41-0.43 for CM276, to 0.44 for SF450b and 0.50 for SF550c. These values are significantly higher than the reference blends described in the study, probably due to the lower proportion of costly plasticisers. An advantage of the mixtures proposed by the author appears to be the possibility to flexibly adjust their properties directly to the given technology and production conditions. The disadvantage is the time-consuming and costly control of input raw materials, difficult in the conditions of a workplace with a limited budget and number of workers. A major risk has been the supply of raw materials in small quantities, which is only possible, for example, in the case of cement and limestone, by purchasing from a retail chain, where, as the author assumes, the quality requirements and variations in raw material properties are not as high across multiple production batches. These mixes also have the disadvantage of being more difficult to prepare in terms of time, space, equipment and labour, since the dry ingredients must be mixed first and then the fresh mix prepared. In addition, the preparation of material in small quantities carries the risk of weighing errors, as well as humidity and temperature variations in the production environment.

In the experimental part, the 3D printing mortars designed by the author proved to be fully functional and capable of fulfilling the thesis objectives, i.e. printing prefabricated parts with fine layers and high print quality. The CM276 mix showed lower buildability values, so it was limited to objects with mainly vertical walls and

low slenderness. In the case of printing slender geometries with a tendency to bulge, the technology of temporary printing supports with sand backfill was used. This technology proved to be ineffective due to the time, labour, unreliability and the effect of sand on the surface of the elements. It is questionable to what extent the buildability of this mix could be improved by adding a setting accelerator. The second cement-based material developed was CX450. Its stability during printing was ensured in 2D panel technology by resting the layers on an inclined printing board, so buildability was not addressed further. The mixture facilitated a very demanding project of four embossed panels, which were produced in top quality. Very promising printing results were also achieved using the author's proposed Sorfix-based cementless blends SF450b and SF550c. In 3D printing of prefabricates with fine layers and high print quality, in quantities up to 50 kg and with the chosen technology, they are demonstrably comparable to the tested cement-based mixes. To confirm the possibility of fully replacing cement-based mixes with a more environmentally friendly Sorfix-based alternative, printing jobs of 75-100 kg batches would need to be carried out, as well as strength and shrinkage tests.

The composition of the commercially available mixes Redrock, Flow 3D 100 and Sikacrete 751 3D was not known to the author, but it can be assumed that they differ from the previously described mixes mainly by the addition of a powdered setting accelerator in addition to the type and proportion of ingredients. The great advantage of the industrial mixes is the simpler and faster preparation consisting only in mixing with water, which takes only about 5-6 minutes. In the case of F3D100, this advantage was unfortunately lost due to the low shelf life of the chosen packaging and the variation in quality from batch to batch. The problem with premix mixes is their limitation to the technology with which they were developed and tested and the purpose, where there is a difference between a mix for printing buildings with massive layers and a mix for fine layers with requirements for final quality and the possibility of colour tinting. None of the premix mixtures tested were applicable for printing fine layers of 18-25 mm width given a printing technology with mixing of material in batches without adjustments. Without knowing the composition of the mixtures, adjusting the premix recipe is very risky. The properties of the F3D100 blend could have been adapted to the target purpose by the high addition of a hardening retarder, unfortunately the intervention in the recipe caused the formation of rust spots and thus rendered it unusable for design elements. A combination of CX450 proprietary compound and F3D100 industrial compound appeared to be the most promising, unfortunately due to the quality variation of F3D100, even this solution proved to be unworkable for commercial application after five batches were delivered.

Based on the experiments performed, the author suggests that for 1K mixtures, the open time is composed of two time-varying components, the first of which is thixotropic in nature with a rapid rise and can be reset by repeated agitation. The second component has a slow rise and cannot be reset. As hydration progresses over time, the irreversible component dominates. 1K material is therefore to some extent more suitable for experiments, as it allows multiple print jobs to be performed with a single batch of material and reduces waste due to its longer and somewhat resettable open time. With 2K compounds, where solidification is provided by

acceleration in the nozzle, the printed filament is irreversibly hydrated by the accelerator, cannot be reused and becomes waste.

Strength tests of the mature material were carried out as part of the work. In the case of CM276, flexural tensile strength tests were performed which demonstrated the orthotropic nature of the 3D printed test specimens. The achieved strength values ranged between 3.4-10.6 MPa in the case of stress perpendicular to the interlayer joint and 7.7-16.0 MPa in the direction along the interlayer joint, so it can be said that the effect of weakening in the interlayer joint weakens the tensile strength by about 50%. Strength tests were also carried out on relief panels fabricated by 3D printing on an inclined plate of CX450 material. One load test was performed on an unreinforced panel of 25 x 325 x 1450 mm on a 1340 mm span. The resultant force of 0.367 kN at failure corresponds to strength of 3.63 MPa, which is consistent with the tensile strength results of CM276 material. However this value is only indicative and would need to be confirmed by testing according to the applicable standard as for CM276.

On the basis of the tests carried out and the handling of the prints, it can be stated that the width of 18-32 mm, in combination with the strength of the material, appears to be sufficient to withstand the stress of the prints under the load of its own weight and normal handling. Only layer fragments of a 5-15 mm in size were chipped off during handling-induced loading of the edge of the element in contact with the hard ground due to the concentration of the self-weight to one point. The author is not aware of any major damage or deformation during handling or use of the prints.

The durability of the products when exposed to outdoor weathering is also critical for commercial use. As part of the project, several dozen products were placed outdoors for 1-3 years, thus exposing them to several dozen freeze cycles [Fig 101]. No changes other than natural aging were observed in the CM276 and CX450 products. The only problem occurred in the HCA-added F3D100 and F3D100-CX450 material, where the rain caused the formation of irremovable rust stains within a few days and weeks, which prevented the commercial use of the prints.

A batch mixing technology was chosen for material preparation because of experimentation and smaller volumes of material. In order to ensure this, different types of mixing equipment were tested. Mixing in quantities up to 1 kg was carried out on a laboratory mixer. Mixing in the range of 6-60 kg was carried out on two types of mixing stations. Mixing in the range of 6-100 kg was carried out with single or double whisk stirrers. The use of a double whisk stirrer proved to be the most effective, reducing the mixing time to 5-10 minutes compared to 15-25 minutes for the mixing station. However, the disadvantage of the stirrer compared to the mixing station is the need to involve one extra physically fit worker.

Due to the unavailability of specialized pumps for 3D printing, injection pumps were chosen as the pumping device for transporting the fresh mixture to the nozzle. Within the project, the Sanax S8 peristaltic pump and the Sanax DT screw pump were selected for testing based on a review of pumps and inline mixing stations. Due to pumping stability and ease of maintenance, the Sanax S8 pump was selected and used for all subsequent print tasks. The pumping system, consisting of the pump and the feed hose, was highly flexible and this resulted in delays when changing the pumping performance. However, this flexibility also compensated for the pump

fluctuations and surges caused by imperfect filling and the cyclic nature of the peristaltic unit. It can be assumed that if a stiffer hose was used, the delay in pumping performance would be eliminated, but the compensation for surges would have to be accommodated in other means. The use of the pump to convey mixtures with a significantly stiffer consistency than that for which the peristaltic unit and pump motor are designed began to cause mechanical wear on the pumping unit after a year of operation, which had to be replaced twice over the years. Pump operation was also limited by overheating of the pump, which led to an automatic protective shutdown of the machine. This occurred when the air temperature was higher and the pump was operated for more than two hours. On one occasion, the motor burned out and had to be replaced.

Batch mixing technology was limited by the deterioration of material consistency over time. This problem was addressed in three different ways. The first method was to increase the pumping power, but the effect was limited by the pump stage 6. In addition, as pump wear increased, pumping solid materials at maximum power resulted in pump overload, subsequent failure and thus failure to complete the print job. The solidifying consistency also had to be eliminated at the nozzle by varying the print speed and the nozzle extrusion rate by continuously increasing the values of the scripted coefficients v and f in Pronterface. This was eventually necessary for most scripts with print times over 30 minutes. Maintaining consistency was also addressed by additionally sprinkling water into the material in the hopper. However, the volume of water added in this way, as well as evaporation on the surface and on contact with the filling equipment, is very difficult to determine. Filling of the S8 pump was done with a wooden stick, metal spoon or funnel, or in the case of stiffer consistencies, with rubber-gloved hands. The contact area at the material contact point and the temperature of the tools varies and is very difficult to quantify, thus having different effects on the overall evaporation of water from the mixture.

The operator's work was very demanding, filling the S8 pump required considerable physical strength, pressure regulation required considerable experience and foresight, and coordination of all activities required coolness.

The key element of the whole technology is the 3D printer. Based on the determination of key parameters, a Cartesian type of structure with 3 DOF with a print area of 1 x 1 x 1 m was designed. Based on the specifications of the key parts, the design of the machinery was subsequently performed in Autodesk Fusion 360 environment. An 8-bit Arduino Mega 2560 control board, operated by Arduino 1.8.9, was selected as the control unit. The printer was subsequently fabricated by an external supplier with considerable input from the author. The fabrication of the printer was carried out on a limited budget by craftsmen with standard tooling, yet the device achieves speed and accuracy, with margins sufficient for high quality printing. During the operation of the printer, the weakness of the proposed solution became apparent, which is the limited computational power of the Arduino controller. This is overwhelmed in the case of more complex models with larger amounts of data in GCode, the system jams, the limit switch on the Z-axis trips and multiple reboots are required. The firmware setup of the printer was performed in the Marlin 1.1 environment. The fixed position and size of the print area also proved to be a disadvantage of the Cartesian printer with a fixed print pad, limiting the printing of

multiple jobs in a row. In the case of printing objects filling most of the print space, or large objects with a risk of collapse, further printing is only possible after the printout has taken several hours to mature, limiting the number of large jobs to one per day.

The printer control was designed in Pronterface. This application allows running GCode scripts as well as executing HOME commands and direct control of individual printer axes. The ability to continuously adjust nozzle movement and extrusion speeds during printing in Pronterface, depending on changes in material consistency, proved very useful. Pronterface proved to be a functional solution during hundreds of print jobs, but unfortunately it does not allow control simulation of print jobs, which had to be performed in the NC viewer web interface.

The project also addressed the methods of nozzle extrusion. Extrusion from a nozzle connected directly to the pump hose proved to be unusable due to surge transfer and pressure variations in the quality of the layers. In addition, it was necessary to control the extrusion directly in the control script. For this purpose, 5 options of printheads were designed with an extrusion auger driven by a stepper motor controlled by the printer control unit. The variants differed, apart from the shape and material design, mainly in the way of pressure compensation, guaranteeing uniform extrusion. The project showed that the print head with pressure compensation by a lateral outlet at the beginning of the auger achieves the most uniform extrusion and thus layer quality. Unfortunately this solution requires one additional manpower to operate the outlet. Due to the frequent change of the bin with discharged material, it is only possible for a printer with a print area limited by the human reach, i.e. about 1.5 m. Moreover, changing the bin during printing limits the speed of the print head and thus the printing speed. However, for the production of prefabricates on the given printer, the solution proved to be fully satisfactory. The advantage of the proposed solution is the low cost and simplicity of the solution, which uses human operators instead of sensors and data linking the pump and nozzle to the system. After the necessary training, the operator is able to control the quality and the width of the layers very efficiently. The nozzle outlet pressure compensation method is an affordable low-end solution for print quality control in 1K technologies. It is definitely not suitable for prints of several meters and high print speeds. It is also limited for 3DOF printers where the print head orientation is not changed. It seems particularly suitable for low cost and experimental projects.

The models of printed objects were created in the CAD application Rhinoceros or in its parametric plugin Grasshopper, where the GCode print scripts were subsequently generated. For this purpose, the author created several hundred original scripts in Grasshopper format, allowing automated generation of models, their slicing into three different types of print paths, assignment of parameters v and f to individual sections of the print path and extension of the subsequent GCode with data about the print job, necessary for material preparation and production planning. Verification of the printability of the models was not carried out as part of this process due to the difficulty of simulating the highly complex printing process and print material behaviour. The Rhinoceros applications with the Grasshopper plugin proved to be a great and affordable solution, allowing easy geometry adjustment and flexible adjustment of print job parameters in case of creating a high-quality parametric

model. It is therefore a very effective tool for print quality control and efficient production planning of 3D printed prefabricates.

A fundamental issue related to the sustainability and economics of the whole technology is material consumption and waste production. As the width of the layers during printing also changes with changing consistency, it is only possible to estimate the consumption, especially for prints over 25 kg, indicatively. In order to complete a print job before running out of material, it is therefore necessary to increase the batch by a certain margin. If this reserve is not used up, waste is then generated. In most cases, the printout itself becomes waste if the printout is not completed due to insufficient material reserve.

Simulating of printing process and material behaviour as described on page 19 would be beneficial to verify printability of collapse sensitive geometries prior to the full-scale testing. The published methodology has to be augmented by quality criteria. To employ simulation of printing into the design process, the properties of the fresh material and additional boundary conditions linked with the quality have to be studied.

As part of the project, an original technology of 3D printing of relief panels on inclined plates was developed. This technology enabled the printing of functional relief panels with dimensions of 660 x 1400 mm and a thickness of 25mm. Due to their mechanical durability, surface quality and low weight, these panels are a cost-comparable alternative to decorative panels made of stone or concrete, with the advantage of the possibility of creating a customized relief within each panel.

Essential for the evaluation of the presented 3D printing technology is the assessment of the efficiency of the production process. For every successful print job there were 1-5 unsuccessful attempts, depending on the complexity of the object shape. In the case of shape-complex elements, time and material consuming prototyping was necessary to find a shape that would allow printing in high quality. This involved the identification of the appropriate geometry, slicing method and parameters of the printing technology and material. As Case Study No. 7 showed, even after finding the optimum parameters for the model, technology and material, the successful repeatability of the process is not guaranteed due to the difficulty of affecting changes in external conditions.

The number of workers required for a print job made with the given technology from one batch of material is 2 people. Two persons are responsible for the preparation of the printing apparatus and material, testing and subsequent cleaning and washing of the apparatus. During the print job, one person operates the pump and the print head outlet, the other person operates the printer and adjusts the print parameters. In the case of multiple batch printing, a third person is required to prepare the multiple batches and assist the pump and printer operator. Depending on the size of the object and the length of the print run, the time required for a single job is between 2 and 5 hours. In the case of two people, the time commitment is 4 to 10 hours, in the case of three people 6 to 15 hours. At a cost of 40 Euro/hour, the job cost per print is between 160 and 600 Euro per piece (excluding the cost of designing the element, generating the GCode and prototyping).

The thesis proved the functionality of the 3D printing technology proposed in the project on the basis of several hundred print jobs. The printing material was 1K

cement-based or cement-free mortars without setting accelerator. The batch mixing technology allowed printing objects up to 180kg in a controlled indoor environment. The uniqueness of the technology is the ability to eliminate material and machine imperfections as well as environmental influences through a trained operator to achieve high quality printing with fine detail. Due to its considerable complexity, this process requires intense physical and mental effort by the operator. Unfortunately, maintaining high print quality in the long term is subject to fluctuations in the properties of the raw materials and also wear and tear on the machinery. According to the author, the high sensitivity of the material to changes in external and internal conditions fundamentally limits the use of the presented technology for printing in situ and also for printing large objects on the scale of buildings.

Structure of the 3D printing process
(The duration of the activities is estimated based on the experiments carried out)

1. **Preparation of the printing equipment (about 30-60 minutes depending on the number of people)**

    1.1. Setting up the print head and mounting it on the printer

    1.2. Preparation of the print area of the printer

    1.3. Inspection and cleaning of the mechanical parts of the printer

    1.4. Connecting the printer to PC and network, printer start-up

    1.5. Moving the print head to the cleaning position, loading the GCode with the print task

    1.6. Checking and preparing working tools

    1.7. Setting up the peristaltic pump unit

    1.8. Connecting hose to pump and printhead

    1.9. Flushing the pump, hose and printhead with a quantity of water

2. **Material preparation (approx. 20-60 minutes depending on print size and type of mix)**

    2.1. Weighing of dry mix components

    2.2. Mixing of the dry mix (no need for premix mixes)

    2.3. Weighing of water and additives

    2.4. Mixing of fresh mix

    2.5. Mix relaxation

    2.6. Filling the pump hopper

3. **Mix testing (approx. 10-20 minutes)**

   3.1. Indicative consistency test by spilling (optional)

   3.2. Pumpability test

   3.3. Displacement test

   3.4. Printing test, specification of printing parameters

4. **Print task (10-60 minutes according to script)**

   4.1. Continuous filling of the pump hopper

   4.2. Continuous feeding of the pump unit

   4.3. Continuous operation of the print head outlet

   4.4. Continuous monitoring of print quality

   4.5. Continuous change of print parameters in Pronterface (in case of deterioration of consistency)

   4.6. Continuous wetting of the material in the hopper by spraying (in case of deteriorating consistency)

   4.7. Continuous preparation of additional batches (in case of multi-batch printing)

   4.8. Termination of the print job

5. **Post-production of the print (5-20 minutes)**

   5.1. Print relaxation

   5.2. Moving the printout to the curing zone (if necessary to free up print space for other print jobs, for prints up to 25kg)

   5.3. Treatment of the print with spray or PE film

6. **Equipment washing and cleaning (30-60 minutes depending on the number of people)**

   6.1. Pressing the remaining mixture out of the pump and hose with water

   6.2. Switching off and disconnecting the printer

   6.3. Disposal of remaining material

   6.4. Disassembly and washing of the pump peristaltic unit

   6.5. Disassembly and washing of the printhead

   6.6. Washing the tools

8. CONCLUSION

Based on results and its discussion summarized in this thesis, it is possible to draw the following conclusions and recommendations.

- The 1K materials, in conjunction with the appropriate off-site technology, allow for layer widths of 17 to 32 mm. Ensuring buildability is possible for selected geometries without the use of a hardening accelerator.

- The tensile strength of 3D printed materials in a hardened state varies by up to 50% depending on the orientation of the layers.

- The Sanax S8 peristaltic pump is a viable alternative for printing from 1K compounds but requires surge compensation within the printhead. A physically fit and experienced operator is required to continuously fill the peristalsis unit with 1K mortars. Significant wear and tear on the pump must be anticipated when using stiff mixtures.

- Pressure and surge compensation in the nozzle can be effectively provided by a printhead outlet at the upper part of the discharge auger, but the operation of the outlet requires an extra operator. The simplicity and low cost of the solution make it suitable for experimental and low-budget projects.

- The development of a suitable device for integrated material preparation and pumping is an option to ensure continuous production and transport of material to the nozzle. It has to facilitate supply without pressure fluctuations, bubbles or changes in consistency.

- From the available literature, it is clear that despite the common principles in 3D printing projects, there are large differences in technologies and material composition. The project has shown that in order to master this technology it is necessary to reflect local conditions in terms of both raw materials and technical facilities.

- To sustain properties of material within the workable range, daily tests of the input raw materials and the storage of bulk and liquid components under constant conditions, as specified in the technical data sheets, are indispensable. Ensuring such a quality control system requires significant human and financial resources, which are only available to organisations with a strong background.

- The project has demonstrated that 1K technology, despite its undeniable potential, has its limits and there is considerable opportunity for optimisation. For wider commercial applicability, the printing process needs to be further optimised and changes in environmental conditions minimised or responded to flexibly. For this reason, the entire process of material preparation, pumping, printing and curing needs to be closely monitored both inside the production system and externally, i.e. to track changes in the production environment. To facilitate such a system it is necessary to implement a control system that interconnects the mixer, pump and mixing nozzle. These devices need to be

equipped with pressure and temperature sensors to monitor and control the behaviour of the material in real time depending on changing internal and external conditions. To address all quality linked aspects of the process, it is necessary to indicate latent trends and to reflect them in a reasonable number of parameters. The criterion for the term „reasonable" can be based on the needs of the AI regarding the sufficient size and training data set. The question is what would be the robustness of such complex technology and equipment when applied in real construction conditions and what would be the return on investment in the development or acquisition of such a technology.
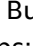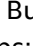
- Switching to 2K technology seems to be a sensible solution to the problems associated with maintaining print quality and the laboriousness of 1K technology. The advantage would be using the material with a processing time exceeding the time of the material preparation and printing process, i.e. about 2 hours, together with ensuring the buildability by rapid accelerating material in the nozzle.

- The application of 3D printing must take into account the fact that the structuring of the environment in the construction will probably always be at a lower level than in, for example, an automotive factory, even in the case of precast concrete production. This approach appears to be very problematic in terms of the requirement for robustness of the technology, arising from the nature of current construction and the high labour requirements.

- The integral part of the suggested production technology is the trainee process, based on on-site training. Rather than on a large scale, apprentice approach on a smaller scale is necessary.

- In order to shorten the prototyping process to a minimum and to take into account quality criteria in the design of the elements, it will be necessary to develop software, simulating in real time not only the printability and stability of the geometry, but also the quality of the 3D printing.

Fig.100. Illustrative selection of printouts from various materials, fabricated during 3 years of a 3DCP research as a part of this thesis

BIBLIOGRAPHY

[1]   QUIRK, Vanessa. How 3D Printing Will Change Our World. In: Www.archdaily.com [online].
       Zurich: DAAily platforms AG [cit. 2023-02-11]. [Online] hyperlink:
       https://www.archdaily.com/253380/how-3d-printing-will-change-our-world

[2]   STOTT, Rory. Chinese Company Showcases Ten 3D-Printed Houses. In:
       Www.archdaily.com [online]. 2014 [cit. 2018-03-05].

[3]   ADLUGHMIN. World's First 3D Printed Castle is Complete: Andrey Rudenko Now to Print a
       Full-size House. In: 3D print [online]. 3DR Holdings LLC, 2014 [cit. 2023-02-11]. [Online]
       hyperlink: https://3dprint.com/12933/3d-printed-castle-complete/

[4]   CONTOUR CRAFTING CORPORATION. New Press Release: Contour Crafting Corporation
       gets Investment from Doka Ventures, leases 33000+ sq-ft space in El Segundo to start
       production of construction 3D printers [online]. In: [cit. 2018-03-05]. [Online] hyperlink:
       http://contourcrafting.com/press-release/

[5]   SCOTT, Clare. Dubai and Cazza Construction Technologies Announce Plans to Build
       World's First 3D Printed Skyscraper. In: Https://3dprint.com [online]. 2017 [cit. 2018-03-
       05].

[6]   WAM. 25% of Dubai's buildings will be 3D printed by 2030, says Sheikh Mohammed
       [online]. In: The Gulf Today, 2016 [cit. 2018-03-06]. [Online] hyperlink:
       http://gulftoday.ae/portal/ea6e7ae1-b73a-4fa5-8572-26a52eeb042d.aspx

[7]   VELKÁ BRITÁNIE. UK National Strategy for Additive Manufacturing / 3D Printing. In: .
       London, 2017. [Online] hyperlink: http://am-uk.org/wp-content/uploads/2017/11/AM-
       UK_Strategy_Publication_Amends_Novermber_Digital.pdf

[8]   How To Build A Lunar Base With 3D Printing. In: TGDaily [online]. [cit. 2023-02-11]. [Online]
       hyperlink: https://tgdaily.com/science/space/69207-how-to-build-a-lunar-base-with-
       3d-printing/

[9]   Mars Habitat. In: Foster + Partners: Projects - Industrial and Research [online]. [cit. 2018-
       03-06]. [Online] hyperlink: https://www.fosterandpartners.com/projects/mars-habitat/

[10]   LUXFORD, Charlotte. Can 3D printing help solve the global housing crisis?. In: Medium
       [online]. San Francisco: A Medium Corporation [cit. 2023-02-11]. [Online] hyperlink:
       https://medium.com/the-omnivore/can-3d-printing-help-solve-the-global-housing-
       crisis-42d91bfb08f3

[11]   CHIUSOLI, Alberto. 3D Printing for Sustainable Living. In: WASP [online]. Massa Lombarda
       [cit. 2023-02-11]. [Online] hyperlink: https://www.3dwasp.com/en/3d-printing-for-
       sustainable-living/

[12]   ROUSSEL, Nicolas. Rheological requirements for printable concretes. Cement and
       Concrete Research [online]. 2018, 112, 76-85 [cit. 2023-02-19]. ISSN 00088846. [Online]
       hyperlink: doi:10.1016/j.cemconres.2018.04.005

[13]   DUBALLET, R., O. BAVEREL a J. DIRRENBERGER. Classification of building systems for
       concrete 3D printing. In: Automation in Construction [online]. 2017, , s. 247-258 [cit. 2023-
       02-15]. ISSN 09265805. [Online] hyperlink: doi:10.1016/j.autcon.2017.08.018

[14]   Mobile 3D-printer Apis Cor: Building by future standards. In: Apis Cor [online]. [cit. 2023-02-13]. [Online] hyperlink: https://apis-cor.com

[15]   GOSSELIN, C., R. DUBALLET, Ph. ROUX, N. GAUDILLIèRE, J. DIRRENBERGER a Ph. MOREL. Large-scale 3D printing of ultra-high performance concrete – a new processing route for architects and builders. Materials & Design [online]. 2016, 100, 102-109 [cit. 2018-10-04]. ISSN 02641275. [Online] hyperlink: doi:10.1016/j.matdes.2016.03.097

[16]   ANTON, Ana, Lex REITER, Timothy WANGLER, Valens FRANGEZ, Robert FLATT a Benjamin DILLENBURGER. A 3D concrete printing prefabrication platform for bespoke columns. Automation in Construction [online]. 2021, 122 [cit. 2023-03-02]. ISSN 09265805. [Online] hyperlink: doi:10.1016/j.autcon.2020.103467

[17]   GARCÍA CUEVAS, Diego a Gianluca PUGLIESE. Advanced 3D printing with Grasshopper: clay and FDM. First published. Independently published, 2020. ISBN 9798635379011.

[18]   ANTON, Ana, Angela YOO, Patrick BEDARF, Lex REITER, Timothy WANGLER a Benjamin DILLENBURGER. Vertical Modulations [online]. In: . s. 596-605 [cit. 2023-03-01]. [Online] hyperlink: doi:10.52842/conf.acadia.2019.596

[19]   LIM, S., R.A. BUSWELL, T.T. LE, S.A. AUSTIN, A.G.F. GIBB a T. THORPE. Developments in construction-scale additive manufacturing processes. Automation in Construction [online]. 2012, 21, 262-268 [cit. 2023-02-26]. ISSN 09265805. [Online] hyperlink: doi:10.1016/j.autcon.2011.06.010

[20]   Baumit BauMinator: Zukunft in Beton [online]. In: . [cit. 2023-03-01]. [Online] hyperlink: https://www.additive-fertigung.com/bericht/cc---contour-crafting__3242/baumit__bauminator__zukunft__in__beton-2018-03-27

[21]   CHEN, Yu, Shan HE, Yidong GAN, Oğuzhan ÇOPUROğLU, Fred VEER a Erik SCHLANGEN. A review of printing strategies, sustainable cementitious materials and characterization methods in the context of extrusion-based 3D concrete printing. Journal of Building Engineering [online]. 2022, 45 [cit. 2023-02-23]. ISSN 23527102. [Online] hyperlink: doi:10.1016/j.jobe.2021.103599

[22]   TATERSALL, G.H. a P.G.F. BANFILL. The Rheology of Fresh Concrete. London: Pitman, 1983. ISBN 0273085581.

[23]   ROUSSEL, N., G. OVARLEZ, S. GARRAULT a C. BRUMAUD. The origins of thixotropy of fresh cement pastes. Cement and Concrete Research [online]. 2012, 42(1), 148-157 [cit. 2023-02-20]. ISSN 00088846. [Online] hyperlink: doi:10.1016/j.cemconres.2011.09.004

[24]   LE, T.T., S.A. AUSTIN, S. LIM, R.A. BUSWELL, R. LAW, A.G.F. GIBB a T. THORPE. Hardened properties of high-performance printing concrete. Cement and Concrete Research [online]. 2012, 42(3), 558-566 [cit. 2018-03-06]. ISSN 00088846. [Online] hyperlink: doi:10.1016/j.cemconres.2011.12.003

[25]   LE, T., S. AUSTIN, S. LIM, R. BUSWELL, A. GIBB a T. THORPE. Mix design and fresh properties for high-performance printing concrete. Materials and Structures [online]. 2012, 45(8), 1221-1232 [cit. 2018-03-06]. ISSN 1359-5997. [Online] hyperlink: doi:10.1617/s11527-012-9828-z

[26] NERELLA, V.N., M. NÄTHER, A. IQBAL, M. BUTLER a V. MECHTCHERINE. Inline quantification of extrudability of cementitious materials for digital construction. Cement and Concrete Composites [online]. 2019, 95, 260-270 [cit. 2023-02-20]. ISSN 09589465. [Online] hyperlink: doi:10.1016/j.cemconcomp.2018.09.015

[27] LEE, Seung, Hong KIM, Etsuo SAKAI a Masaki DAIMON. Effect of particle size distribution of fly ash–cement system on the fluidity of cement pastes. Cement and Concrete Research [online]. 2003, 33(5), 763-768 [cit. 2023-02-26]. ISSN 00088846. [Online] hyperlink: doi:10.1016/S0008-8846(02)01054-2

[28] CLAISSE, P.A., M.H. OMARI a P. LORIMER. Workablity of cement pastes. ACI Materials Journal. 2001, 98(6), 476-482. [Online] hyperlink: http://www.claisse.info/My%20papers/Paper%2016.pdf

[29] MA, Guowei a Li WANG. A critical review of preparation design and workability measurement of concrete material for largescale 3D printing. Frontiers of Structural and Civil Engineering [online]. 2018, 12(3), 382-400 [cit. 2023-02-26]. ISSN 2095-2430. [Online] hyperlink: doi:10.1007/s11709-017-0430-x

[30] NERELLA, Venkatesh, Martin KRAUSE a Viktor MECHTCHERINE. Direct printing test for buildability of 3D-printable concrete considering economic viability. Automation in Construction [online]. 2020, 109 [cit. 2023-02-19]. ISSN 09265805. [Online] hyperlink: doi:10.1016/j.autcon.2019.102986

[31] MALAEB, Zeina, Hussein HACHEM, Adel TOURBAH, Toufic MAALOUF, Nader ZARWI a Farook HAMZEH. 3D Concrete Printing: Machine and Mix Design: Machine and Mix Design. International Journal of Civil Engineering and Technology. 2015, 6, 14-22.

[32] KAZEMIAN, Ali, Xiao YUAN, Evan COCHRAN a Behrokh KHOSHNEVIS. Cementitious materials for construction-scale 3D printing: Laboratory testing of fresh printing mixture. Construction and Building Materials [online]. 2017, 145, 639-647 [cit. 2023-02-10]. ISSN 09500618. [Online] hyperlink: doi:10.1016/j.conbuildmat.2017.04.015

[33] TRTNIK, Gregor, Goran TURK, Franci KAVČIČ a Violeta BOSILJKOV. Possibilities of using the ultrasonic wave transmission method to estimate initial setting time of cement paste. Cement and Concrete Research [online]. 2008, 38(11), 1336-1342 [cit. 2023-02-26]. ISSN 00088846. [Online] hyperlink: doi:10.1016/j.cemconres.2008.08.003

[34] ÖZTÜRK, T., J. RAPOPORT, J. POPOVICS a S. SHAH. Monitoring the setting and hardening of cement-based materials with ultrasound. Concrete Science and Engineering. RILEM Publications SARL, 1999, 1(2), 83-91. ISSN 1295-2826.

[35] LIM, S., R.A. BUSWELL, T.T. LE, S.A. AUSTIN, A.G.F. GIBB a T. THORPE. Developments in construction-scale additive manufacturing processes. In: Automation in Construction. 2012, , s. 262-268. ISSN 09265805. [Online] hyperlink: doi:10.1016/j.autcon.2011.06.010

[36] PERROT, A., D. RANGEARD a A. PIERRE. Structural built-up of cement-based materials used for 3D-printing extrusion techniques. Materials and Structures [online]. 2016, 49(4), 1213-1220 [cit. 2023-02-26]. ISSN 1359-5997. [Online] hyperlink: doi:10.1617/s11527-015-0571-0

[37] KETEL, Sabrina, Gabriel FALZONE, Bu WANG, Newell WASHBURN a Gaurav SANT. A printability index for linking slurry rheology to the geometrical attributes of 3D-printed

components. Cement and Concrete Composites [online]. 2019, 101, 32-43 [cit. 2023-02-27]. ISSN 09589465. [Online] hyperlink: doi:10.1016/j.cemconcomp.2018.03.022

[38]   TRIPATHI, Avinaya, Sooraj NAIR a Narayanan NEITHALATH. A comprehensive analysis of buildability of 3D-printed concrete and the use of bi-linear stress-strain criterion-based failure curves towards their prediction. Cement and Concrete Composites [online]. 2022, 128 [cit. 2023-02-28]. ISSN 09589465. [Online] hyperlink: doi:10.1016/j.cemconcomp.2022.104424

[39]   WANGLER, Timothy, Nicolas ROUSSEL, Freek BOS, Theo SALET a Robert FLATT. Digital Concrete: A Review. Cement and Concrete Research [online]. 2019, 123 [cit. 2023-02-27]. ISSN 00088846. [Online] hyperlink: doi:10.1016/j.cemconres.2019.105780

[40]   WOLFS, R.J.M., F.P. BOS a T.A.M. SALET. Early age mechanical behaviour of 3D printed concrete: Numerical modelling and experimental testing. Cement and Concrete Research [online]. 2018, 106, 103-116 [cit. 2018-10-04]. ISSN 00088846. [Online] hyperlink: doi:10.1016/j.cemconres.2018.02.001

[41]   SUIKER, A.S.J. Mechanical performance of wall structures in 3D printing processes: Theory, design tools and experiments. International Journal of Mechanical Sciences [online]. 2018, 137, 145-170 [cit. 2023-02-28]. ISSN 00207403. [Online] hyperlink: doi:10.1016/j.ijmecsci.2018.01.010

[42]   WOLFS, R. a A. SUIKER. Structural failure during extrusion-based 3D printing processes. The International Journal of Advanced Manufacturing Technology [online]. 2019, 104(1-4), 565-584 [cit. 2023-02-28]. ISSN 0268-3768. [Online] hyperlink: doi:10.1007/s00170-019-03844-6

[43]   VANTYGHEM, G., T. OOMS a W. DE CORTE. FEM modelling techniques for simulation of 3D concrete printing. In: Proceedings of the fib Symposium: Conference was postponed due to Covid-19. (Accepted) [online]. Shanghai, China, 2020 [cit. 2023-02-11]. [Online] hyperlink: https://arxiv.org/abs/2009.06907

[44]   OOMS, Ticho, Gieljan VANTYGHEM, Ruben VAN COILE a Wouter DE CORTE. A parametric modelling strategy for the numerical simulation of 3D concrete printing with complex geometries. Additive Manufacturing [online]. 2021, 38 [cit. 2023-02-11]. ISSN 22148604. [Online] hyperlink: doi:10.1016/j.addma.2020.101743

[45]   REITER, Lex, Timothy WANGLER, Nicolas ROUSSEL a Robert FLATT. The role of early age structural build-up in digital fabrication with concrete. Cement and Concrete Research [online]. 2018, 112, 86-95 [cit. 2023-03-01]. ISSN 00088846. [Online] hyperlink: doi:10.1016/j.cemconres.2018.05.011

[46]   PANDA, Biranchi, Jian LIM a Ming TAN. Mechanical properties and deformation behaviour of early age concrete in the context of digital construction. Composites Part B: Engineering [online]. 2019, 165, 563-571 [cit. 2023-03-01]. ISSN 13598368. [Online] hyperlink: doi:10.1016/j.compositesb.2019.02.040

[47]   BOS, Freek, Rob WOLFS, Zeeshan AHMED a Theo SALET. Additive manufacturing of concrete in construction: potentials and challenges of 3D concrete printing. Virtual and Physical Prototyping [online]. 2016, 11(3), 209-225 [cit. 2018-06-14]. ISSN 1745-2759. [Online] hyperlink: doi:10.1080/17452759.2016.1209867

[48] FENG, Peng, Xinmiao MENG, Jian-Fei CHEN a Lieping YE. Mechanical properties of structures 3D printed with cementitious powders. Construction and Building Materials [online]. 2015, 93, 486-497 [cit. 2023-02-28]. ISSN 09500618. [Online] hyperlink: doi:10.1016/j.conbuildmat.2015.05.132

[49] ZAREIYAN, Babak a Behrokh KHOSHNEVIS. Effects of interlocking on interlayer adhesion and strength of structures in 3D printing of concrete. Automation in Construction [online]. 2017, 83, 212-221 [cit. 2023-02-28]. ISSN 09265805. [Online] hyperlink: doi:10.1016/j.autcon.2017.08.019

[50] ASPRONE, Domenico, Costantino MENNA, Freek BOS, Theo SALET, Jaime MATA-FALCÓN a Walter KAUFMANN. Rethinking reinforcement for digital fabrication with concrete. Cement and Concrete Research [online]. 2018, 112, 111-121 [cit. 2023-02-28]. ISSN 00088846. [Online] hyperlink: doi:10.1016/j.cemconres.2018.05.020

[51] ROBERT MCNEEL & ASSOCIATES. Rhinoceros [Software]. Version 7 SR26 Educational. 2021 [cit. 2023-02-12]. [Online] hyperlink: https://www.rhino3d.com/download/rhino-for-windows/7/latest. System requirements: Windows 11, 10 or 8.1.; size 293.8 MB .

[52] PROJECTSILKWORM. Silkworm: 3D printing plugin for Grasshopper [Software]. Version 0.1.1 2012-12-22. 2012. [Online] hyperlink: www.food4rhino.com/en/app/silkworm. System requirements: Rhino 4 -7 for Windows; size 92 kB .

[53] VANTYGHEM, Gieljan a Ticho OOMS. Concre3DLab. In: Food4Rhino [online]. 2021 [cit. 2023-02-11]. [Online] hyperlink: www.food4rhino.com/en/app/concre3dlab

[54] PEGNA, Joseph. Exploratory investigation of solid freeform construction. Automation in Construction [online]. 1997, 5(5), 427-437 [cit. 2023-02-13]. ISSN 09265805. [Online] hyperlink: doi:10.1016/S0926-5805(96)00166-5

[55] KHOSHNEVIS, Berokh. Innovative rapid prototyping process makes large sized, smooth surfaced complex shapes in a wide variety of materials. Materials Technology. 1998, 13(2), 52–63.

[56] KHOSHNEVIS, Behrokh. Automated construction by contour crafting—related robotics and information technologies. In: Automation in Construction [online]. 2004, , s. 5-19 [cit. 2018-03-11]. ISSN 09265805. [Online] hyperlink: doi:10.1016/j.autcon.2003.08.012

[57] KHOSHNEVIS, Behrokh, Dooil HWANG, Ke YAO a Zhenghao YEH. Mega-scale fabrication by Contour Crafting. International Journal of Industrial and Systems Engineering [online]. 2006, 1(3), 301-320 [cit. 2018-03-06]. ISSN 1748-5037. [Online] hyperlink: doi:10.1504/IJISE.2006.009791

[58] BUSWELL, R.A., R.C. SOAR, A.G.F. GIBB a A. THORPE. Freeform Construction: Mega-scale Rapid Manufacturing for construction. In: Automation in Construction [online]. 2. 2007, , s. 224-231 [cit. 2023-02-10]. ISSN 09265805. [Online] hyperlink: doi:10.1016/j.autcon.2006.05.002

[59] THORPE, Tony, Alistair GIBB, Simon AUSTIN, Richard BUSWELL, John WEBSTER, Thanh LE a Sungwoo LIM. Fabricating construction components using layer manufacturing technology. In: Global Innovation in Construction Conference 2009 (GICC'09), [online]. Loughborough University, 2009 [cit. 2023-02-13].

[60]   GOEHRKE, Sarah Anderson. Concrete Plans: CyBe's Berry Hendriks Describes Plans to 3D Print with Mortar. In: Https://3dprint.com [online]. New York: 3DR Holdings LLC, 2015 [cit. 2023-02-10]. [Online] hyperlink: https://3dprint.com/35727/cybe-berry-hendriks-concrete/

[61]   Total Kustom: Rudenko's 3D Concrete Printer [online]. 20, 2015 [cit. 2023-02-15]. [Online] hyperlink: http://www.totalkustom.com

[62]   ADLUGHMIN. Architect Plans to 3D Print a 2-story Home in Minnesota Using a Homemade Cement Printer. In: 3DR Holdings [online]. [cit. 2023-02-15]. [Online] hyperlink: https://3dprint.com/2471/3d-printed-home-in-minnesota/

[63]   BUREN, Alec. Technical University Eindhoven takes massive 11x5x4m concrete 3D printer into production. In: 3Ders [online]. [cit. 2023-02-13]. [Online] hyperlink: https://www.3ders.org/articles/20151023-technical-university-eindhoven-takes-massive-concrete-3d-printer-into-production.html

[64]   LANGENBERG, Erno. Mapping 20 years of 3D printing in Architecture [online]. In: . [cit. 2023-02-13]. [Online] hyperlink: https://www.elstudio.nl/?p=1904

[65]   ČSN EN 206+A2: Beton - Specifikace, vlastnosti, výroba a shoda. 10/2021. Praha: CEN, 2021.(Czech National Code. Concrete - Specifications, properties, production and compliance)

[66]   ČESKOMORAVSKÝ CEMENT, A.S. – ZÁVOD RADOTÍN. CEM I 42,5 R Portlandský cement EN 197-1: Technický list. Praha, 2017, 2 s. (Portland cement, manufacturer ČESKOMORAVSKÝ CEMENT ,Technical Data Sheet)

[67]   CEMEX CZECH REPUBLIC, S.R.O. CEM I 42,5 R Prachovice: Technický list. Praha, 2022, 2 s. [Online] hyperlink: www.cemex.cz/documents/46856796/52314696/TL__01__CEM+I+42%2C5+R__v02.pdf/ (Portland cement, manufacturer CEMEX ,Technical Data Sheet)

[68]   ČEZ ENERGETICKÉ PRODUKTY, S.R.O. Sulfátovápenaté pojivo SORFIX pro výrobu betonu: Technický list. Hostivice, 2022, 5 s. [Online] hyperlink: https://www.cezep.cz/cs/aktuality/ekologicke-pojivo-sorfix-141806 (SORFIX Sulfate-Lime Binder for concrete production: Technical Data Sheet)

[69]   ČEZ ENERGETICKÉ PRODUKTY, S.R.O. Sorfix: Bettersizer ST Particle Size Analysis Report. 2021-03-18. 1 s.

[70]   KRKONOŠSKÉ VÁPENKY KUNČICE, A.S. Vápenec velmi jemně mletý, tř. V – VI 5600 druh č. 10 (druh B): Technický list. Kunčice, 2017. [Online] hyperlink: https://www.kvk.cz/content/dam/dms/cz-kvk/e/tds-5600.pdf (Limestone very finely ground, cl. V - VI, 5600 Species No 10 (Species B). (Technical Data Sheet)

[71]   MASTER BUILDERS SOLUTIONS CZ S.R.O. MasterLife MS 120 D: Technický list. 2020. [Online] hyperlink: https://assets.master-builders-solutions.com/cs-cz/mbs-masterlife-ms-120-d-tl.pdf). (Technical Data Sheet)

[72]   SKLOPÍSEK STŘELEČ, A.S. Mikromleté písky: Technický list. 07-2020. Microground sands. Technical Data Sheet

[73]   SKLOPÍSEK STŘELEČ, A.S. Slévárenský písek - ST 53: Křivka zrnitosti. 07-2020. 1 s. (Foundry sand - ST 53: Grain size curve)

[74]   SKLOPÍSEK STŘELEČ, A.S. Sportovní písky - ST53: Technical Data Sheet. 07-2020.

[75]   SKLOPÍSEK STŘELEČ, A.S. Technický písek ST 06-12: Křivka zrnitosti. 07-2020. (Technical sand - ST 53: Grain size curve)

[76]   SKLOPÍSEK STŘELEČ, A.S. Technické písky: Technický list. 07-2020. (Technical sands: Technical Data Sheet)

[77]   MASTER BUILDERS SOLUTIONS CZ S.R.O. MasterFiber 006: Technical Data Sheet. 28-08-2018.

[78]   MASTER BUILDERS SOLUTIONS CZ S.R.O. MasterGlenium ACE 430: Technical Data Sheet. 28-08-2018.

[79]   MASTER BUILDERS SOLUTIONS CZ S.R.O. MasterMatrix SDC 100: Technical Data Sheet. 28-08-2018.

[80]   MASTER BUILDERS SOLUTIONS CZ S.R.O. MasterRoc HCA20: Technical Data Sheet. 28-08-2018.

[81]   MASTER BUILDERS SOLUTIONS CZ S.R.O. MasterKure 220WB: Technical Data Sheet. 28-08-2018.

[82]   MASTER BUILDERS SOLUTIONS CZ S.R.O. MasterFlow 3D 100: Technical Data Sheet. Chrudim, 2021.

[83]   SIKA CZ, S.R.O. Sikacrete 751 3D: Product data sheet. Brno, 2022, 3 s.

[84]   COSTANZI, Chris Borg. 3D Printing Concrete onto Flexible Surfaces [online]. Delft, 2016 [cit. 2018-10-04]. [Online] hyperlink: https://repository.tudelft.nl/islandora/object/uuid:84d36c2e-8969-4432-b1a5-c9c02e6304f6/datastream/OBJ1/download. MSc. Thesis. Delft University of Technology, Faculty of Architecture and the Build Environment.

[85]   MA, Guowei, Zhijian LI a Li WANG. Printable properties of cementitious material containing copper tailings for extrusion based 3D printing. Construction and Building Materials [online]. 2018, 162, 613-627 [cit. 2023-03-05]. ISSN 09500618. [Online] hyperlink: doi:10.1016/j.conbuildmat.2017.12.051

[86]   HANSSEN, Trygwe. ELKEM AS. EMMA: Elkem Materials Mixture Analyser [Software]. 3.5.2.11. Elkem AS, 2012. [Online] hyperlink: https://content.elkem.com/Elkem-Materials-Mixture-Analyser. System requirements: Windows 7; size 5.88 MB .

[87]   SNOP, Roman. ČEZ ENERGETICKÉ PRODUKTY, S.R.O. Ekologické pojivo Sorfix. Praha, 2021, 8 s. [Online] hyperlink: https://www.cezep.cz/webpublic/file/edee/sorfix/pojivo-sorfix.pdf
(Ecological binder Sorfix.)

[88]   Arduino: Mega 2560. In: Arduino [online]. Monza [cit. 2023-03-06]. [Online] hyperlink: https://docs.arduino.cc/hardware/mega-2560

[89] ARDUINO. Arduino: 1.8.9. [Software]. GNU General Public Licence. 2018. [Online] hyperlink: https://www.arduino.cc/en/software. System requirements: Win 7. Size: 31,5 MB.

[90] Marlin: 1.1 [Software]. GNU General Public Licence. [Online] hyperlink: https://marlinfw.org/meta/download/. System requirements: Win7. Size: 4.9 MB.

[91] Pronterface: Printrun 1.6.0 [Software]. GNU General Public Licence. [Online] hyperlink: https://github.com/kliment/Printrun. System requirements: Windows 8.1-10; size 60.1 MB.

[92] LUCIANO, Xander. NC Viewer: GCode Viewer and Machine Simulator [online]. 2018 [cit. 2023-02-11]. [Online] hyperlink: https://ncviewer.com

[93] SVAZ VÝROBCŮ BETONU ČR. Evropská směrnice pro samozhutnitelný beton: Specifikace, výroba a použití. 1.0.0. Praha: Svaz výrobců betonu ČR, 2005, 65 s. [Online] hyperlink: https://www.svb.cz/assets/pdf/smernicescc.pdf (European guidelines for self-compacting concrete: Specification, production and use: Association of Concrete Producers of the Czech Republic)

[94] ETHERINGTON, Rose. Building Bytes 3D printed bricks by Brian Peters. In: Dezeen [online]. London: Dezeen Limited, 2012 [cit. 2023-03-12]. [Online] hyperlink: https://www.dezeen.com/2012/10/31/building-bytes-3d-printed-bricks-brian-peters/

[95] Prvok: Jak Prvok přišel na svět. In: Scoolpt [online]. České Budějovice [cit. 2022-10-24]. Dostupné z: https://www.scoolpt.com/pribeh-prvoka/ (3D printed house Prvok. How Prvok was born)

[96] HUNČÍK, Martin. Využití pojiva na bezcementové bázi k návrhu malty pro 3D tisk. Praha, 2022. Bachelor thesis. Czech Technical University, Faculty of Civil Engineering. Vedoucí práce Michal Kovářík. (Using a cement-free binder to design a mortar for 3D printing)

LIST OF FIGURES

LIST OF TABLES